



**Characterisation and Molecular Manipulation of  
Barley  $\beta$ -amylase**

by

**YUEFANG MA**

M. Sc.

Hangzhou University

Hangzhou, China

This thesis submitted for the degree  
of Doctor of Philosophy at Adelaide University

Department of Plant Science  
Waite Campus, Adelaide University  
Glen Osmond, South Australia

March, 2001

## **Declaration**

---

The work presented in this thesis has not previously been submitted to any University or other tertiary institution for the award of any other degree or diploma. To the best of my knowledge and belief, the thesis contains no material previously published or written by another person, except where due reference has been made in the text. I give consent to this copy of my thesis, when deposited in the University Library, being available for photocopying and loan.

**Yuefang Ma**

## Acknowledgments

---

Special thanks must go to my supervisors Dr. D. E. Evans, Prof. Peter Langridge and Dr. Sue Logue, not only for their academic direction and help, but also for their continual support and encouragement throughout my study. I would also like to acknowledge Dr. Doug Stewart for his advice in the early stages of my study.

I am very grateful to Mr Jason Eglinton for his valuable comments and suggestions during the course of my study. I also appreciate the help from Dr. Maria Hrmova and Dr. Andrew Harvey with the kinetic assays and protein modelling, and specially thank Dr. Neil Shirley for his advice and assistance with DNA sequencing and synthesis of primers.

I would like to express my sincere thanks to staff and students in Professor Langridge's laboratory and the South Australian Barley Improvement Program for their technical advice and friendship. Many thanks to all my colleagues within the Department of Plant Science for their generous help and cooperation during my study.

Financial support for this research project was provided by the Australian Grains Research and Development Corporation and was much appreciated.

Finally, and most importantly, I would like to express my deep gratitude to my family-parents, husband and son, for their love, support and patience throughout my study.

## Table of contents

---

<b>Title</b>	i
<b>Declaration</b>	ii
<b>Acknowledgments</b>	iii
<b>Table of contents</b>	1
<b>Abbreviations</b>	8
<b>Thesis summary</b>	10
<b>Publications</b>	12
<b>Thesis introduction</b>	14
<b>Chapter 1</b>	
<b>Literature review</b>	19
1. 1 Introduction	19
1. 2 Barley $\beta$ -amylase genes	19
1. 2. 1 Endosperm-specific $\beta$ -amylase gene	19
1. 2. 2 Ubiquitous $\beta$ -amylase gene	22
1. 3 Synthesis of barley endosperm-specific $\beta$ -amylase	23
1. 4 Release of barley $\beta$ -amylase	24
1. 5 Primary structure of barley $\beta$ -amylase	25
1. 6 Action pattern of $\beta$ -amylase	26
1. 7 Biochemical characteristics of barley $\beta$ -amylase	26
1. 8 Heterogeneity of barley $\beta$ -amylase	28

1. 9 Three-dimensional structure of barley $\beta$ -amylase	30
1. 9. 1 Overall structure of barley $\beta$ -amylase	31
1. 9. 2 Substrate-binding site	32
1. 9. 3 Catalytic site	34
1. 10. Conclusion	35
<b>Chapter 2</b>	
<b>General materials and methods</b>	38
2. 1 Materials	38
2. 1. 1 Enzymes	38
2. 1. 2 Kits	38
2. 1. 3 Substrates	39
2. 1. 4 Other Materials	39
2. 1. 5 Synthetic oligodeoxyribonucleotides	40
2. 1. 6 Bacterial strains	40
2. 2 Methods	
2. 2. 1 Purification of barley $\beta$ -amylase from malt	40
2. 2. 1. 1 Crude extraction	40
2. 2. 1. 2 Ammonium-sulphate precipitation	41
2. 2. 1. 3 Anion exchange chromatograph	41
2. 2. 1. 4 Size exclusion chromatograph	42
2. 2. 2 $\beta$ -Amylase analysis	42
2. 2. 2. 1 SDS-PAGE	42
2. 2. 2. 2 Immuno-blotting analysis	43

2. 2. 2. 3 IEF	44
2. 2. 2. 4 Irreversible thermal inactivation	45
2. 2. 2. 5 Measurement of $\beta$ -amylase activity	45
2. 2. 2. 6 Preparation of reduced substrates	46
2. 2. 2. 7 Estimation of starch molecular weight	46
2. 2. 2. 8 Measurement of protein concentration	47
2. 2. 2. 9 $\beta$ -Amylase kinetic assay	47
2. 2. 2. 10 Molecular Modelling	48
2. 2. 3 Cloning of barley $\beta$ -amylase cDNAs	48
2. 2. 3. 1 Total RNA extraction	48
2. 2. 3. 2 RNA electrophoresis	49
2. 2. 3. 3 Reverse Transcription PCR	49
2. 2. 3. 4 DNA electrophoresis	50
2. 2. 3. 5 Purification of DNA fragments	51
2. 2. 3. 6 Ligation of PCR products	51
2. 2. 3. 7 Transformation	52
2. 2. 3. 8 Mini-prep of plasmid DNA	53
2. 2. 3. 9 Quantification of DNA	53
2. 2. 3. 10 DNA sequencing	54
2. 2. 4 Expression of barley $\beta$ -amylase cDNA	55
2. 2. 4. 1 Restriction digestion	55
2. 2. 4. 2 Dephosphorylation	55
2. 2. 4. 3 Ligation	56
2. 2. 4. 4 Transformation	56

2. 2. 4. 5 Orientation determination	57
2. 2. 4. 6 Expression	57
2. 2. 4. 7 Extraction of recombinant $\beta$ -amylase	58
2. 2. 4. 8 Affinity purification	59
2. 2. 4. 9 Removal of 6xHis-tag	59
2. 2. 5 Site-directed mutagenesis	60
2. 2. 5. 1 Mutagenic reaction	60
2. 2. 5. 2 Digestion of the parental supercoiled dsDNA	60
2. 2. 5. 3 Transformation	60
2. 2. 5. 4 DNA sequencing of the mutated $\beta$ -amylase	61
<b>Chapter 3</b>	
<b>Kinetic study of barley <math>\beta</math>-amylases</b>	62
3. 1 Introduction	64
3. 2 Materials and methods	65
3. 2. 1 Materials	65
3. 2. 2 $\beta$ -Amylase purification and analysis	65
3. 3 Results	66
3. 3. 1 Purity of the purified $\beta$ -amylases	66
3. 3. 2 Kinetic properties of $\beta$ -amylases	68
3. 3. 3 Inhibition of $\beta$ -amylase by maltose	72
3. 4 Discussion	73

## Chapter 4

<b>Removal of the four C-terminal glycine-rich repeats enhances thermostability and substrate binding affinity of barley <math>\beta</math>-amylase</b>	79
4. 1 Introduction	80
4. 2 Materials and methods	81
4. 2. 1 Materials	81
4. 2. 2 PCR primer design	72
4. 2. 3 Cloning of barley $\beta$ -amylase cDNAs	84
4. 2. 4 Production of recombinant $\beta$ -amylases	85
4. 3 Results	86
4. 3. 1 Thermostability of native $\beta$ -amylases	86
4. 3. 2 Production of recombinant $\beta$ -amylases	87
4. 3. 3 Thermostability of recombinant $\beta$ -amylases	89
4. 3. 4 Kinetics of recombinant $\beta$ -amylases	90
4. 3. 5 Structural analysis	91
4. 4 Discussion	94
<b>Chapter 5</b>	
<b>A single amino acid substitution that determines the IEF band pattern of barley <math>\beta</math>-amylase</b>	99
5. 1 Introduction	100
5. 2 Materials and methods	101
5. 2. 1 Materials	101
5. 2. 2 Site-directed mutagenesis	101
5. 2. 3 Electrophoresis	103



5. 2. 4 Electrostatic calculations	103
5. 3 Results	104
5. 3. 1 IEF band patterns of native $\beta$ -amylases	104
5. 3. 2 IEF band patterns of recombinant $\beta$ -amylases	104
5. 3. 3 Production of mutant $\beta$ -amylases	105
5. 3. 4 IEF band patterns of mutant $\beta$ -amylases	107
5. 3. 5 IEF band patterns with reducing agents	108
5. 3. 6 Electrostatic potential of $\beta$ -amylase	109
5. 4 Discussion	111
<b>Chapter 6</b>	
<b>The amino acid substitutions of barley <math>\beta</math>-amylase that improve thermostability and substrate-binding affinity</b>	115
6. 1 Introduction	117
6. 2 Materials and methods	118
6. 2. 1 Sequence alignment of barley $\beta$ -amylases	118
6. 2. 2 Site-directed mutagenesis	118
6. 2. 3 Production of mutant $\beta$ -amylases	119
6. 3 Results	119
6. 3. 1 Sequence comparison of barley $\beta$ -amylases	119
6. 3. 2 Production of mutant $\beta$ -amylases	120
6. 3. 3 Thermostability of barley $\beta$ -amylases	122
6. 3. 4 Kinetics of barley $\beta$ -amylases	125
6. 3. 5 Structural analysis of $\beta$ -amylases	126

6. 4 Discussion	130
<b>General discussion</b>	135
<b>Appendix A Results of <math>\beta</math>-amylase purification</b>	143
<b>Appendix B Results of <math>\beta</math>-amylase clone and recombinant protein analysis</b>	148
<b>Appendix C Buffers, stock solutions and media</b>	154
<b>References</b>	159

## List of abbreviations

---

A	adenine
ATP	adenosine 5'-triphosphate
BBA-7s	the sevenfold mutant of barley $\beta$ -amylase
bp	base pair
BSA	bovine serum albumin
C	cytosine
CsCl	cesium chloride
cDNA	complementary DNA
CIAP	calf intestinal alkaline phosphatase
DEPC	diethyl pyrocarbonate
DNA	deoxyribonucleic acid
dNTP	2'-deoxy nucleotide 5'-triphosphates
DMSO	dimethyl sulfoxide
dp	average degree of polymerisation
DP	diastatic power
DTT	dithiothreitol
EDTA	ethylenediaminetetraacetic acid
EGTA	ethyleneglyco-bis-( $\beta$ -aminoethyl ether)N'N'-tetraacetic acid
G	guanine
hr	hour
IEF	isoelectric focusing
IPTG	isopropyl $\beta$ -thiogalactopyranoside
kb	kilobase
kDa	kilodalton
LB	luria broth
LSD	least significant difference

MES	2-(N-morpholino)ethanesulfonic acid
$\beta$ -ME	2-mercaptoethanol
min	minute
MOPS	3-(N-Morpholino)propanesulfonic acid
mRNA	messenger ribonucleic acid
ng	nano gram
nmole	nano molar
PAGE	polyacrylamide gel electrophoresis
PBS	phosphate buffered saline
PCR	polymerase chain reaction
pI	isoelectric point
RNA	ribonucleic acid
rpm	revolutions per minute
SDS	sodium dodecyl sulphate
sec	second
TBS	Tris buffered saline
Tris-HCl	tris(hydroxymethyl) amino methane hydrochloride
Triton X-100	$\alpha$ -[4-(1,1,3,3-tetramethylbutyl)phenyl]- $\omega$ -hydroxypoly(oxy-1,2-ethanediyl)
Tween 20	polyoxyethylenesorbitan monolaurate
UV	ultraviolet
X-Gal	bromo-(5)-4-chloro-3-indolyl- $\beta$ -D-galactopyranoside

## Thesis summary

---

There are three allelic  $\beta$ -amylase forms, termed Sd1, Sd2L and Sd2H.  $\beta$ -Amylase also undergoes proteolytic modification with approximately 4 kDa cleaved from the C-terminal region of the 60 kDa protein (535 amino acids) after germination. Barley grain and malt (germinated barley) Sd1 and Sd2L  $\beta$ -amylases were purified and used to investigate the enzymatic characteristics. The results demonstrated that the two allelic  $\beta$ -amylases had different characteristics, and that proteolytic cleavage after germination increased the enzyme's thermostability and substrate-binding affinity. Subsequently, further investigations were conducted to understand the molecular basis for the influences of the proteolytic cleavage and amino acid substitutions on the enzyme's properties.

To gain insight into the effect of proteolytic cleavage on enzyme properties, Sd1 and Sd2L  $\beta$ -amylase cDNAs with different deletions in the 3' translational region were cloned, and recombinant  $\beta$ -amylases were generated. Different deletions in the C-terminal region of the protein were found to have different effects on thermostability, although all of the deletions increased the substrate-binding affinity. Complete deletion of the four C-terminal glycine-rich repeats significantly increased the enzyme's thermostability, while incomplete deletion with one repeat remaining did not. Structural analysis suggested that the increased thermostability by the complete deletion of the four glycine-rich repeats might be due to the removal of the unstable C-terminal loop.

The molecular basis for the different properties of the three allelic  $\beta$ -amylases was investigated by site-directed mutagenesis. Sequence alignment of all three allelic  $\beta$ -amylases revealed six amino acid substitutions, and the contributions of these substitutions to the enzymatic characteristics were evaluated by site-directed mutagenesis. Results showed that the R115C mutation, which resulted in an additional hydrogen bond, was responsible for the difference in kinetic properties. The R115C substitution was also found to be the determinant for the two distinct IEF band patterns of barley  $\beta$ -amylase since it altered both the net charges on the protein surface and intermolecular interactions by disulfide bonds.

The different thermostabilities of the three allelic  $\beta$ -amylase forms were due to two amino acid substitutions (V233A and L347S), which increased the enzyme's thermostability index  $T_{50}$  by 1.9°C and 2.1°C, respectively. Although both the V233A and L347S mutations increased thermostability, they affected the thermostability in different ways. The replacement of L347 with serine increased the thermostability by slowing the thermal unfolding of the protein during heating, while the mutation of V233 with alanine accelerated the refolding after heating.

The knowledge of the three preferred residues (C115, A233 and S347) for increased thermostability and substrate-binding affinity of the enzyme was subsequently used to develop a mutant which demonstrated improved enzyme characteristics. Consequently, this investigation recommends a superior  $\beta$ -amylase, which has potential for application in the genetic improvement of malting barley.

## Publications arising from this thesis

---

- Ma, Y. F., Stewart, D. C., Eglinton, J. K., Logue, S. J., Langridge, P. and Evans, D. E. (2000a) Comparative enzyme kinetics of two allelic forms of barley (*Hordeum vulgare* L.) *beta*-amylase. *J. Cereal Sci.* 31, 335-344.
- Ma, Y. F., Eglinton, J. K., Evans, D. E., Logue, S. J. and Langridge, P. (2000b) Removal of the four C-terminal glycine-rich repeats enhances the thermostability of barley  $\beta$ -amylase. *Biochemistry* 39, 13350-13355.
- Ma, Y. F., Evans, D. E., Logue, S. J. and Langridge, P. Mutations of barley  $\beta$ -amylase that improve its thermostability and substrate-binding affinity. Submitted to *Mol. Gen. Genet.*
- Ma, Y. F., Langridge, P., Logue, S. J., Evans, D. E. A single amino acid substitution that determines the IEF band pattern of barley *beta*-amylase. Submitted to *J. Cereal Sci.*
- Ma, Y. F., Stewart, D. C., Eglinton, J. K., Logue, S. J., Langridge, P. and Evans, D. E. (1998) A kinetic study of two forms of  $\beta$ -amylases from barley grain and malt. In 'Proceedings of the 48th Australian Cereal Chemistry Conference', O'Brien L. *et al.* ed. pp 291-195.

Ma, Y. F., Evans, D. E., Logue, S. J. and Langridge, P. (2000) Proteolytic cleavage at the C-terminus improves the thermostability and substrate-binding affinity of barley  $\beta$ -amylase. In 'Proceedings of 6th International Congress of Plant Molecular Biology', The International Society for Plant Molecular Biology ed. pp S27-22.

Ma, Y. F. Evans, D. E. Logue, S. J. and Langridge, P. Improving the thermostability and substrate binding affinity of barley  $\beta$ -amylase by protein engineering. In 'Proceedings of 8th International Barley Genetic Conference', Logue S. ed. 3, 111-113,



## Thesis introduction

---

$\beta$ -Amylase, 1,4  $\alpha$ -glucan maltohydrolase (EC 3.2.1.2), catalyses the release of maltose from the non-reducing end of starch. The enzyme is not only physiologically important for supplying energy for the germinating grain, but also economically significant for the brewing industry because it plays a vital role in hydrolyzing cereal grain starch and releasing maltose, an easily fermentable sugar used by yeast to produce alcohol.

Barley is the primary cereal used in brewing beer due to its high content of hydrolytic enzymes and to its husk, which is required for the lautering stage. Beer is made by the conversion of fermentable sugars, including glucose, fructose, sucrose, maltose and maltotriose (Table 1) into alcohol by yeast. In barley grain, the most abundant component is starch, which comprises approximately two-thirds of the dry weight of the grain. For brewing, barley grains must be modified by a process called malting (Figure 1), which results in the synthesis or release of the starch-degrading enzymes. Malting is essentially a biological process in which the barley is imbibed with water for 1-2 days (steeping), allowed to germinate for 4-5 days and dried at above 80 °C (kilning) to stabilize the malt product and produce the characteristic malt flavors and colors.

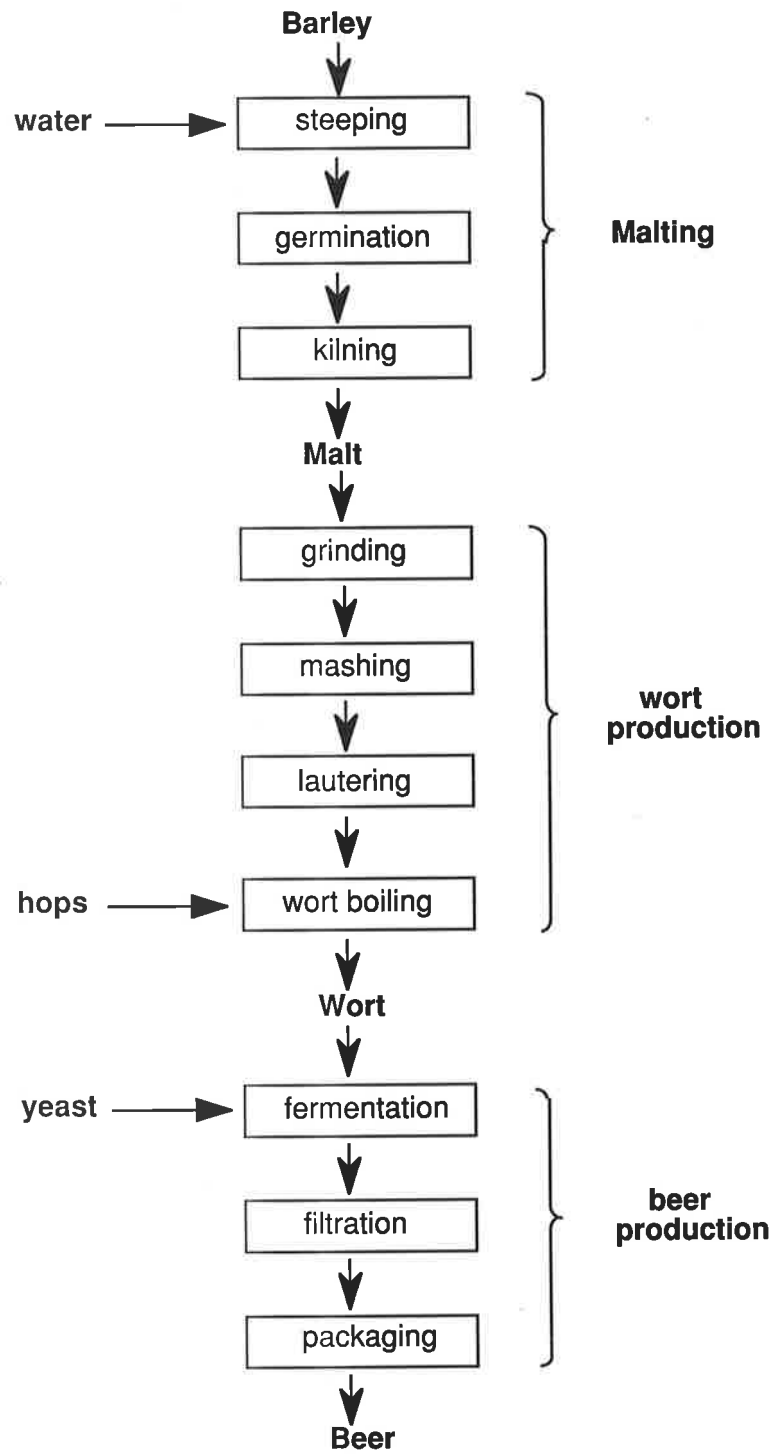


Figure 1 Simplified scheme of the malting and brewing processes.

Table 1. The normal composition of fermentable extract in pale beers (extracted from Kunze 1996)

Fermentable sugars	g in 100 mL of 12 % (w/v) wort	% of fermentable extract
Hexoses (glucose, fructose and sucrose)	0.9-1.2	11.2
Sucrose	0.4-0.5	5.1
Maltose	5.6-5.9	65.4
Maltotriose	1.4-1.7	17.6
Total	8.8	100

The majority of the starch in barley grain is hydrolyzed during the mashing stage (Figure 1) when ground malt is mixed with water in ratios typically 3:1 to 4:1. During brewing, mashing is typically performed either isothermally at approximately 65 °C (infusion mash) or using a ramped temperature profile from approximately 45 °C to 70 °C (temperature programmed mash). Temperatures above 60 °C are required for starch gelatinisation, which in turn is necessary for the rapid and complete enzymatic degradation of starch. Hydrolysis of starch into fermentable sugars is accomplished primarily by four enzymes: (1). <sup>ex - Amylase</sup>  $\beta$ -Amylase is an exo-acting-enzyme, which randomly attacks the starch chain in the middle to produce oligosaccharides, or limit dextrins containing  $\alpha$ -1,4-linked glucose residues. (2).  <sup>$\beta$  amylose</sup>  $\alpha$ -Amylase is an endo-acting-enzyme, which cleaves starch from the non-reducing ends of each starch chain to produce  $\beta$ -maltose, a disaccharide. (3). Limit dextrinase is an endo-acting-enzyme, which hydrolyses  $\alpha$ -1,6-linkages, and thus removes the branches in amylopectin or

$\alpha$ -limit dextrin. (4).  $\alpha$ -Glucosidase is an exo-acting-enzyme, which primarily cleaves  $\alpha$ -1,4-linkages to produce glucose. The activities of these four starch-degrading enzymes are collectively called “diastatic power” (DP). In the brewing industry, DP is a key parameter of malting quality since it is a measure of the capacity of the malt to degrade starch into fermentable sugars (Hayter and Allison 1975; Delcour and Verschaeve 1987). Therefore, the improvement of DP has become a critical objective in Australian barley breeding programs that seek to improve malt quality, especially where large quantities of un-malted adjunct are used.

Although DP describes the collective activities of starch degrading enzymes, only  $\beta$ -amylase has been consistently and significantly correlated with DP (Delcour and Verschaeve 1987; Arends *et al.* 1995; Gibson *et al.* 1995). The activities of the other enzymes have generally been poorly correlated with DP. Therefore, as a major contributor to DP, a sufficiently high level of  $\beta$ -amylase activity is essential for completely hydrolyzing of starch into fermentable sugars during the mashing stage of brewing. However,  $\beta$ -amylase activity is apparently the rate limiting enzyme in starch hydrolysis during mashing in most commercial malts (MacGregor 1996; Sjöholm *et al.* 1995), although the efficiency of  $\beta$ -amylase is influenced by other starch degrading enzymes, particularly limit dextrinase (MacGregor *et al.* 1999; Stenholm and Home 1999).

Apparent sub-optimal levels of  $\beta$ -amylase activity during mashing are predominantly due to the quality, rather than the quantity of the enzyme. Barley  $\beta$ -amylase

represents approximately 1-2 % of the total barley protein (MacGregor *et al.* 1971; Hejgaard and Boisen 1980; Evans *et al.* 1997a) and is relatively thermolabile compared with other starch-degrading enzymes (Sjöholm *et al.* 1995), so that a significant proportion of the  $\beta$ -amylase activity is lost during the mashing process. Thus it would be of great benefit to Australian barley to increase the  $\beta$ -amylase thermostability and/or hydrolytic capacity by protein engineering. This thesis describes the molecular investigation of the enzymatic characteristics of three allelic barley  $\beta$ -amylases and the improvement of the enzymes' characteristics by molecular manipulation.

# Chapter 1

## Literature Review

---

### 1. 1 Introduction

An improved knowledge of barley  $\beta$ -amylase will help identify potential strategies to increase the production of fermentable sugars during mashing, and improve the malting quality of barley varieties. This literature review describes current knowledge of  $\beta$ -amylase in barley, with emphasis placed on those aspects relevant to malting quality and fermentability.

### 1. 2 Barley $\beta$ -amylase genes

Two  $\beta$ -amylase loci have been identified in the barley genome, designated *Bmy1* and *Bmy2*. *Bmy1* is located on the long arm of chromosome 4H and codes for the endosperm-specific  $\beta$ -amylase (Kreis *et al.* 1987; Rorat *et al.* 1991). *Bmy2* is located on the short arm of chromosome 2H and codes for ubiquitous  $\beta$ -amylase (Kreis *et al.* 1988; Shewry *et al.* 1988).

#### 1. 2. 1 Endosperm-specific $\beta$ -amylase gene

Three endosperm-specific  $\beta$ -amylase alleles, termed *Bmy1*-Sd1, *Bmy1*-Sd2L and *Bmy1*-Sd2H, have been identified at the *Bmy1* locus among cultivated barleys (Eglinton *et al.* 1998). The corresponding enzymes are referred to as Sd2L, Sd1 and Sd2H, and possess low, intermediate, and high thermostability, respectively (Eglinton *et al.* 1998). These

three allelic  $\beta$ -amylases have also been identified by Kihara *et al.* (1998; 1999) as type A (corresponding to Sd2H), type B (corresponding to Sd1) and type C (corresponding to Sd2L). The different characteristics of the allelic  $\beta$ -amylase forms have a significant effect on the fermentability of barley varieties (Eglinton *et al.* 1998; Kihara *et al.* 1998; 1999).

Sd2L and Sd2H  $\beta$ -amylase cDNAs have been cloned and sequenced from barley varieties Hiproly (Kreis *et al.* 1987) and Haruna nijo (Yoshigi *et al.* 1994a). The cDNAs are 1,754 and 1,775 bp in length, respectively. Sd2L and Sd2H genomic DNAs of  $\beta$ -amylase have also been isolated from barley varieties Adorra and Haruna nijo, and found to consist of 3,825 bp and contain seven exons and six introns (Yoshigi *et al.* 1995; Erkkilä *et al.* 1998). A *Bmy1* allele of a wild barley *H. spontaneum* (Erkkilä *et al.* 1998) was also sequenced and showed identical sequence to the *Bmy1*-Sd2H allele from Haruna nijo (Yoshigi *et al.* 1995). An alignment of all the published  $\beta$ -amylase sequences revealed three amino acid substitutions (Figure 1. 1). The three substitutions were as follows: Ala-233, Ser-347, Met-527 in Sd2H  $\beta$ -amylase and Val-233, Leu-347, Ile-527 in Sd2L  $\beta$ -amylase. Kaneko *et al.* (2000) also suggested several further amino acid substitutions (C115, E165, A430, T520 ) for type B  $\beta$ -amylase (variety: Harrington) and reported that the thermostability of  $\beta$ -amylase is determined by amino acid substitutions of the  $\beta$ -amylase gene. It has yet to be shown which substitution(s) are responsible for the different enzyme characteristics of the allelic  $\beta$ -amylase forms.

1 MEVNVKGNVYVQVYVMLPLDAVSVNNRFEKGDDELRAQLRKLVEAGVDGVMVDVWWGLVEGK 60  
2 .....  
3 .....  
4 .....

1 GPKAYDWSAYKQLFELVQKAGLKLQAIMSFHQCGGNVGDAVNIPIQWVRDVGTRDPDIF 120  
2 .....  
3 .....  
4 .....

1 YTDGHGTRNIEYLTTLGVDNQPLFHGRSAVQMYADYMTSFRENMKDFLDAGVIVDIEVGLG 180  
2 .....  
3 .....  
4 .....

1 PAGEMRYPSPYQSHGWSFPGIGEFICYDKYLQADFKAAAAAVGHPEWEPNDVGQYNDTP 240  
2 .....V.....  
3 .....A.....  
4 .....A.....

1 ERTQFFRDNGTYLSEKGRFFLAWYSNNLIKHGDRILDEANKVFLGYKVQLAIKISGIHWW 300  
2 .....  
3 .....  
4 .....

1 YKVP SHAAELTAGYYNLHDRDGYRTIARMLKRHRASINF TCAEMRDLEQSSQAMSAPEEL 360  
2 .....L.....  
3 .....S.....  
4 .....S.....

1 VQQVLSAGWREGLNVACENALPRYDPTAYNTILRNARPHGINQSGPPEHKLFGFTYLRLS 420  
2 .....  
3 .....  
4 .....

1 NQLVEGQNYVNFKTFVDRMHANLPRDPYVDPMAPLPRSGPEISIEMILQAAQPKLQPPFF 480  
2 .....  
3 .....  
4 .....

1 QEHTDLPVGPTGGMGGQAEGPTCGMGGQVKGPTGGMGGQAEDPTSGIGGELPATM  
2 .....M.....  
3 .....M.....  
4 .....M.....



Figure 1. 1. Amino acid sequence alignment of published barley  $\beta$ -amylase sequences obtained from GeneBank. 1. Sd2L  $\beta$ -amylase from Hiproly (the accession number is X52321), 2. Sd2L $\beta$ -amylase from Adorra (the accession number is AF061203), 3. Sd2H  $\beta$ -amylase from Haruna nijo (the accession number is D21349), 4.  $\beta$ -amylase from wild barley *H. Spontaneum* (the accession number is AF061204). The numbers at the end of each line refer to the amino acid position. The search codes for  $\beta$ -amylase sequences from Hiproly, Adorra, Haruna nijo, and *H. spontaneum* are X52321, AF061203, D21349, and AF061204, respectively. The multiple sequence alignment was performed using the Pileup program (ANGIS).

$\beta$ -Amylase encoded by the endosperm-specific  $\beta$ -amylase gene accounts for 1-2% of the total soluble proteins in a seed (Hejgaard and Boisen 1980; MacGregor *et al.* 1971; Evans *et al.* 1997a). Because it is such an abundant protein, it has been suggested that it may function as a storage protein (Giese and Hejgaard 1984; Shewry *et al.* 1988). This may be significantly important in the brewing industry, where a large amount of starch needs to be rapidly and completely converted into fermentable sugars.

### **1. 2. 2 Ubiquitous $\beta$ -amylase gene**

The mRNA level of ubiquitous  $\beta$ -amylase was 30 to 40-fold lower than that of endosperm-specific  $\beta$ -amylase (Rorat *et al.* 1995). The gene is not detected in the endosperm, but present in other seedling organs such as leaves and roots (Shewry *et al.* 1988). In addition, ubiquitous  $\beta$ -amylase lacks the C-terminal glycine-rich repeats

(Sadowski *et al.* 1993), which are present in the endosperm-specific  $\beta$ -amylase gene (Kreis *et al.* 1987; Yoshigi *et al.* 1994a). The differences between the endosperm and the ubiquitous  $\beta$ -amylases suggest that they may have different physiological roles during seed development and germination. Ubiquitous  $\beta$ -amylase has been suggested to play a role in germination-related starch breakdown (Daussant and Laurière 1990; Daussant *et al.* 1991).

### **1. 3 Synthesis of barley endosperm-specific $\beta$ -amylase**

Unlike the other starch-degrading enzymes, such as  $\alpha$ -amylase, that are synthesised during germination, barley  $\beta$ -amylase is synthesised and accumulated in the sub-aleurone endosperm during the development of the grain (Laurière *et al.* 1986). The highest level of the  $\beta$ -amylase mRNA occurs 20 days after pollination and the corresponding enzymatic protein accumulates throughout seed development (Rorat *et al.* 1995). Okada *et al.* (2000) recently isolated the promoter of the  $\beta$ -amylase gene, and revealed that the promoter region contains a TATA box and a CCAAT box-like sequence. However, there was no characteristic sequence similar to the endosperm box, TGTAAGTNAATNNG(A/G)TGAGTCAT, which is known as a common sequence in the promoter region of prolamine genes and seems to be associated with seed specific expression (Hammond-Kosack *et al.* 1993). Therefore, it seems that the expression mechanism of the  $\beta$ -amylase promoter differs from that of the prolamine promoter. In addition, the expression of barley  $\beta$ -amylase is also controlled by the intron III of the *Bmy1* gene (Erkkilä *et al.* 1998). A reduction in the length of the intron III resulted in increased expression levels of barley  $\beta$ -amylase.

#### 1. 4 Release of barley $\beta$ -amylase

$\beta$ -Amylase accumulates in barley grain in two forms; a free form, and a bound form which is present as insoluble complexes with other seed proteins and glutenins, and deposited around starch granules (Laurière *et al.* 1986; Hara-Nishimura *et al.* 1986; MacGregor *et al.* 1971; Hejgaard 1976). Free  $\beta$ -amylase can be extracted with water and salt solutions, while the bound form requires the addition of reducing agents (Grime and Briggs 1995) or proteolytic enzymes for extraction (Lundgard and Svensson 1986; 1987; Guerin *et al.* 1992; Sopanen and Laurière 1989). The bound fraction has also been shown to contain a 'latent' fraction which can be extracted with detergent and reducing agents (Evans *et al.* 1997b). Free  $\beta$ -amylase is soluble and active, while bound and latent  $\beta$ -amylases are not soluble, thus not active. A substantial proportion of the bound fractions are released during germination so as to meet the requirements of starch degradation during mashing (Sopanen and Laurière 1989).

The release of  $\beta$ -amylase by endogenous protease has been shown to result in a reduction in the molecular weight, causing a shift of pI to the more basic (Lundgard and Svensson 1986; Guerin *et al.* 1992; Evans *et al.* 1997a). Approximately four kDa was shown to be removed from the C-terminal tail by proteolytic cleavage after germination, producing several isoforms with different termination positions at the C-terminus (A533, Q519-G528, Q508 and G493-Q497, respectively) (Lundgard and Svensson 1987). This observation indicates that the proteolytic cleavage of barley  $\beta$ -amylase is non-specific, but stepwise from the C-terminus. It is unclear, however, what is the implication of the cleavage on the enzyme's characteristics. The cleavage did not cause

any change in the enzyme's activity (Evans *et al.* 1997; Lundgard and Svensson 1987), while a removal of 54 amino acid residues from the C-terminal tail (terminating Q481) resulted in a significant decrease in the thermostability, but an increase in substrate-binding affinity of a recombinant protein (Yoshigi *et al.* 1995a). Further investigations are required to determine the effects of proteolysis on the enzyme characteristics of  $\beta$ -amylase.

### 5 Primary structure of barley $\beta$ -amylase

Barley  $\beta$ -amylase is composed of 535 amino acids, with a relative molecular mass of 59.7 kDa (Kreis *et al.* 1987; Yoshigi *et al.* 1994a). An interesting feature of the primary structure of barley  $\beta$ -amylase is that the C-terminal tail of the protein has four glycine-rich repeated sequences of 11 amino acid residues (Figure 1. 2). In comparison, soybean  $\beta$ -amylase, which shares 67.7% identity with barley  $\beta$ -amylase, lacks the four glycine-rich repeats and is 45 residues shorter than barley  $\beta$ -amylase (Totsuka and Fukazawa 1993 ).

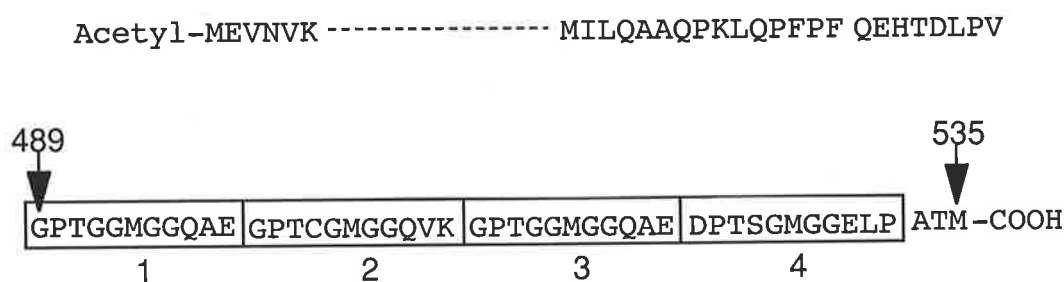


Figure 1. 2. Amino acid sequence of the C-terminal tail of barley  $\beta$ -amylase deduced from cDNA. The four glycine-rich repeats are boxed.

Barley  $\beta$ -amylase contains five sulfhydryl groups, but no intra-molecular disulfide bonds are formed (Yoshigi *et al.* 1994a; Lundgard and Svensson 1987). It was reported that the sulfhydryl groups are involved in the active site because the enzyme activity decreases or disappears when treated with various sulfhydryl reagents (Mikami *et al.* 1994). However, x-ray crystallographic analysis of  $\beta$ -amylase revealed that none of the cysteine residues were involved at the catalytic site, but were concerned with the substrate-binding sites (Shinke 1988).

### **1. 6 Action pattern of $\beta$ -amylase**

$\beta$ -Amylase catalyses the successive liberation of  $\beta$ -maltose from the non-reducing ends of  $\alpha$ -1,4-D-glucans. The action pattern for  $\beta$ -amylase is multiple attack (Nakatani, 1997), where the enzyme, after cleaving off a maltose unit, detaches from the amylose chain to attack another chain. Therefore, the hydrolysis of amylose (unbranched) by  $\beta$ -amylase may potentially reach 100 %, while the hydrolysis of amylopectin will be stopped near the  $\alpha$ -1, 6-glucosidic linkage branched points, leaving  $\beta$ -limit dextrins.

### **1. 7 Biochemical characteristics of barley $\beta$ -amylase**

The enzymatic properties of barley  $\beta$ -amylase have been reported by a number of studies on purified protein (Lundgard and Svensson 1987; Shinke 1988; Yoshigi *et al.* 1994b; 1995a). The optimum pH value of barley  $\beta$ -amylase is 5.2, and the pH stability is between 4.5 and 8.0 (Shinke 1988). The optimal temperature for Sd2H barley  $\beta$ -amylase activity is 55 °C in both recombinant and native enzymes (Yoshigi *et al.*

1995b). The thermostability ( $T_{50}$ ) of recombinant and native Sd2H barley  $\beta$ -amylases are also similar, being 57.4 °C and 56.8 °C, respectively (Yoshigi *et al.* 1995b). However, recombinant  $\beta$ -amylase has higher substrate-binding affinity for starch than native enzyme with the  $K_m$  values for starch 2.53 mg/mL (recombinant) and 4.33 mg/mL (native enzyme), respectively (Yoshigi *et al.* 1995a). Amylose is a relatively poor substrate for barley  $\beta$ -amylase (Yoshigi *et al.* 1995a), as it is for the  $\beta$ -amylases from pea (Lizotte *et al.* 1990), sweet-potato (Baba and Kainuma 1987), and potato (Vikso-Nielsen 1997) compared with starch and amylopectin.

The thermostability of barley  $\beta$ -amylase has a significant influence on the fermentability of barley varieties (Figure 1. 3). Barley  $\beta$ -amylase is relatively thermolabile compared with soybean  $\beta$ -amylase (Yoshigi *et al.* 1995b). Amino acid substitutions of barley  $\beta$ -amylase with corresponding amino acid residues of soybean  $\beta$ -amylase (S295A, I297V, S351P and A376S) (Totsuka and Fukazawa 1993 ) or heat-stable  $\beta$ -amylase from *Clostridium thermosulfurogenes* (M185L, S350P and Q352D) (Kitamoto *et al.* 1988) have been shown to result in an increased thermostability (Yoshigi *et al.* 1995b). These reports suggest that amino acid substitutions are responsible for the thermostability of  $\beta$ -amylase. In addition, barley  $\beta$ -amylase is 45 amino acid residues longer than soybean  $\beta$ -amylase at the C-terminal tail. It is not known if the longer C-terminal tail also affects the thermostability of the protein.

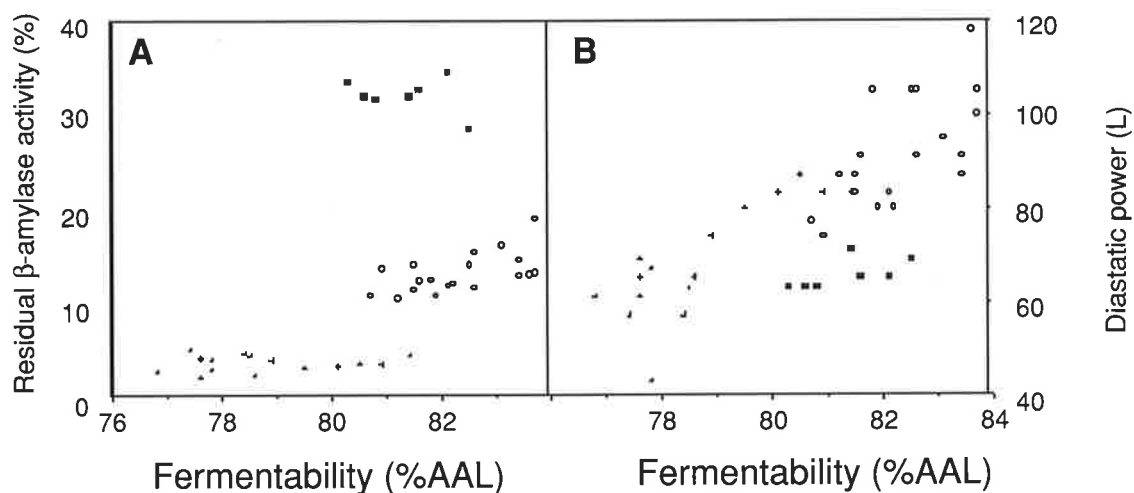


Figure 1. 3. Relationship between  $\beta$ -amylase thermostability and wort fermentability in 42 commercial malt samples.  $\circ$  Sd1,  $\blacksquare$  Sd2H,  $+$  Sd2L (reproduced from Eglinton *et al.* 1998).

### 1. 8 Heterogeneity of barley $\beta$ -amylase

Barley  $\beta$ -amylase is heterogeneous and exists in a number of forms with different isoelectric points (pI) in the range of 5-7 (Visuri and Nummi 1972; Lundgard and Svensson 1987; Shewry *et al.* 1988; Evans *et al.* 1997a). Various explanations have been suggested for the occurrence of the multiple isoenzyme forms. The most probable reason for the multiple forms of barley  $\beta$ -amylase may be polymerization through sulfhydryl groups (Nummi *et al.* 1965; Visuri and Nummi 1972; Briggs 1973; LaBerge and Marchylo 1986; Hejgaard 1976; 1978; LaBerge *et al.* 1983), or various degrees of

peptide cleavage or “ragged ends” at the C-terminus by proteolytic actions (Lundgard and Svensson 1986; 1987; Sopanen and Laurière 1989; Evans *et al.*, 1997a).

Among the three allelic  $\beta$ -amylase forms (Sd1, Sd2L and Sd2H), two IEF band patterns have been identified in cultivated barley, termed Sd1 and Sd2 (Allison 1973; Eglinton and Evans *et al.* 1996; Evans *et al.* 1997a) (Figure 1. 4). Sd2L and Sd2H have the same IEF band pattern (Eglinton *et al.* 1998). The IEF band patterns of barley  $\beta$ -amylase are closely associated with the major malting quality parameters, DP (Swanston 1980; Swanston 1983; Evans *et al.* 1997a) and fermentability (Eglinton *et al.* 1998; Kikara *et al.* 1998; 1999). It has been suggested that the patterns can be used as a biochemical marker to predict DP in barley breeding programs (Swanston 1980; Swanston 1983).

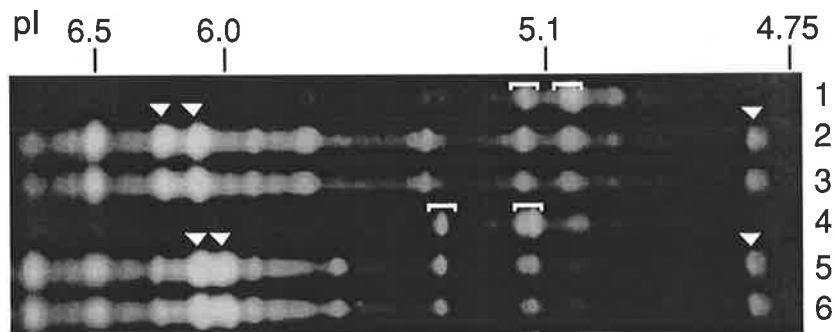


Figure 1. 4 IEF gel of barley grain and malt extracts stained for  $\alpha$ - and  $\beta$ -amylase activity. Lane 1, Sd1 barley grain; lane 2, Sd1 malt; lane 3, Sd1 kilned malt; Lane 4, Sd2L barley grain; lane 5, Sd2L malt; lane 6, Sd2L kilned malt. Square parentheses denote distinctive bands of barley grain Sd1 and Sd2 band patterns and arrowheads denote main  $\alpha$ -amylase bands (reproduced from Evans *et al.* 1997a).



Approaches in barley breeding to improve malting quality have traditionally relied on the measurement of standard malt quality parameters, such as DP and malt extract, as the primary selection tools. These parameters, however, are composites of a number of factors, thus are not precise measurements. They are also slow and laborious procedures, in which the results will vary with the environmental conditions. The IEF technique is a simple and reproducible method for examining genetic variation in  $\beta$ -amylase. Thus, the  $\beta$ -amylase IEF band patterns provide an option for more precisely selecting specific  $\beta$ -amylase alleles that are important for malting quality. However, the reason for the different band patterns is still unknown. An understanding of the molecular basis underlying the different band patterns of barley  $\beta$ -amylase is no doubt important for applying the band pattern as a marker into barley breeding programs. Therefore, it would be useful to gain a closer insight, at the molecular level, of the IEF band patterns.

### **1. 9 Three-dimensional structure of barley $\beta$ -amylase**

The three dimensional structure of  $\beta$ -amylase was first determined in soybean  $\beta$ -amylase (SBA) at 3.0 Å resolution (Mikami *et al.* 1993). The crystal structures of the sevenfold mutant of barley  $\beta$ -amylase (BBA-7s) (Mikami *et al.* 1999), sweet potato (Cheong *et al.* 1995), *Bacillus cereus*  $\beta$ -amylase (Nanmori, *et al.* 1993) have also been determined by x-ray crystallographic analysis. The investigations of the three-dimensional structures of these  $\beta$ -amylases have greatly contributed to the elucidation of the function of  $\beta$ -amylase.

### 1. 9. 1 Overall structure of barley $\beta$ -amylase

The overall structure of BBA-7s is very similar to that of SBA (Mikami *et al.* 1999). The enzyme has a  $\beta/\alpha$  barrel structure (Figure 1. 5). Like all  $\beta/\alpha$  barrel structures, barley  $\beta$ -amylase has a core of eight twisted parallel  $\beta$ -stands arranged close together into a barrel. Of a total of 535 amino acid residues, 188 are contained in this  $\beta/\alpha$  barrel structure. These residues form all eight of the  $\beta$ -stands (44 amino acid residues, Q11-L16, D46-W54, H83-S89, E173-G178, Q289-I292, S336-F339, N374-E378 and F414-Y416) and  $\alpha$ -helices (144 residues, L29-A43, W67-G81, S147-A169, S254-L284, R423-R334, A356-G327, Q385-A396 and N421-A441). The remaining residues form 15 loops that connect the  $\beta$ -stands with the  $\alpha$ -helices of the core structure of  $\beta$ -amylase. The loops on the N-terminal side (L'1-L'7) are generally shorter than those on the C-terminal side (L1-L8). The three longest loops L3 (F90-F120), L4 (L179-S254) and L5 (K293-R423) form a smaller lobe that extends from the C-terminal end of the  $\beta$ -barrel core. There is a similarity of folding of L3, L4 and L5. Each of those loops includes an  $\alpha$ -helix. The common motif is loop1-helix-loop2. The large  $\beta/\alpha$  core and the smaller globular region formed by the long loops L3, L4 and L5 basically resemble the single-domain structure of barley  $\beta$ -amylase.

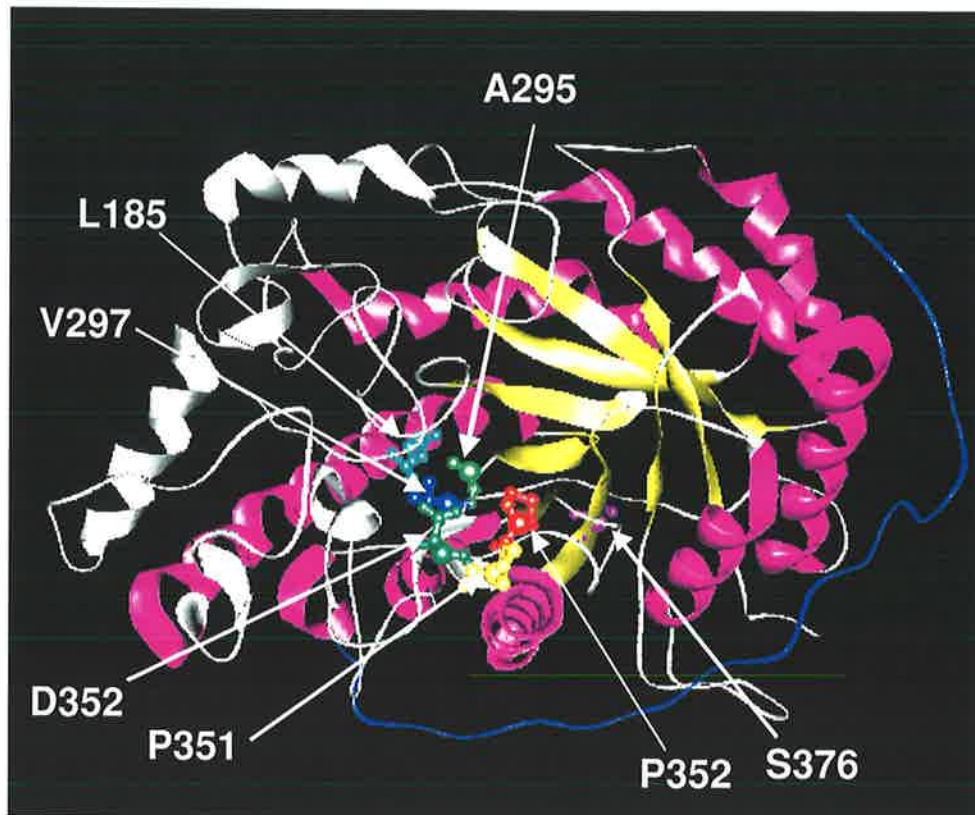


Figure 1. 5. Ribbon model and the seven mutated sites of BAA-7s. The eight  $\alpha$ -helices are coloured pink, the eight  $\beta$ -stands are yellow, the 15 loops are coloured white, the C-terminal tail is coloured blue.

### 1. 9. 2 Substrate-binding site

A cavity-type deformation (about  $30 \times 15 \times 18 \text{ \AA}$ ) is present on the surface of the lobe region of the protein, which leads to a funnel-shaped pocket created by the eight C-terminal side loops (L1-L8). This pocket contains the substrate binding site and the catalytic site (Figure 1. 6). According to the structure solved by Mikami *et al.* (1999), 19 amino acid residues (L20, D53, L89, H93, D101, A184, E186, R188, Y192, K295, G298, H300, W301, T342, E380, N381, A382, L419 and R420) are involved in the

substrate-binding with subsites (Glc, Glc 2, Glc 3 and Glc 4) by making a total 26 hydrogen-bonds and 20 C-C contacts. Six amino acid residues (V99, Y192, W198, F200, M346, and L383) are involved in the substrate-binding via a number of van der Waals contacts.

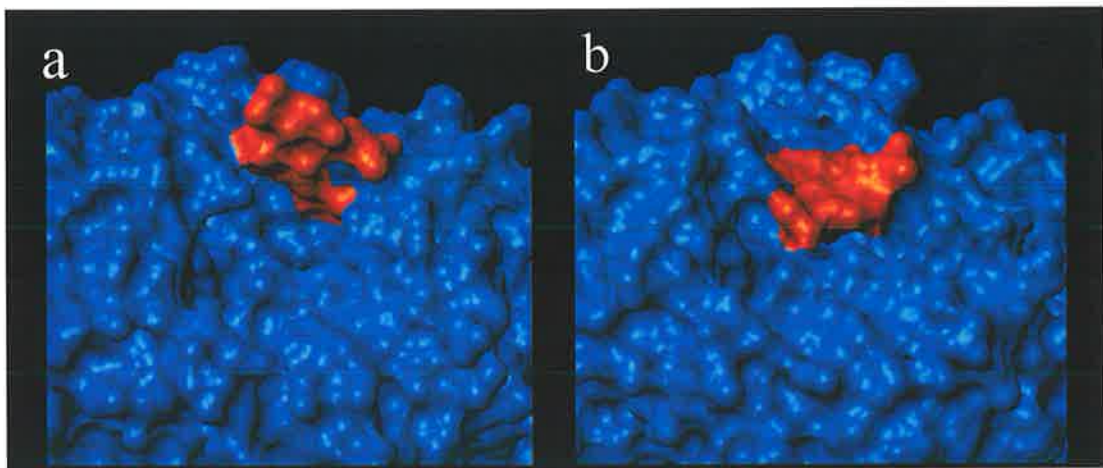


Figure 1. 6 A model of barley  $\beta$ -amylase showing the active site pocket of the enzyme. (a) view into the pocket showing the van der Waals protein surface. The hinged loop L3 (coloured orange) is shown in the unliganded open conformation. (b) the hinged loop L3 in the closed conformation, showing the van der Waals protein surface extending over the reaction centre. This allows the methyl groups of V95 to interact with those of L381 (This figure is provided by Mr J. Eglinton).

### 1. 9. 3 Catalytic site

In the ( $\beta/\alpha$ )-barrel domain, the active site is located in the bottom of the funnel-shaped pocket. The functional residues comprise parts of L3, L4, L5, L6 and L7. It is evident that most of the highly conserved residues of  $\beta$ -amylases are located at these loop regions, especially those of L3 (Uozumi *et al.* 1991; Totsuka and Fukazawa 1993). Based on the complexing of SBA with maltose (Mikami *et al.* 1993), two oppositely disposed glutamic acids (E186 and E380) have been identified as catalytic residues. Both of the glutamic acid residues are conserved in all reported plant and microbial  $\beta$ -amylase sequences (Mikami *et al.* 1994). Glu 186 functions as a general acid (with pKa 8.2) and is presumed to donate a proton to the oxygen in the cleavage site to yield the  $\beta$ -maltose product. Glu 380 acts as a general base with pKa 3.5 in hydrolysing  $\alpha$ -1, 4-glucoside linkages (Mikami *et al.* 1993; Nitta *et al.* 1989; Totsuka *et al.* 1994).

A significant feature of  $\beta$ -amylase is a flexible loop comprising residues 96-103. These residues are identical in all reported  $\beta$ -amylase sequences. This loop in the closed conformation forms part of the active site, and is capable of a hinge-type motion (Totsuka and Fukazawa 1996). In the open conformation, substrate binding is allowed at the active site and the product can be released (Totsuka and Fukazawa 1996; Laederach *et al.* 1999). Therefore, the open/close movement of this loop plays an important role in  $\beta$ -amylase catalysis (Mikami *et al.* 1994).

## 1. 10. Conclusion

$\beta$ -Amylase plays a critical role in starch hydrolysis during brewing and helps to produce the main yeast fermentable sugar, maltose. Endosperm-specific  $\beta$ -amylase is a major barley grain protein that accounts for 1-2% of the total seed protein (MacGregor 1971; Hejgaard and Boisen 1980; Evans *et al.* 1997a). There is only one locus for the endosperm-specific  $\beta$ -amylase (*Bmy1*), but three alleles at the locus have so far been identified among cultivated barleys. The three allelic  $\beta$ -amylase forms have different thermostabilities, which is related to the fermentability of mashes prepared from barley varieties (Eglinton *et al.* 1998; Kihara *et al.* 1998). However, the molecular basis for the different thermostabilities of these allelic  $\beta$ -amylase forms remains to be explained. A fundamental understanding of the molecular mechanisms will provide valuable knowledge that can be applied to improve the  $\beta$ -amylase characteristics via molecular engineering.

The barley  $\beta$ -amylase residues that participate in substrate binding and catalytic action are located in the loop regions of the molecule (Mikami *et al.* 1999). These regions do not contribute to the structural stability of the protein. This structure physically separates the residues that contribute to the stability of the protein from those that are responsible for its specificity. Such an arrangement has obvious evolutionary advantages for changing function without affecting the structural stability of the protein or changing the structural stability of the protein without affecting the substrate-binding

and catalytic action of the enzyme. As a result, this arrangement provides an excellent target for genetically redesigning the protein *in vitro*.

Comparing the sequences and tertiary  $\beta$ -amylase structures of homologous proteins from thermophilic and mesophilic organisms has been the preferred approach to uncovering general trends in sequence and structure evolution that is related to stability, and has led to the development of strategies for increasing the stabilities of proteins (Vogt *et al.* 1997; Thompson and Eisenberg 1999). The three-dimensional structure of Sd2H  $\beta$ -amylase has already been solved (Mikami *et al.* 1999). These previous investigations provide the opportunity to analyse the differences in the sequences and structures of the three allelic  $\beta$ -amylases, which may enable the isolation of important information for improving the characteristics of barley  $\beta$ -amylase. This thesis aims to improve the understanding of the molecular mechanisms controlling the different enzymatic characteristics of the three allelic  $\beta$ -amylases, and to use this knowledge to genetically manipulate the enzyme's hydrolytic capacity, and hence potentially improve the malting quality of barley. Within this framework, the specific aims of this thesis are:

- (1) To purify different allelic  $\beta$ -amylase forms from barley and determine their enzymatic characteristics, in terms of thermostability and kinetic parameters.
- (2) To clone the cDNAs for the different allelic  $\beta$ -amylases and determine the differences in their sequences.

(3) To express the cDNAs and elucidate how the structure influences the enzymatic characteristics of these enzymes.

(4) To manipulate the cDNA by site-directed mutagenesis. The enzymatic characteristics, amino acid substitutions and three dimensional structure of the different types of  $\beta$ -amylase that are discussed above will be used to determine which sites will be investigated.



## Chapter 2

### General materials and methods

---

#### 2. 1 Materials

Buffers, stock solutions and media are described and defined in Appendix C.

##### 2. 1. 1 Enzymes

<b>Enzyme</b>	<b>Source</b>
CIAP	Promega (USA)
Enterokinase	Novagen (USA)
Restriction Endonucleases	Promega (USA)
Superscript™ II	Life Technologies (USA)
T4 DNA ligase	Promega (USA)
<i>Tag</i> DNA polymerase	Promega (USA)

##### 2. 1. 2 Kits

<b>Kit</b>	<b>Source</b>
Betamyl assay	Megazyme (Ireland)
GeneClean (Bio 101)	Bresatec (USA)
pGEM-T easy vector	Promega (USA)
pQE-30 expression vector	Qiagen (USA)
Bio-Rad protein assay	Bio-Rad (USA)
Site-directed mutagenesis	Stratagene (USA)
QIAprep spin plasmid	Qiagen (USA)

### **2. 1. 3 Substrates**

<b>Substrates</b>	<b>Source</b>
Amylose EX-I	Hayashibara Biochemical Lab., Inc. (Japan)
Amylose EX-III	Hayashibara Biochemical Lab., Inc. (Japan)
Glucitol	Sigma (USA)
Maltitol	Seikagaku Corporation (Japan)
Maltopentaose	Sigma (USA)
Maltotriitol	Seikagaku Corporation (Japan)
Potato starch	Sigma (USA)

### **2. 1. 4 Other materials**

<b>Material</b>	<b>Source</b>
Amicon ultrafiltration cell	Amicon (USA)
Anti-His antibody	Qiagen (USA)
Bio-gel P-60 (fine grade)	Bio-Rad (USA)
DE-52	Whatman (UK)
GAR-HRP	Bio-Rad (USA)
Goat anti-rabbit-IgG	Sigma (USA)
Nitrocellulose membranes	Bio-Rad (USA)
SeeBlue marker	Novex (USA)

## 2. 1. 5 Synthetic oligodeoxyribonucleotides

PCR primers and the mutagenic deoxy-oligonucleotide primers for the desired mutagenic changes were synthesized using an Applied Biosystems (USA) DNA Synthesizer (Model 381A) and subsequently purified by reverse-phase High-Performance Liquid Chromatography (HPLC) by Dr Neil Shirley in the Department of Plant Science, Adelaide University.

## 2. 1. 5 Bacterial strains

*E. coli* DH5 $\alpha$ : F<sup>-</sup>,  $\phi$ 80dlacZ $\Delta$ M15, endA1, recA1, hsdR17(rk<sup>-</sup>.mk<sup>+</sup>), supE44, thi-1. gyrA96, relA1,  $\Delta$ (lacZYA-argF), U169,  $\lambda$ <sup>-</sup>.

*E. coli* M15 (pREP4): NaI<sup>s</sup> str<sup>s</sup> rif<sup>s</sup>, lac<sup>-</sup> ara<sup>-</sup> gal<sup>-</sup> mtl<sup>-</sup> F<sup>+</sup> recA<sup>+</sup> uvr<sup>+</sup>.

Epicurian Coli: recA1 endA1 gyrA96 thi-1 hsdR17 supE44 relA1 lac [F<sup>+</sup> proAB lacI<sup>q</sup>Z $\Delta$ M15 Tn10 (Tet<sup>r</sup>)]<sup>c</sup>.

## 2. 2 Methods

### 2. 2. 1 Purification of barley $\beta$ -amylase from malt

All purification steps were carried out in a cold room (4 °C).

#### 2. 2. 1. 1 Crude extraction

1 kg of green malt was combined with 1.5 L of  $\beta$ -amylase extraction buffer and blended in a large Waring blender. A further 1.5 L of extraction buffer was added and stirred for 2 hrs. The extract was collected by centrifugation at 10,000 g for 5

min. A cloudy, viscous, and light-brown supernatant was obtained and the insoluble residue was discarded.

### **2. 2. 1. 2 Ammonium-sulphate precipitation**

The  $\beta$ -amylase extract was initially fractionated by ammonium sulphate precipitation. Dry ammonium sulphate was added slowly with stirring to give 20 % saturation. pH was maintained with 1N  $\text{NH}_4\text{OH}$ . The mixture was stirred for 1 hr, then centrifuged at 10,000 g for 10 min. The supernatant was again precipitated by adding ammonium sulphate to 60 % saturation, stirred overnight, and centrifuged at 10,000 g for 10 min. The precipitate was redissolved and dialysed against 4L of 15 mM Tris-HCl buffer, pH 7.0.

### **2. 2. 1. 3 Anion exchange chromatography**

The dialysed fraction was applied and passed into a 5 x 15 cm column of Diethylaminoethyl cellulose (DE-52) equilibrated with 15 mM Tris-HCl buffer (PH 7.0) at 1.8 mL/min flow rate. The column was washed with the same buffer at the same flow rate. Coloured material was retained on the column, while the  $\beta$ -amylase passed through the column and was collected in a fraction collector. Protein concentrations were measured by optical densities at 280 nm. The first column flow-through gave the separation shown in Appendix A, Figure A1. The enzyme fractions (determined by measuring the  $\beta$ -amylase activity) were pooled and concentrated by Amicon ultrafiltration cell (PM 30 filter) to concentrations of about 5 mg/mL. During ultrafiltration, the fraction was equilibrated in Tris-HCl buffer, pH 8.5. The pooled fraction was loaded onto a second DE-52 column (5 x 40 cm)

equilibrated with 15 mM Tris-HCl buffer, pH 8.5, at a flow rate of 1.0 mL/min. Unbound proteins were washed from the column with the same buffer, and bound proteins were eluted into 18 mL fractions by a gradient from 0 to 0.15 M NaCl at a flow rate of 1.8 mL/min. Three active peaks were detected from the second DE-52 column (Appendix A, Figure A2). The resulting fractions were pooled and concentrated by ultrafiltration cell (Amicon) and the buffer was changed to 50 mM acetate buffer containing 0.1 M NaCl, 10 mM DTT, pH 5.0.

#### **2. 2. 1. 4 Size exclusion chromatography**

2 mL of the pooled enzyme solution from the second anion exchange column was loaded onto a 1 m x 1.6 cm Bio-gel P60 column equilibrated with 50 mM acetate buffer containing 0.1 M NaCl, 10 mM DTT, pH 5.0, and run through the column with a flow rate of 0.1 mL/min. The chromatography of these separations is presented in Appendix A, Figure A3. The active fractions were pooled and the enzyme was concentrated with an ultrafiltration cell. The purity of the preparation obtained from size exclusion chromatography was checked by SDS-PAGE and it was stored at -20 °C in concentrated form (>1.0 mg/mL) as a suspension in 75 mM carbonate buffer containing 5 mM DTT and 5 % glycerol, pH 8.0, and flushed briefly with nitrogen gas. Enzyme yield and specific activities and purification factors are presented in Appendix A, Table A1 and Table A2.

#### **2. 2. 2 $\beta$ -amylase analysis**

##### **2. 2. 2. 1 SDS-PAGE**

SDS-PAGE was performed on 12.5 % polyacrylamide gels according to the method of Laemmli (1970). For the preparation of enzyme extracts, 50 mg mature barley or malt flour was incubated with 1 mL of 0.05 M Tris-HCl, pH 6.8, containing 4 % SDS, 5 M urea and 143 mM  $\beta$ -ME for 1 hr at room temperature, then centrifuged at 10,000 g for 3 min. The protein sample (approximately 0.5  $\mu$ g) was mixed with 5x protein loading buffer, heated at 94 °C for 7 min. to denature the protein, then chilled on ice, loaded on SDS-PAGE gels and run at 130 V in a mini-protein electrophoresis cell (Bio-Rad). SeeBlue markers were used as molecular weight standards.

#### **2. 2. 2. 2 Immuno-blotting analysis**

Immuno-blotting analysis was performed as described by Evans *et al.* (1997a). Briefly, the separated proteins were transferred to a nitrocellulose membrane at 100 V with cooling in a Mini Trans-blot cell (Bio-Rad) for 1 hr. After transfer, the membrane was blocked with 5 % milk powder in PBS for 30 min, and rinsed with PBS twice. Then the membrane was incubated in a 1:5000 diluted solution of rabbit anti- $\beta$ -amylase serum that had been raised against Schooner barley  $\beta$ -amylase in PBS containing 1 % (w/v) BSA at room temperature overnight, and washed three times with TPBS (PBS containing 0.05 % Tween 20) and twice with PBS. For detection of the primary antibody-antigen reaction, the membrane was incubated in a 1:5000 diluted solution of goat anti-rabbit IgG horseradish peroxidase conjugate with PBS buffer containing 1 % (w/v) BSA at room temperature for 3 hrs, followed by washing the membrane three times with TPBS, twice with PBS and three times with TBS, respectively. For colour development, the membrane was immersed in

freshly made HRP colour development solution until the purple-band appeared, then the development was stopped by incubating the membrane in a 0.3 % oxalic acid solution.

### **2. 2. 2. 3 IEF**

IEF of  $\beta$ -amylase was performed at 10 °C on a Multiphor II horizontal electrophoresis unit (LKB, Bromma, Sweden) using ultra-thin (0.4 mm) polyacrylamide gels cast onto Gelbond PAG support film (FMC BioProducts, Rockland, Maine USA). Individual components of the IEF gel were as follows: 1.8 mL of glycerol, 3.3 mL of 30 % acrylamide, 0.5 mL of pH 4.5-5.4 ampholytes (Pharmacia), 0.5 mL of pH 5-7 ampholytes, 25  $\mu$ L of TEMED, 50  $\mu$ L of 10 % ammonium persulphate, and 11.8 mL of water. Prior to addition of the catalysts the solution was degassed under vacuum in a sonicator bath. The anode electrode buffer was 0.04 M L-glutamic acid, and the cathode electrode buffer was 0.2 M L-histidine. The electrode wicks were soaked in electrode solution and blotted free of the excess prior to application. Light paraffin oil was used to provide even contact between the cooling plate and the PAG backing. Gels were pre-focused for 20 min at 5 W constant power, following by focussing at 10 W constant power with upper limits of 2200 V and 50 mA for 2.5 hrs. The focused proteins were stained for  $\beta$ -amylase activity with I/KI solution as described previously (Guerin, *et. al.* 1992). pI values were estimated relative to native IEF markers (Bio-Rad).

#### **2. 2. 2. 4 Irreversible thermal inactivation**

Irreversible thermal inactivation of the purified recombinant  $\beta$ -amylases was assayed by the determination of  $T_{50}$  values.  $T_{50}$  value is the temperature at which 50 % of initial enzymatic activity is lost after heat treatment. The assay method was as follows: purified  $\beta$ -amylases were diluted to 0.1 mg/mL with  $\beta$ -amylase dilution buffer containing 2.8 mg/mL BSA. This is the mean protein concentration of crude extracts measured with the Bradford Coomassie blue binding assay (Bradford 1976). The diluted enzymes were incubated at a range of temperatures from 50 °C to 62.5 °C for 30 min. After incubation, the enzyme solutions were immediately cooled in ice, and the residual  $\beta$ -amylase activity was measured using the Betamyl assay. The  $T_{50}$  value was determined by linear interpolation between the data points closest to 50 % remaining activity.

#### **2. 2. 2. 5 Measurement of $\beta$ -amylase activity**

$\beta$ -Amylase activity was determined using the Betamyl assay as described by Megazyme. The assay was performed by mixing the diluted enzyme (50  $\mu$ L) in  $\beta$ -amylase dilution buffer with 50  $\mu$ L of substrate mixture containing  $\alpha$ -glucosidase (200 U) and the specific "Betamyl" substrate p-nitrophenylmaltopentaoside (PNPG5) (4.75 mg/mL). The enzyme concentrations were adjusted by the initial reaction rate which is linear only with enzyme concentrations that give reaction absorbance values of 0.2-0.8. After incubation for 10 min at 40 °C, the reaction was terminated by adding 750  $\mu$ L of Trizma base (1 %, w/v). The absorbance was read



at 410 nm. One unit of activity is defined as the amount of enzyme that catalyses the release of 1  $\mu\text{mol}$  of maltose/min under the experimental conditions.

#### **2. 2. 2. 6 Preparation of reduced substrates**

The reduced substrates were prepared by reduction with sodium borohydride ( $\text{NaBH}_4$ ) by the method of Takeda *et al.* (1973). 2 g of substrate (potato soluble starch, amylose EX-I, amylose EX-III, or maltopentaose) was dissolved in 20 mL of DMSO with mild heating. After solubilisation, 180 mL of distilled water and 20 mL of 0.2 M  $\text{NaBH}_4$ -0.01 N NaOH were added and the solution was kept at 40 °C for 1 hr. The excess  $\text{NaBH}_4$  was removed by adding 20 mL of 5.15 M acetic acid. The solution was then neutralised with 5 M NaOH. The reduced starch was precipitated by adding a 2x volume of cold ethanol. The precipitate of reduced starch was washed three times with methanol. The product was then dried over silica gel in a desiccator.

#### **2. 2. 2. 7 Estimation of the molecular weight of starch**

The reducing ends of a series of starch solutions with different concentrations (mg/mL) were measured by the Somogyi-Nelson method (Nelson 1944). The number of molecules was estimated using a glucose standard curve since each molecule has only one reducing end. The average molecular weight of the soluble starch was calculated by dividing the amount of starch in a solution by the number of molecules.

## **2. 2. 2. 8 Measurement of protein concentration**

Protein concentrations were determined using the Coomassie blue-binding assay (Bradford 1976). Briefly, 0.2 mL of Coomassie protein assay reagent was added to 0.8 mL of diluted protein solution, and mixed by inversion. The absorbance at 595 nm of the supernatant was measured within 1 hr, and the sample concentration was determined by reference to a standard curve prepared using BSA.

## **2. 2. 2. 9 $\beta$ -Amylase kinetic assay**

The reduced substrates were used for the kinetic analysis of  $\beta$ -amylase. Both enzyme and substrate concentrations were tested to force the rate of hydrolysis to measurable levels, and special care was taken to ensure that initial reaction rates were measured throughout. The assay was performed by mixing the purified enzymes (50 ng) with substrate solution (2-200  $\mu$ M for native  $\beta$ -amylases, 1-100  $\mu$ M for recombinant  $\beta$ -amylases) containing 50 mM acetate buffer, pH 5.0, in a final volume of 500  $\mu$ L. Under these conditions, the reaction rates were linear for at least 15 min. After incubation at 40 °C for 3, 6, 9, and 12 min, the amount of reducing sugars produced by the action of  $\beta$ -amylase on the substrates was determined using the Somogyi-Nelson method (Nelson 1944). Briefly, after incubation of the tube at 40 °C, the reaction was stopped by adding of 500  $\mu$ L of freshly diluted Somogyi reagent (4 parts Somogyi I : 1 part Somogyi II). The tubes were boiled for 10 min, and cooled on ice, following which, 500  $\mu$ L of freshly diluted Nelson/acid reagent (1 part Nelson reagent: 2 parts 0.75 M sulphuric acid) was added. The tubes were vortexed to liberate all gases, and allowed to stand for at least 5 min, followed by

centrifugation of the tubes for 10 min at 5,000 g. The absorbance of the supernatant at 660 nm was read, and the amount of reducing sugars was calculated by reference to a maltose standard curve. The kinetic data was processed by a non-linear-regression analysis based on the Michaelis-Menten equation using the EZ-FIT software (Perella 1988).

### **2. 2. 2. 10 Molecular Modelling**

The solved crystal structure of BBA-7s (PDB identifier 1B1Y) was used to construct a homology-based model of barley  $\beta$ -amylase using the Swiss-Model (Peitsch 1995; 1996). Molecular visualisation and analysis were performed using program SPDBV 3.5 (Guex and Peitsch 1997). The quality of the model was confirmed by the Ramachandran plot (Ramakrishnan and Ramachandran 1965) or the root-mean-square backbone deviation (Chothia and Lesk 1986).

### **2. 2. 3 Cloning of barley $\beta$ -amylase cDNAs**

#### **2. 2. 3. 1 Total RNA extraction**

The method of Cox and Goldberg (1988) was used in the extraction of total RNA with minor modification. Briefly, 1 g of developing barley grain was ground to a fine powder with liquid nitrogen with a mortar and pestle, followed by homogenisation with 3 mL of REB buffer. The slurry was transferred to a pre-chilled Corex centrifuge tube and immediately centrifuged at 5,000 g at 4 °C for 5 min. The supernatant was transferred to a fresh tube and CsCl (1g/mL supernatant) was added. The solution was carefully layered onto the top of 3 mL of CsCl cushion (9.65 g of CsCl dissolved in TE buffer to a final volume of 10 mL) in an

ultracentrifuge tube, and centrifuged at 38,000 g for 16 hrs at 4 °C. The supernatant was removed and the RNA pellet resuspended in 0.4 mL of REB buffer. The solution was extracted with phenol/chloroform/isoamyl-alcohol, and the RNA precipitated with one-tenth volume of 3 M sodium acetate and 2.5 volume of cold ethanol at -20 °C overnight. The pellet of RNA was washed with 70 % ethanol and dried briefly under vacuum, then suspended in TE buffer. The OD<sub>260</sub> of the RNA samples was determined using a spectrophotometer, and the RNA concentration (μL/mL) calculated using OD<sub>260</sub> x 40 x dilution.

#### **2. 2. 3. 2 RNA electrophoresis**

The quality of RNA was assessed by electrophoresis to view the integrity of ribosomal RNA bands with UV light. Agarose gel (1.2 %) containing MOPS buffer and 3 % formaldehyde was prepared. 2.5 μL of the total RNA (approximately 10 μg) was mixed with 2.0 μL of 10xMOPS, 10 μL of deionised formamide, and 3.5 μL of formaldehyde, heated at 65 °C for 10 min and chilled on ice. 2 μL of 10x RNA loading buffer was added to each sample. The RNA samples were loaded into gel and run in 1xMOPS buffer at 60 V for 2-3 hrs. The gels were then stained in 1 μg/mL ethidium bromide for 15 min, followed by destaining in water for 30 min to view ribosome bands with UV light (Appendix B, Figure B1).

#### **2. 2. 3. 3 Reverse Transcription PCR (RT-PCR)**

For the isolation of barley β-amylase cDNAs, the first-strand cDNA was synthesised using the total RNA as a template and oligo (dT) as primer. Briefly, approximately

7.5  $\mu\text{g}$  of the total RNA was denatured in the presence of 50  $\mu\text{M}$  oligo-(dt)-primer in 2  $\mu\text{L}$  of RNase-free  $\text{H}_2\text{O}$  by heating to 70  $^\circ\text{C}$  for 10 min, followed by cooling on ice for 5 min. The annealed RNA-primer mixture was then subjected to reverse transcription under the following conditions: 50 mM Tris-HCl, 2  $\mu\text{L}$  of 0.1 M DDT, 4  $\mu\text{L}$  of 2.5 mM dNTPs (1 mM each dNTP) and 400 units of SuperScript<sup>TM</sup> II RT in a final volume of 20  $\mu\text{L}$ . The mixture was incubated at 45  $^\circ\text{C}$  for 1 hr. To purify the cDNA, the reaction mixture was mixed with one tenth volume of 3 M sodium acetate (pH 4.8) and 2 volumes of pure ethanol, and allowed to precipitate at -80  $^\circ\text{C}$  for half hr. The cDNA was pelleted at 12,000 g, 4  $^\circ\text{C}$  for 15 min, washed with 70 % ethanol, dried and dissolved in 10  $\mu\text{L}$  of water.

The first-strand cDNA was used for PCR amplification which was carried out in a total reaction volume of 25  $\mu\text{L}$  containing 1  $\mu\text{L}$  of the first strand cDNA mixture, 1xPCR buffer, 50  $\mu\text{M}$  of each primer, 0.2 mM of each dNTP, 2.5  $\mu\text{L}$  of 25 mM  $\text{MgCl}_2$ , and 0.4 units of *Taq* DNA polymerase. The temperature profile for the thermocycler was 95  $^\circ\text{C}$  for 4 min, 35 cycles of denaturation (94  $^\circ\text{C}$  for 30 sec), annealing (55  $^\circ\text{C}$  for 1 min) and extension (72  $^\circ\text{C}$  for 1.5 min), and the PCR reaction terminated at 4  $^\circ\text{C}$ . Three independent PCR reactions were performed.

#### **2. 2. 3. 4 DNA electrophoresis**

The PCR products (5 $\mu\text{L}$ ) were mixed with 2  $\mu\text{L}$  of 10xDNA sample loading buffer, and separated on agarose gels. The gels were prepared from 1.0 % (w/v) solution of

agarose in 1xTAE Buffer. Preparation of phage  $\lambda$ DNA digested with EcoR I or phage  $\lambda$ DNA digested with Bste II/Sal I were used as molecular weight markers.

Gels were electrophoresed in 1xTAE buffer at 60 V. After electrophoresis, the gels were stained in ethidium bromide [10 $\mu$ g/mL (w/v) in water] for 20 min, and destained in water before photography under short-wave length UV light using Polaroid 667 film (Appendix B, Figure B2).

### **2. 2. 3. 5 Purification of DNA fragments**

The slice of agarose containing the PCR fragments was excised from agarose gel with a surgical blade under long-wave length UV light, and stored in an Eppendorf tube. A GeneClean Kit (Bio 101) was used to purify the DNA fragment from the agarose gel according to the manufacturer's instructions. Briefly, the pieces of excised gels were dissolved with 2.5x 6 M NaI (w/v) at 50 °C. An appropriate volume of glass milk (typically 5-10  $\mu$ L) was added. The mixture was placed on ice for 5 min, allowing DNA to bind to glass particles. The particles were pelleted by centrifugation for 30 sec and washed three times with new wash solution. The particle-bound DNA was redissolved with H<sub>2</sub>O at 50 °C for 3 min, and spun briefly to pellet the particles. The purified DNA was carefully transferred to a new tube and stored at -20 °C.

### **2. 2. 3. 6 Ligation**

PCR fragments were ligated into a pGEM-T Easy vector in an insert : vector molar ratio of 3:1. The ligation was carried out in a volume of 20  $\mu$ L containing 1xligation

buffer, 1  $\mu\text{L}$  of pGEM-T Easy vector, 2  $\mu\text{L}$  of the PCR product, and 1  $\mu\text{L}$  of T4 DNA ligase. The mixture was incubated for 2 hrs at room temperature and kept at 4  $^{\circ}\text{C}$  before transformation.

### **2. 2. 3. 7 Transformation**

Transformation was performed using *E coli* DH5 $\alpha$  competent cells. The competent cells were prepared as follows: a single *E coli* DH5 $\alpha$  colony was inoculated into 2 mL of SOB medium and grown overnight in a 37  $^{\circ}\text{C}$  shaker. 0.5 mL of the overnight culture was added to 50 mL of SOB medium, followed by incubation at 37  $^{\circ}\text{C}$  with vigorous shaking until an OD<sub>600</sub> of approximately 0.5 was achieved. The cell suspension was pelleted at 5,000 g, 4  $^{\circ}\text{C}$  for 12 min and resuspended with 8.5 mL of TFB buffer. The bacteria were pelleted by centrifugation as previously after incubating on ice for 10 min. The cell pellet was resuspended in 2 mL of TFB buffer and placed on ice. 70  $\mu\text{L}$  of redistilled DMSO was added to the bacterial suspension and mixed by swirling the tube gently. The cell suspension was mixed with 157.5  $\mu\text{L}$  of 1M DTT and incubated on ice for a further 10 min after which the DMSO step was repeated, then divided into 400  $\mu\text{L}$  aliquots, frozen in liquid nitrogen, and stored at -80  $^{\circ}\text{C}$  for transformation.

For transformation, an individual aliquot of competent cells was thawed on ice. 5  $\mu\text{L}$  of each ligation mixture was then mixed with a 100  $\mu\text{L}$  of competent cells, and incubated on ice for 30 min. The cells were heat shocked at 42  $^{\circ}\text{C}$  for 90 sec, then

allowed to recover by incubation at 37 °C for 60 min after addition of 400 µL of SOC (1 mL of SOB medium containing 7 µL of 50 % glucose). The transformation suspension was plated out onto solid LB medium containing 50 µg/mL ampicillin, and incubated at 37 °C overnight. Desired single colonies were selected for plasmid DNA analysis.

### **2. 2. 3. 8 Mini-prep of plasmid DNA**

A QIA Spin miniprep kit was used in plasmid isolation as described by the manufacturer's instructions. A single white colony, carrying the recombinant plasmid, was inoculated into 1.5 mL of LB medium with 50 µg/mL ampicillin and grown at 37 °C overnight with shaking. Cells were pelleted by centrifugation at 12,000 g for 2 min. The suspension was discarded, and the cell pellet was resuspended in 250 µL of P1 buffer and placed on ice for 10 min. Cells were lysed by the addition of 250 µL of P2 buffer. The resulting solution was added to 350 µL of N3 buffer, mixed immediately, but gently, by inverting the tube several times, followed by centrifugation at 12,000 g for 15 min. The resulting supernatant was applied to a QIA prep column and centrifuged for 45 sec. The flow-through was discarded, and the column washed by the addition of 0.75 mL of 70 % ethanol and centrifuged for 45 sec. Residual ethanol was completely removed by centrifuging the column for an additional 1 min at maximum speed. To elute the DNA, 50 µL of water was added to the center of the membrane. The column was allowed to stand for 1 min, and was then centrifuged for an extra 1 min.



### **2. 2. 3. 9 Quantification of DNA**

2-5  $\mu\text{L}$  of DNA sample was diluted into 1 mL of water. The absorbance between 200-300 nm was determined by scanning the sample against a water blank. DNA concentration ( $\mu\text{g}/\text{mL}$ ) was calculated using  $\text{OD}_{260} \times 50 \times$  dilution times.

### **2. 2. 3. 10 DNA sequencing**

DNA sequencing was performed using both commercially available primers and specific primers with an ABI automated DNA Sequencer (Applied Biosystems Inc.). A *Taq* DyeDeoxy Terminator Cycle Sequencing kit was used in dideoxy-mediated sequencing reactions. The reaction mix contained 0.4  $\mu\text{g}$  of DNA, 3  $\mu\text{L}$  of 3.2  $\mu\text{mol}$  primer, 8  $\mu\text{L}$  of terminator ready reaction mix made up to a final volume of 20  $\mu\text{L}$  by the addition of water. The amplification profile was 25 cycles at 96  $^{\circ}\text{C}$  for 10 sec, 50  $^{\circ}\text{C}$  for 5 sec and 60  $^{\circ}\text{C}$  for 4 min. The PCR reaction was terminated at 4  $^{\circ}\text{C}$ .

After the reactions were completed, the entire 20  $\mu\text{L}$  of reaction solution was carefully transferred to a clean 1.5 mL Eppendorf tube containing 50  $\mu\text{L}$  of 95 % ethanol and 2  $\mu\text{L}$  of 3 M sodium acetate (pH 4.6), and mixed thoroughly. The tube was placed on ice for 15 min to precipitate the DNA. The DNA was pelleted at 12,000 g at 4  $^{\circ}\text{C}$  for 15 min, washed with 70 % ethanol, and the pellet dried on a heating block at 95  $^{\circ}\text{C}$  for 10 min. The DNA was then separated electrophoretically and analysed using an ABI automated DNA Sequencer by Dr Neil Shirley in the

Department of Plant Science, Adelaide University. The sequence data was analysed using SeqEd program.

## **2. 2. 4 Expression of barley $\beta$ -amylase cDNA**

### **2. 2. 4. 1 Restriction digestion**

5  $\mu$ g of purified  $\beta$ -amylase plasmid and pQE-30 expression vector were digested with 3  $\mu$ L of restriction endonuclease BamH 1 using the buffer system supplied by the manufacturers at 37 °C for 2 hrs.

### **2. 2. 4. 2 Dephosphorylation**

The digested pQE-30 vector was extracted with phenol/chloroform (containing one volume of redistilled phenol equilibrated in 50 mM Tris-HCl (pH 8.0) and one volume of chloroform), followed by centrifugation at 10,000 g. The supernatant was mixed with one tenth volume of 3 M sodium acetate (pH 4.8) and 2 volumes of pure ethanol. The mixture was incubated at -20 °C for 1 hr to precipitate DNA, followed by centrifugation at 12,000 g, 4 °C for 15 min. The DNA pellet was washed with cold 70 % (v/v) ethanol, dried under vacuum for 1-2 min and resuspended in 42  $\mu$ L of 10 mM Tris-HCl (pH 8.0). 5  $\mu$ L of 10xCIAP buffer and 2  $\mu$ L of CIAP (1U/ $\mu$ L) were added to dephosphorylate the DNA at 37 °C for 15 min, followed by incubation at 56 °C for 15 min. An additional 5  $\mu$ L of CIAP was added and

incubated at 37 °C for 15 min, then 56 °C for 15 min. The reaction was stopped by adding 300 µL of dephosphorylation stop buffer. The reaction solution was extracted with equal volumes of phenol/chloroform and precipitated with ethanol. Finally, the dephosphorylated vector was resuspended in 10 µL of water.

#### **2. 2. 4. 3 Ligation**

Both BamH 1 digested β-amylase and dephosphorylated pQE-30 vector were electrophoresed on 1 % agarose gel and purified with GeneClean as described in chapter 2, section 2. 2. 3. 5. The β-amylase fragment was ligated into pQE-30 expression vector as described in chapter 2, section 2. 2. 3. 6, and used for transformation to *E. coli*.

#### **2. 2. 4. 4 Transformation**

Transformation was performed using M15[pREP4] competent cells. The competent cells were prepared in bulk and stored at -80 °C according to the manufacturer's instructions. Briefly, a single *E. coli* M15[pREP4] colony was inoculated into 10 mL of LB medium containing 25 µg/mL kanamycin and grown overnight in a 37 °C shaker. 1 mL of overnight culture was added to 100 mL of LB medium containing 25 µg/mL kanamycin, followed by incubation at 37 °C with vigorous shaking until an OD<sub>600</sub> of approximately 0.5 was reached. The culture was cooled on ice for 5 min and pelleted by centrifugation at 5,000 g at 4 °C for 5 min. The cells were resuspended gently with 30 mL of TFB 1 buffer, and the suspension was kept on ice for an additional 90 min. The cells were collected by centrifugation as previously,

and the cell pellet resuspended in 4 mL of ice-cold TFB2 buffer. Cells were divided into 200  $\mu$ L aliquots and frozen in liquid nitrogen, then stored at -80 °C for transformation.

The transformation was performed as described in chapter 2, section 2. 2. 3. 7, except for an addition of 500  $\mu$ L of Psi broth after heat shock at 42 °C for 90 sec.

The cell transformation suspension was plated out onto LB-agar plates containing 25  $\mu$ g/mL kanamycin and 100  $\mu$ g/mL ampicillin, and incubated at 37 °C overnight.

Single colonies were picked to check orientation.

#### **2. 2. 4. 5 Orientation determination**

Both orientations of the  $\beta$ -amylase insert were expected in the expression plasmids as both 5' and 3' ends of the  $\beta$ -amylase fragment were BamH 1 recognition sites. To determine the orientation of the insert in pQE-30 transformants, the plasmid was isolated as described in chapter 2, section 2. 2. 3. 8. 2  $\mu$ g of the plasmids was digested with 2  $\mu$ L of restriction endonuclease Hind III using the buffer system supplied by the manufacturers at 37 °C for 2 hrs. According to the restriction map of  $\beta$ -amylase cDNA (Appendix B, Figure B3), the plasmid with the right orientation was expected to release a 455 bp fragment after Hind III digestion (Appendix B, Figure B4 line 1), while the plasmid with the reverse orientation would release a 1248 bp fragment by Hind III digestion (Appendix B, Figure B4 line 2). Plasmids with the correct orientations were selected for expression.

#### **2. 2. 4. 6 Expression**

*E. coli* M15 harbouring  $\beta$ -amylase was grown at 37 °C in LB medium supplemented with 100  $\mu\text{g}/\text{mL}$  Ampicillin and 25  $\mu\text{g}/\text{mL}$  Kanamycin. When the absorbance of the culture at 600 nm reached approximately 0.5, IPTG was added to the culture medium to a final concentration of 0.1 mM and the sample was immediately shifted to 22 °C. The induction continued for a further 8 hrs.

#### **2. 2. 4. 7 Extraction of recombinant $\beta$ -amylase**

Small scale extraction was carried out to check the expression of the recombinant protein according to the manufacturer's instructions. 2 mL of cell culture induced with IPTG was pelleted by centrifugation at 12,000 g at room temperature for 1 min. The pellet was frozen at -20 °C overnight. The cell pellets were suspended in 300  $\mu\text{L}$  of sonication buffer containing 1 mM lysozyme, and lysed by an ultrasonicator (Model Sonifier B-12, Branson Ultrasonic PTY. LTD) at 40 W. This was repeated four times (10 sec duration) with intermittent cooling on ice. The supernatant (containing soluble  $\beta$ -amylase) was obtained by centrifuging the crude lysate at 12,000 g at 4 °C for 15 min, and used to check the overexpression of  $\beta$ -amylase in *E. coli* by SDS-PAGE and immuno-blotting analysis as described in chapter 2, sections 2. 2. 2. 1 and 2. 2. 2. 2 (Appendix B, Figure B5).

Large scale extraction was performed to purify the recombinant  $\beta$ -amylase. 500 mL of cell culture was harvested by centrifugation at 4,000 g, 4 °C in JA14 for 12 min. The cell pellet was resuspended in 7-8 mL of sonication buffer, and frozen at -20 °C overnight. The frozen cell suspension was thawed and lysed by sonication using the same procedure as for small scale extraction. The soluble protein was removed by centrifugation at 12,000 g, 4 °C for 15 min.

#### **2. 2. 4. 8 Affinity purification**

8 mL of supernatant containing soluble protein was mixed with 4 mL of Ni-NTA resin equilibrated with sonication buffer, and stirred in a cold room (about 4 °C) for 1 h. The resin was then loaded into a 1.6 cm diameter column, and washed with 100 mL of sonication buffer containing 20 mM imidazole, and 100 mL of wash buffer containing 20 mM imidazole at 0.5 mL/min flow rate. The recombinant protein was eluted with 250 mM imidazole in wash buffer. The imidazole was exchanged with 1x rEK cleavage buffer in an Amicon centricon-30 microconcentrator (Amicon, USA).

#### **2. 2. 4. 9 Removal of 6xHis-tag**

Purified protein (0.2 mg) was digested by the addition of 4U enterokinase in 1x rEK cleavage buffer to give a final volume of 80  $\mu$ L. After incubation at 23 °C for 16 hrs, the digested mixture was loaded on a Ni-NTA column to remove the undigested proteins. The complete cleavage of the 6xHis-tag was detected by immuno-blot analysis as described in chapter 2, section 2. 2. 2. 2 using anti-His antibody. Successful cleavage resulted in the removal of a peptide from fusion proteins

upstream of the enterokinase cleavage site. No band was evident at the size corresponding to the target protein (Appendix B, Figure B6). Finally, enterokinase was removed by size exclusion chromatography as described in chapter 2, section 2.

2. 1. 4.

## **2. 2. 5 Site-directed mutagenesis**

### **2. 2. 5. 1 Mutagenic reaction**

The mutagenic reaction mixture contained 20 ng of the dsDNA template, 125 ng of each mutagenic oligonucleotide primer, 1  $\mu$ L of dNTP mix, 5  $\mu$ l of 10xreaction buffer and 2.5 units of PfuTurbo DNA polymerase in a final volume of 50  $\mu$ L. The mixture was reacted at 95 °C for 2 min, followed by 30 cycles at 95 °C for 30 sec, 55 °C for 1 min, and 68 °C for 15 min, followed by 16 hrs at 10 °C.

### **2. 2. 5. 2 Digestion of the parental supercoiled dsDNA**

10  $\mu$ L of the amplified product was electrophoresed on a 1 % agarose gel to check for sufficient amplification. The remaining 40  $\mu$ L of amplification product was added to 1  $\mu$ L of the Dpn I restriction enzyme (10 U/ $\mu$ L), followed by incubation at 37 °C for 1 h to digest the parental supercoiled dsDNA.

### **2. 2. 5. 3 Transformation**

The Epicurian Coli XL1-Blue supercompetent cells were used for the transformation of mutant  $\beta$ -amylase. The cells were thawed on ice. 50  $\mu$ L of the supercompetent cells were mixed with 2  $\mu$ L of the Dpn I-treated DNA. The mixture was incubated on ice for 30 min. The cells were heat shocked at 42 °C for 45 sec, then allowed to recover by incubation in a 37 °C shaker for 1 h after addition of 500  $\mu$ l of NZY Broth. The cell transformation suspension was plated out onto LB-agar plates containing 100  $\mu$ g/mL ampicillin that had been prepared with 20  $\mu$ L of 10 % (w/v) X-gal and 20  $\mu$ L of 100 mM IPTG, and incubated at 37 °C overnight.

#### **2. 2. 5. 4 DNA sequencing of the mutated $\beta$ -amylase**

Plasmids were isolated from single colonies of transformants as described in chapter 2, section 2. 2. 3. 8, and DNA sequencing of the mutated  $\beta$ -amylase was performed as described in chapter 2, section 2. 2. 3. 10 to confirm that only the desired mutation occurred during the manipulations.



## Chapter 3

### Kinetic study of barley $\beta$ -amylase

---

#### Abstract

Sd1 and Sd2L  $\beta$ -amylases were purified from barley grain and malt of varieties Franklin and Schooner. Kinetic parameters were measured using the purified enzymes. The  $K_m$  value for malt  $\beta$ -amylase was lower than that of mature grain  $\beta$ -amylase for both varieties when potato starch was used as a substrate, although  $k_{cat}$  was similar. This indicated that proteolysis after germination increased the affinity of  $\beta$ -amylase for potato starch, but did not affect the catalytic capacity. No significant kinetic differences were observed between  $\beta$ -amylase from mature grain and malt of the two barley varieties when amylose (dp 100 and 18) and maltopentaose were used as substrates. Kinetic differences were also observed between the two allelic  $\beta$ -amylase forms. Sd1 malt  $\beta$ -amylase exhibited a lower  $K_m$  value for potato starch than Sd2L malt  $\beta$ -amylase, suggesting that Sd1  $\beta$ -amylase may be better able to hydrolyse starch than Sd2L  $\beta$ -amylase. As the degree of polymerisation of the substrates decreased from approximately 740 to 5 (maltopentaose), the  $K_m$  values for  $\beta$ -amylase increased, whilst  $k_{cat}$  values decreased. The hydrolytic product of  $\beta$ -amylase, maltose, was found to be a weak competitive inhibitor of both Sd1 and Sd2L malt  $\beta$ -amylase with respect to potato

starch and amylose. Glucose and maltotriose were not inhibitors of malt  $\beta$ -amylase at concentrations found in wort produced during the brewing process.

### 3. 1 Introduction

Three endosperm-specific  $\beta$ -amylase alleles, *Bmy1-Sd1*, *Bmy1-Sd2L* and *Bmy1-Sd2H*, have been identified in cultivated barley at the *Bmy1* locus on chromosome 4H. The corresponding enzymes are referred to as Sd1, Sd2L and Sd2H, respectively (Eglinton *et al.* 1998). However, only two distinct IEF band patterns have been identified (Sd1 and Sd2), as Sd2L and Sd2H exhibit an identical band pattern. These allelic forms of barley  $\beta$ -amylase have been found to have differences in thermostability (Eglinton *et al.* 1998; Kihara *et al.* 1998). However, it is not known whether they have different kinetic properties.

$\beta$ -Amylase is synthesised during barley grain development (Hardie 1975), and undergoes proteolytic modification after germination with approximately 4 kDa cleaved from the C-terminal region (Lundgard and Svensson 1986). It has been suggested that this proteolysis activates  $\beta$ -amylase (Sopanen and Laurière 1989; Guerin *et al.* 1992). However, no significant effect of proteolysis on  $\beta$ -amylase activity was observed by Evans *et al.* (1997b). Yoshigi *et al.* (1994b; 1995a) reported a reduction in  $K_m$  value for recombinant barley  $\beta$ -amylase after 54 amino acid residues (4.9 kDa) were deleted from the C-terminal end. However, no differences in  $K_m$  value were observed between four barley  $\beta$ -amylase forms produced by proteolysis when 4 kDa was cleaved from the C-terminal end (Lundgard and Svensson 1987). In this chapter, the kinetic properties of purified barley grain and malt  $\beta$ -amylases from Sd1 and Sd2L barley varieties were

investigated to resolve what influences allelic difference and proteolytic cleavage have on enzyme function. The potential implications of these differences to malting and brewing properties are discussed.

### **3. 2 Materials and methods**

#### **3. 2. 1 Materials**

Samples of the barley varieties Franklin and Schooner (1996 season) were obtained from the South Australian Barley Improvement Program, and malted in an automated micro-malting unit (Phoenix Bio Systems, Adelaide, Australia) using a standard malting program (Evans 1997a). Malt was removed from the automated micro-malting unit after 4 days of germination and used to purify  $\beta$ -amylase.

#### **3. 2. 2 $\beta$ -Amylase purification and analysis**

$\beta$ -Amylases were purified from malt of the varieties Franklin and Schooner. Purified barley grain  $\beta$ -amylases were obtained from Dr. Evans (Evans *et al.* 1997a). The purified enzymes were used to measure the kinetic parameters. The methods for  $\beta$ -amylase purification (chapter 2, section 2. 2. 1) and kinetic assay (chapter 2, section 2. 2. 2. 9) have been described previously.

### 3. 3 Results

#### 3. 3. 1 Purity of the purified $\beta$ -amylases

The purified  $\beta$ -amylases were free of  $\alpha$ -amylase activity and deemed pure, although a minor band was observed (estimated to be less than 5% total protein) when preparations were examined by SDS-PAGE (Figure 3. 1B, lanes 1 and 3). The minor band was recognised by anti-barley- $\beta$ -amylase antibodies and was assumed to be a minor degradation product of  $\beta$ -amylase (Figure 3. 1D, lanes 1 and 3) as previously identified by Evans *et al.* (1997a). The molecular mass of barley grain  $\beta$ -amylase was estimated to be 60 kDa (Figure 3. 1, lanes 1 and 3), while the enzyme from malt was approximately 56 kDa (Figure 3. 1, lanes 2 and 4). In malt extracts,  $\beta$ -amylase antibodies detected both the 60 kDa and 56 kDa bands (Figure 3. 1A and C, lanes 2 and lane 4). However, only a 56 kDa protein was present after purification.

The purified  $\beta$ -amylases were also examined by IEF (Figure 3. 2). The distinct Sd1 and Sd2L band patterns were consistent with those observed for barley grain and malt extracts by Evans *et al.* (1997a), confirming that the same isoelectric heterogeneity observed in the crude extracts was maintained, and that no artefacts were generated during purification.

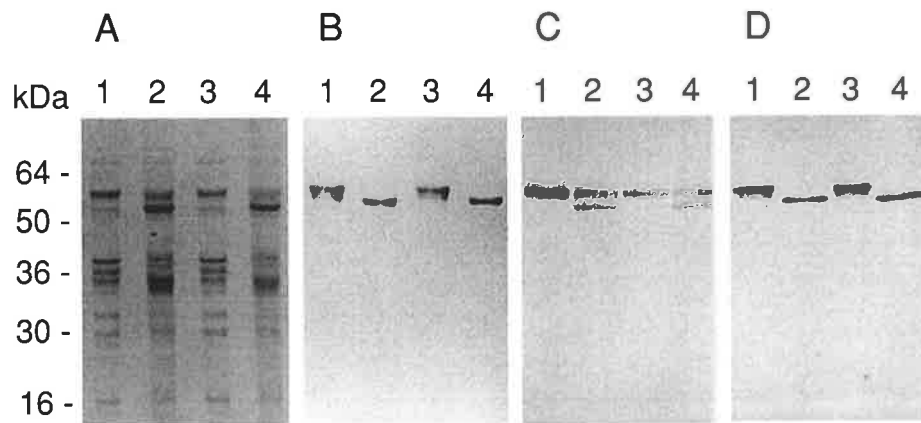


Figure 3. 1. SDS-PAGE and immuno-blot analysis of extracts and purified  $\beta$ -amylases. A and B, SDS-PAGE stained for protein with Coomassie blue R250; C and D, immuno-blot using anti- $\beta$ -amylase polyclonal antibodies; A and C, extracts; B and D, purified protein; lane 1, Sd1 barley grain  $\beta$ -amylase; lane 2, Sd1 malt  $\beta$ -amylase; lane 3, Sd2L barley grain  $\beta$ -amylase; lane 4, Sd2L malt  $\beta$ -amylase.

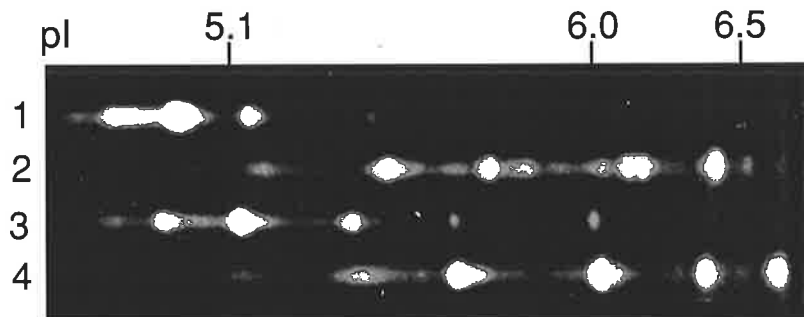


Figure 3. 2. Activity-stained IEF band patterns of purified  $\beta$ -amylase from barley grain and malt. Lane 1, Sd1 barley grain  $\beta$ -amylase; lane 2, Sd1 malt  $\beta$ -amylase; lane 3, Sd2L barley grain  $\beta$ -amylase; lane 4, Sd2L malt  $\beta$ -amylase.

### 3. 3. 2 Kinetic properties of $\beta$ -amylases

Sd1 and Sd2L  $\beta$ -amylases purified from barley grain and malt displayed typical hyperbolic kinetics with reduced potato starch (dp 740), amylose EX-III (dp 100), amylose EX-I (dp 18) and maltopentaose as substrates (Figure 3. 3). The data fitted well to the Michaelis-Menten equation. Barley grain Sd1 and Sd2L  $\beta$ -amylase had the same  $K_m$  value of 20  $\mu$ M (Table 3. 1). After germination the  $K_m$  values for malt Sd1 (4  $\mu$ M) and Sd2L (15  $\mu$ M)  $\beta$ -amylase were significantly reduced. The  $k_{cat}$  values for all four  $\beta$ -amylase forms were similar (642 to 661 U/mg) when potato starch was used as substrate. As the dp of substrates decreased from 740 to 5,  $K_m$  values increased from 4  $\mu$ M to approximately 1000  $\mu$ M, and the  $k_{cat}$  values decreased from approximately 650 to 300 U/mg. The  $K_m$  and  $k_{cat}$  values for Sd1 and Sd2L  $\beta$ -amylase from grain and malt for amylose (dp 100 and 18) and maltopentaose were not significantly different.

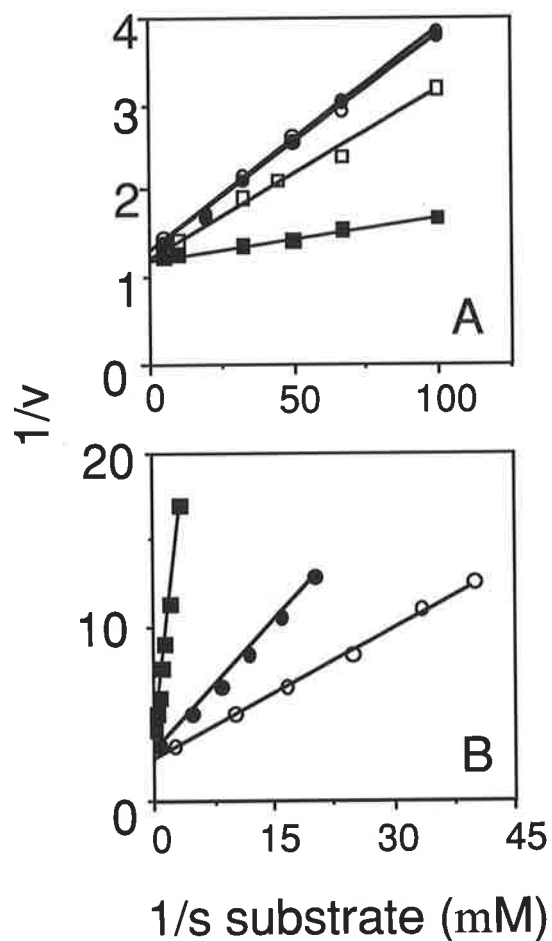


Figure 3.3. The effect of starch and amylose concentrations on barley grain and malt  $\beta$ -amylase activities. A, Activity of  $\beta$ -amylase from Sd1 barley grain (●), Sd1 malt (■), Sd2L barley grain (○), and Sd2L malt (□) were measured with starch as substrate; B, Activity of Sd1 malt  $\beta$ -amylase was measured with amylose EX-III (○), amylose EX-I (●) and maltopentaose (■) as substrates. Reaction rates ( $v$ ) are in  $\mu\text{mol}$  of product/min/ $\mu\text{g}$  of protein. Data are the mean of 3 independent determinations.



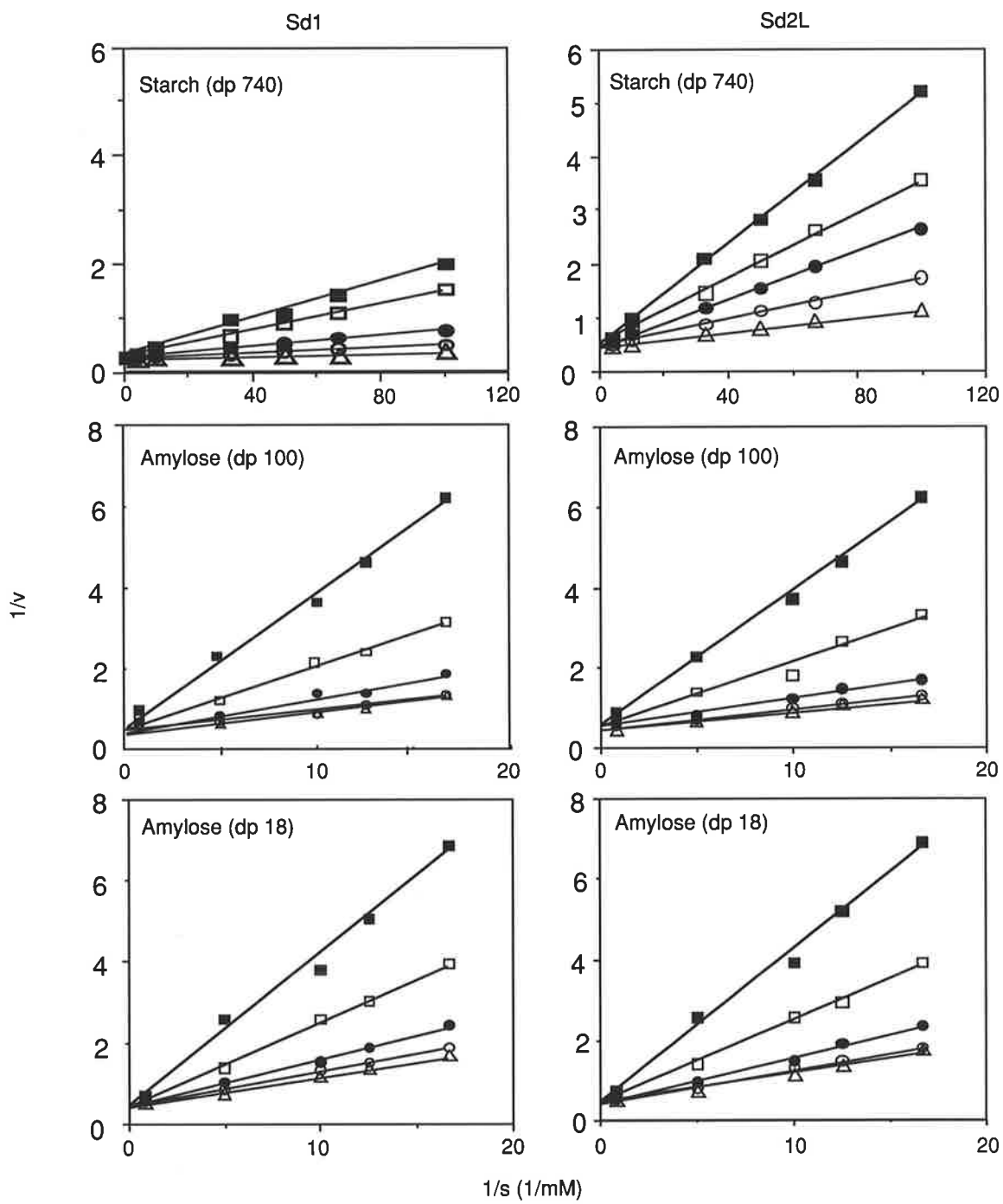


Figure 3. 4. Inhibition of  $\beta$ -amylase by maltose. The concentrations of maltose were 0 ( $\Delta$ ), 10 mM ( $\circ$ ), 50 mM ( $\bullet$ ), 100 mM ( $\square$ ), and 200 mM ( $\blacksquare$ ). Reaction rates ( $v$ ) are in  $\mu\text{mol product}/\text{min}/\mu\text{g protein}$ . Data are the mean of 2 independent determinations.

Table 3. 2. Kinetic constants for the inhibition of Sd1 and Sd2L malt  $\beta$ -amylase by maltose.

Substrates	Sd1 malt $\beta$ -amylase		Sd2L malt $\beta$ -amylase	
	$K_i$ (mM)	Type	$K_i$ (mM)	Type
Potato starch	20	Competitive	22	Competitive
Amylose EX-III	28	Competitive	30	Competitive
Amylose EX-I	29	Competitive	29	Competitive

Variations of less than 10 % from the Michaelis-Menten curve were observed in the inhibition analyses.

### 3. 3. 3 Inhibition of $\beta$ -amylase by maltose

When starch or amylose (dp 100 and 18) were varied at different fixed concentrations of maltose, a pattern of double reciprocal plots which intersected on the ordinate were observed for both Sd1 and Sd2L malt  $\beta$ -amylase (Figure 3. 4). This indicated that maltose was a weak competitive inhibitor with respect to the potato starch and amylose substrates, with  $K_i$  values between 20-30 mM (Table 3. 2). The data fitted well to the equation for competitive inhibition (Cleland 1979), and gave good estimates for the inhibition constants according to the criteria of Mannervik (1982). Although the  $K_i$

values for the Sd1 and Sd2L enzymes with the potato starch were similar, the differences in the slope of the plots reflected differences in  $K_m$  values which have been described earlier. Glucose and maltotriose were not inhibitors of malt  $\beta$ -amylase at 69 mM and 28 mM (data not shown), which are concentrations commonly found in wort (Kunze 1996).

### 3. 4 Discussion

The effect of the removal of approximately 4 kDa (45 amino acid residues) from the C-terminal end after germination on  $\beta$ -amylase function has been contentious. In addition to the release of the bound  $\beta$ -amylase fraction, Sopanen and Laurière (1989) and Guerin *et al.* (1992) suggested that this proteolytic cleavage activated the enzyme. However, Evans *et al.* (1997b) found that this further increase in  $\beta$ -amylase activity could be mainly attributed to the protease mediated release of the latent barley  $\beta$ -amylase fraction. The current study shows that malt  $\beta$ -amylase has a significantly lower  $K_m$  value than grain  $\beta$ -amylase when soluble potato starch is used as a substrate (Table 3. 1). Yoshigi *et al.* (1994a; 1995b) also showed a similar decrease in  $K_m$  for recombinant Sd2H barley  $\beta$ -amylase with 54 amino acid residues (4.9 kDa) removed from the C-terminus when compared to the full length recombinant protein (Table 3. 3).

Similar  $k_{cat}$  values for the grain and malt enzymes in this study indicate that  $\beta$ -amylase is not activated by C-terminal cleavage after germination. No different  $k_{cat}$  values were observed by Lundgard and Svensson (1987) between the four  $\beta$ -amylase forms produced

by proteolysis. Yoshigi *et al.* (1994b; 1995a) also presented similar results for the variety Haruna nijo (Sd2H). Combined, the kinetic investigations suggest that the influence of the C-terminal region on  $\beta$ -amylase activity is limited to influencing substrate binding, possibly by either modifying enzyme conformation or by reducing obstruction to starch binding.

Potato starch was a superior substrate for barley grain and malt Sd1 and Sd2L  $\beta$ -amylase, with the amylose and maltopentaose substrates exhibiting significantly lower  $k_{\text{cat}}$  and higher  $K_{\text{m}}$  values (Table 3. 1). A similar relationship for substrate preference has been observed for Sd2H barley grain and recombinant barley  $\beta$ -amylase (Yoshigi *et al.* 1994b; 1995a), and  $\beta$ -amylase from pea epicotyls (Lizotte *et al.* 1990) sweet-potato tubers (Baba and Kainuma 1987) and potato leaves (Viksø-Nielsen *et al.* 1997). The differences in substrate preference between potato starch and amylose (dp 100) may be due to the increased numbers of sites of attack for starch (Lizotte *et al.* 1990). However, this is not the case for amylose (dp 18) and maltopentaose, as these substrates only have one non-reducing end each. This suggests that the action of  $\beta$ -amylase may be influenced by substrate chain length. No significant kinetic differences were observed between mature grain and malt, or between Sd1 and Sd2L  $\beta$ -amylase for amylose (dp 100 and 18) and maltopentaose (Table 3. 1).

Sd1  $\beta$ -amylase from malt had a significantly lower  $K_{\text{m}}$  value for potato starch than that of Sd2L malt  $\beta$ -amylase (Table 3. 1), indicating that Sd1  $\beta$ -amylase has a higher affinity

for starch. Thus, under conditions where the concentration of starch becomes limiting, such as towards the end of saccharification in the mashing stage of the brewing process, Sd1  $\beta$ -amylases may be better able to hydrolyse starch, thereby improving wort fermentability. This is illustrated in Figure 3. 5, where Sd1  $\beta$ -amylase had a higher velocity than Sd2L  $\beta$ -amylase at the non-saturating 50  $\mu$ M starch concentration. The practical influence of the kinetic differences on wort quality requires further investigation to determine whether substrate specificity influences wort fermentability.

The hydrolysis of starch and amylose by Sd1 and Sd2L malt  $\beta$ -amylase was competitively, but weakly inhibited by the hydrolytic product, maltose, at concentrations less than 170 mM, which is similar to that found in wort during mashing (Kunze 1996) (Table 3. 2). Maltose has been reported to be a competitive inhibitor of  $\beta$ -amylase from pea epicotyl ( $K_i = 11.5$  mM, Lizotte *et al.* 1990), soybean ( $K_i = 5.8$  mM, Nomura *et al.* 1986) and sweet potato ( $K_i = 6$  mM, Misra and French 1960) for starch. It was also a competitive inhibitor of both Sd1 and Sd2L malt  $\beta$ -amylase with amylose (dp 100 and 18) as substrates.

Table 3. 3. Comparison of the  $K_m$  values of published barley  $\beta$ -amylase with results from the present study.

$\beta$ -Amylase	Source	Variety	$\beta$ -Amylase $K_m$ (mg/mL)		
			Soluble starch	Amylose (dp 17-18)	Malto-pentaose
Sd1 (full length) <sup>a</sup>	barley	Gula	2.5	ND	ND
Sd2H (full length) <sup>b</sup>	barley	Haruna nijo	4.33	1.09	1.69
Sd2H (full length) <sup>b</sup>	recombinant	Haruna nijo	2.53	1.35	1.41
Sd2H <sup>c</sup>	recombinant	Haruna nijo	0.917	0.79	1.04
Sd1 <sup>d</sup>	barley	Franklin	2.66	0.60	0.90
Sd1 <sup>d</sup>	malt	Franklin	0.6	0.60	0.90
Sd2L <sup>d</sup>	barley	Schooner	2.66	0.60	0.90
Sd2L <sup>d</sup>	malt	Schooner	1.99	0.60	0.90

<sup>a</sup> data from Lundgard and Svensson (1987); <sup>b</sup> data from Yoshigi *et al.* (1994b); <sup>c</sup> data from Yoshigi *et al.* (1995a); <sup>d</sup> recalculated from Table 3. 1; ND, not determined.

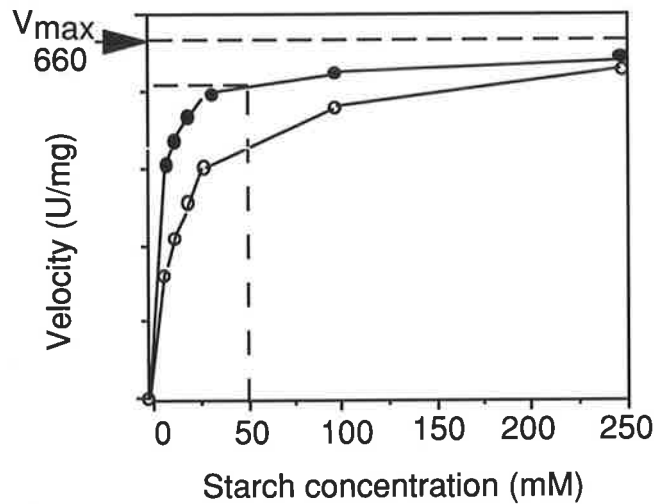


Figure 3. 5. Comparison of the effect of potato starch substrate concentrations on the velocity of hydrolysis by Sd1 (●) and Sd2L (○) malt  $\beta$ -amylase at non-saturating substrate concentrations.

The kinetic analysis in the present study has demonstrated significant differences in the affinity of two allelic forms of barley  $\beta$ -amylase for potato starch. The higher affinity of malt Sd1  $\beta$ -amylase may result in a higher yield of fermentable sugars during the mashing process. In addition, Sd1 and Sd2H  $\beta$ -amylases are more thermostable than Sd2L  $\beta$ -amylase, and have the potential to impact on fermentability (Eglinton *et al.* 1998; Kihara *et al.* 1998). Malt  $\beta$ -amylase activity was weakly and competitively inhibited by the hydrolytic product, maltose. The inhibition of  $\beta$ -amylase by maltose may also influence the production of fermentable sugars during mashing. Simulated mashing experiments are required to assess the practical impact of  $\beta$ -amylase allele  $K_m$ ,

thermostability and maltose inhibition on the production of fermentable sugars for brewing.



## Chapter 4

### **Removal of the four C-terminal glycine-rich repeats enhances thermostability and substrate binding affinity of barley $\beta$ -amylase**

---

#### **Abstract**

Barley  $\beta$ -amylase undergoes proteolytic cleavage in the C-terminal region after germination. To better understand the effect of the proteolytic cleavage on the enzyme's characteristics, recombinant barley  $\beta$ -amylases with specific deletions at the C-terminal tail were generated. The complete deletion of the four C-terminal glycine-rich repeats significantly increased the enzyme's thermostability, but an incomplete deletion with one repeat remaining did not change the thermostability. Although different C-terminal deletions affected the thermostability differently, they all increased the enzyme's affinity for starch. The possible reasons for the increased thermostability and substrate binding affinity due to the removal of the four C-terminal glycine-rich repeats are discussed in terms of the three-dimensional structure of  $\beta$ -amylase.

#### 4. 1 Introduction

Barley  $\beta$ -amylase undergoes proteolytic cleavage at the C-terminal region, and an approximately four kDa segment is cleaved from the C-terminus after germination (Lundgard and Svensson 1986; Evans *et al.* 1997a). This four kDa cleavage (unspecified site) was reported not to affect the thermostability of barley  $\beta$ -amylase, but a 54 amino acid deletion (including the entire four C-terminal glycine-rich repeats and an additional eight amino acid residues upstream of the four repeats) of a recombinant barley  $\beta$ -amylase resulted in a significant decrease in thermostability (Yoshigi *et al.* 1995a). However, the C-terminal cleavage significantly increased the substrate binding affinity, both in recombinant barley  $\beta$ -amylase (Yoshigi *et al.* 1995a) and native barley  $\beta$ -amylases (chapter 3). Moreover, soybean  $\beta$ -amylase is relatively thermostable compared with barley  $\beta$ -amylase (Yoshigi *et al.* 1995b). These two sequences share 66.7% identity (Yoshigi *et al.* 1994a). Their three dimensional structures are very similar except that soybean  $\beta$ -amylase lacks the four glycine-rich repeats (Mikami *et al.* 1999). It seems likely that the proteolytic cleavage of barley  $\beta$ -amylase at the C-terminal tail has both positive and negative effects on the properties of the enzyme. These various influences may be due to the different cleavage sites at the C-terminal tail. Lundgard and Svensson (1986; 1987) reported that the proteolytic cleavage of barley  $\beta$ -amylase is stepwise from the C-terminus, rather than specific. They isolated four major forms which terminated at A533, Q519-G528, Q508 and G493-Q497, respectively, and found that the amount of each component is dependent on the concentrations of proteases (Lundgard and Svensson 1987).

These results suggest that the degree of peptide cleavage in the C-terminal tail is dependent on cleavage conditions. Therefore, it is important for malting barley improvement to clarify how the different cleavage sites affect the characteristics of barley  $\beta$ -amylase.

Three  $\beta$ -amylase alleles, *Bmy1-Sd1*, *Bmy1-Sd2L* and *Bmy1-Sd2H*, have been identified in cultivated barley at the *Bmy1* locus on chromosome 4H (Eglinton *et al.* 1998). The corresponding enzymes exhibit differences in thermostability and are referred to as Sd1 (intermediate thermostability), Sd2L (low thermostability) and Sd2H (high thermostability), respectively. In this chapter, recombinant barley  $\beta$ -amylases with different C-terminal deletions were generated, and the effects of proteolytic cleavage on the thermostability and kinetics properties evaluated.

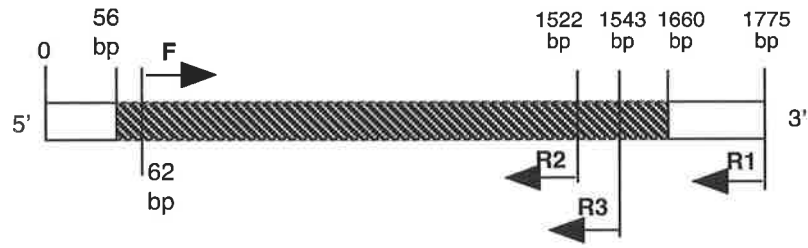
## **4. 2 Materials and methods**

### **4. 2. 1 Materials**

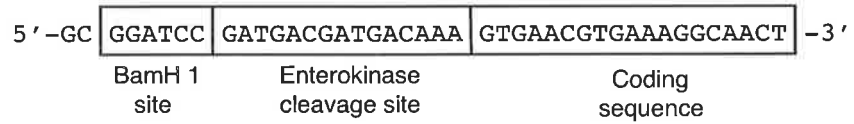
The barley varieties Franklin (Sd1) and Schooner (Sd2L) were used to clone  $\beta$ -amylase cDNAs. Developing grains were harvested 23 days after anthesis, immediately frozen in liquid nitrogen, and stored at  $-80\text{ }^{\circ}\text{C}$ . Native  $\beta$ -amylases were previously purified from barley grain and malt of Franklin and Schooner to homogeneity (chapter 3).

#### 4. 2. 2 PCR primer design

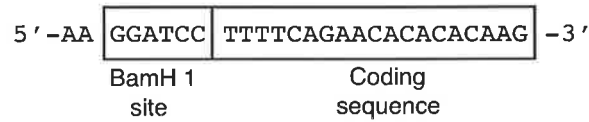
To clone  $\beta$ -amylase cDNAs with deletions at the N- and C-termini, specific forward and reverse primers were designed with the software oligo 4.0 based on the published  $\beta$ -amylase nucleotide sequence (Yoshigi *et al.* 1994a). According to the malt  $\beta$ -amylase sequence, the first two residues (M1 and E2) were removed after germination (Eglinton, unpublished data). The removal of the start codon (M) from the inserted DNA fragment is also recommended by the manufacturer (Qiagen) to prevent internal starts which will result in expressed proteins without the 6xHis tag. Thus the forward primer starts at nucleotide 62 containing 18 nucleotides in the 5' coding region of barley  $\beta$ -amylase gene, and 6 nucleotides encoding for methionine and glutamic acid were removed from the 5' end of the  $\beta$ -amylase coding region (Figure 4. 1). A BamH 1 recognition sequence (GAATCC) was added to the 5' end of the forward primer and two extra bases (GC) were added to the 5' end of the restriction site to ensure that the efficiency of the BamH 1 cleavage was maintained. A enterokinase cleavage site (GATGACGATGACAAA) was also inserted between the BamH 1 site and the N-terminus of the protein to make it possible to remove the 6xHis tag from the purified proteins. Therefore, the forward primer used in the PCR was 5'-GCGAATCCGATGACGATGACAAAAGTGAACGTGAAAGGCAACT-3'.



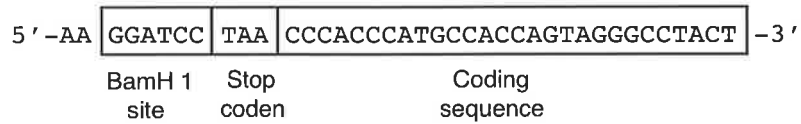
#### Forward primer (F)



#### Reverse primer 1 (R1)



#### Reverse primer 1 (R2)



#### Reverse primer 1 (R3)

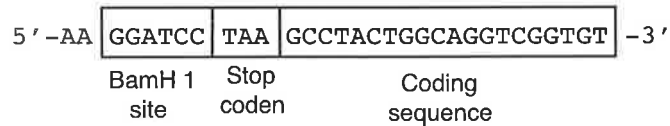


Figure 4. 1 PCR primers designed for amplification of barley  $\beta$ -amylase cDNAs with specific deletions at 5' and 3' ends.  untranslated region;  translated region.

Three reverse primers were designed to amplify PCR fragments with specific deletions at the 3' end suggested by the protein sequence of malt  $\beta$ -amylase (Eglinton, unpublished data). Reverse primer 1 (R1) located in the untranslated region nucleotides 1756 to 1775; reverse primer 2 (R2) containing 28 nucleotides terminates at 3' coding region nucleotide 1543 of barley  $\beta$ -amylase gene (corresponding to G496); reverse primer 3 (R3) containing 20 nucleotides terminates at 3' coding region nucleotide 1552 of barley  $\beta$ -amylase gene (corresponding to G489). A BamH 1 recognition sequence was also added to the 3' end of each reverse primer, following two extra bases (AA) to ensure the cleavage efficiency of restriction enzyme. A stop codon (TAA) was inserted into the reverse primers 1 and 2 between the BamH 1 site and the C-terminus of the protein to ensure expression stop. Therefore, the sequence of reverse primers 1, 2 and 3 used in the PCR were 5'-AAGGATCCCTTTTCAGAACACACAAG-3', 5'-AAGGATCCTAACCCACCCATGCCACCAGTAGGGCCTACT-3', and 5'-AAGGATCCTAAGCCTACTGGCAGGTCGGTGT-3', respectively. The organisations of the primers are shown in Figure 4. 1.

#### **4. 2. 3 Cloning and sequencing of barley $\beta$ -amylase cDNAs**

Total RNA was isolated from developing barley as described in chapter 2, section 2. 3. 3. 1 and used as a template to synthesise the first-strand cDNA. The first-strand cDNA was then used to isolate three cDNAs encoding both Sd1 and Sd2L  $\beta$ -amylases with specific deletions at both the 5' and 3' ends using the specific primers (Figure 4. 1). The forward primer and reverse primer 1 were used to generate a  $\beta$ -amylase without deletions at the C-terminus. The forward primer and

reverse primer 3 were used to generate a  $\beta$ -amylase terminating at G489. A combination of the forward primer and reverse primer 2 was also used to generate a  $\beta$ -amylase terminating at G496. PCR products were cloned into pGEM-T Easy vector as described in chapter 2, section 2.3.3.6, and DNA sequences were confirmed as described in chapter 2, section 2.3.3.10.

#### **4.2.4 Production of purified recombinant $\beta$ -amylases**

BamH 1 fragments were cut from the pGEM-T Easy vector, and sub-cloned into the expression vector pQE-30, then transformed into *E. coli* host strain M15. Cell lines containing the correct orientation of the cDNA inserts were selected for production of the recombinant  $\beta$ -amylases. The 6xHis tag was removed by enterokinase digestion to prevent potential interference in the enzyme analysis. The undigested recombinant proteins were removed by loading the digestion mixture onto a Ni-NTA column. The complete cleavage of the 6xHis-tag from the recombinant  $\beta$ -amylases was monitored with anti-His antibodies. Enterokinase was removed by size exclusion chromatography. The detailed methods used in the production of purified recombinant  $\beta$ -amylases are described in chapter 2, section 2.3.4. The irreversible thermal inactivation and kinetics of  $\beta$ -amylases were measured as described in chapter 2, sections 2.2.2.4-2.2.2.9. Protein modelling and structural analysis were performed as described in chapter 2, section 2.2.2.10.

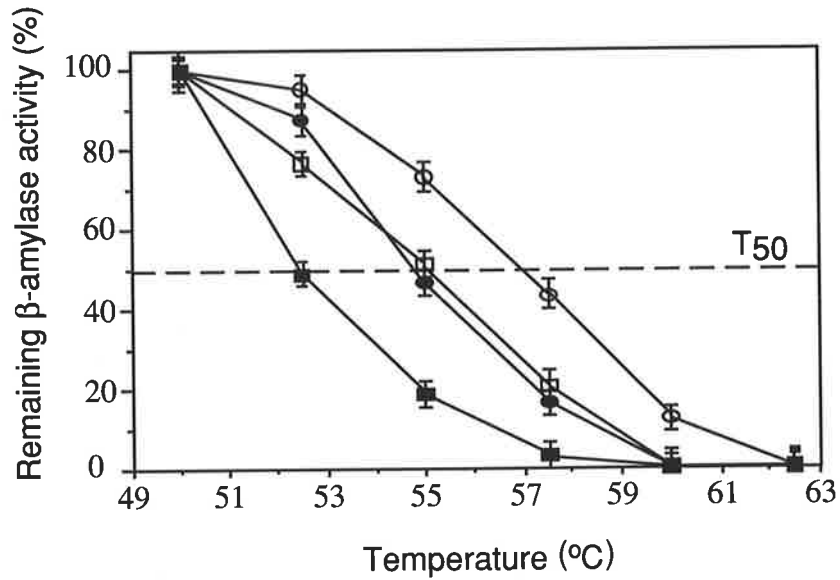


Figure 4. 2 The irreversible thermal inactivation of purified native barley  $\beta$ -amylases. Activity is expressed as a percentage of initial activity. Values are the means of three independent determinations with the standard deviations shown as bars. ○  $\beta$ -amylase from Sd1 germinated malt; ●  $\beta$ -amylase from Sd1 barley grain; □  $\beta$ -amylase from Sd2L malt; ■  $\beta$ -amylase from Sd2L barley grain.

### 4. 3 Results

#### 4. 3. 1 Thermostability of native barley $\beta$ -amylases

The thermostabilities of native barley  $\beta$ -amylases were measured by irreversible thermal inactivation curves (Figure 4. 2) which were used to determine the  $T_{50}$  values. The  $T_{50}$  values for  $\beta$ -amylases from Sd1 barley grain, Sd1 germinated barley, Sd2L barley grain and Sd2L germinated barley were 54.7, 57.0, 52.6 and 55.0 °C, respectively. Therefore,  $\beta$ -amylases from Sd1 and Sd2L malt had 2.3 °C



and 2.4 °C higher  $T_{50}$  values than those of their respective  $\beta$ -amylases from barley grain. The difference in  $T_{50}$  values between the Sd1 and Sd2L enzymes was maintained after germination.

### **Production of purified recombinant $\beta$ -amylases**

Protein sequencing of barley  $\beta$ -amylases has revealed that both the N- and the C-termini are cleaved after germination (Eglinton, unpublished data). This study showed that the first two amino acid residues were removed at the N-terminus, and that there were three cleavage sites (a major site at G489 and two additional sites at H483 and G496) and many ragged-ends at the C-terminal tail. Based on the cleavage sites, cDNA fragments with these specific deletions at the 5' and the 3'-ends were amplified from both Sd1 and Sd2L barley varieties to elucidate whether these deletions affect thermostability and kinetic properties. The cDNA fragment with the deletion at H483 was not included in the present study because the effect of a deletion at Q481 (only two residue differences from H483) on thermostability and affinity for starch has been reported previously (Yoshihi *et al.* 1995a). A fragment amplified by forward primer and reverse primer 1 began at nucleotide 62 and ended at nucleotide 1775, encoding the full length  $\beta$ -amylase without M and E at position 1 and 2 (533 amino acid residues from V3 to M535). The second fragment amplified with forward primer and reverse primer 3 was 1492 bp long, from nucleotide 62 to nucleotide 1522. This cDNA encodes the  $\beta$ -amylase containing 487 amino acid residues from V3 to G489, which is the dominant form after proteolytic cleavage. The third fragment amplified with forward primer and

reverse primer 2 was 1503 bp spanning the region from nucleotide 62 to 1543. This cDNA encodes the  $\beta$ -amylase that contains 494 amino acid residues from V3 to G496, one of the minor species that arises from proteolytic cleavage.

These cDNAs were expressed in *E. coli* as soluble and catalytically active proteins. The recombinant enzymes were designated as Sd1-M535, Sd1-G496, Sd1-G489, Sd2L-M535, Sd2L-G496, and Sd2L-G489, respectively, based on the  $\beta$ -amylase allele and the number of amino acids. Complete removal of the 6xHis tag and enterokinase cleavage site was confirmed with an immunoblot using anti-His antibody, where no bands were detected (Appendix B, Figure B6). The purified recombinant  $\beta$ -amylases are shown in Figure 4. 3.

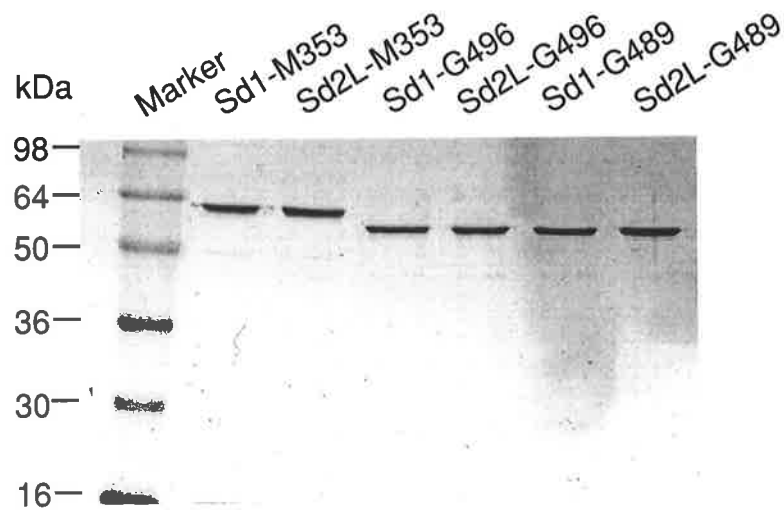


Figure 4. 3. SDS-PAGE of purified barley recombinant  $\beta$ -amylases stained with Coomassie blue R250.

### 4. 3. 3 Thermostability of recombinant $\beta$ -amylases

As shown in Figure 4. 4,  $T_{50}$  values for recombinant  $\beta$ -amylases Sd1-G489, Sd1-G496, Sd1-M535, Sd2L-G489, Sd2L-G496, Sd2L-M535 were 57.6 °C, 55.0 °C, 55.0 °C, 55.2 °C, 52.7 °C and 52.6 °C, respectively. Thus, both Sd1-G489 and Sd2L-G489 had 2.6 °C higher  $T_{50}$  values than those of Sd1-M535 and Sd2L-M535.

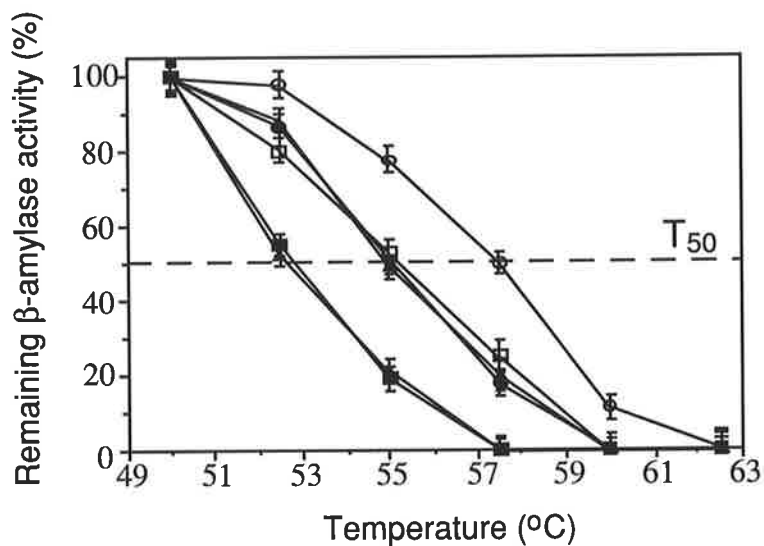


Figure 4. 4. Irreversible thermal inactivation of purified recombinant  $\beta$ -amylases.

The activities are expressed as percentages of the initial activity. Values are the means of three independent determinations with the standard deviations shown as bars. ○ Sd1-G489; △ Sd1-G496; ● Sd1-M535; □ Sd2L-G489; ▲ Sd2L-G496; ■ Sd2L-M535.

However, the  $T_{50}$  values of Sd1-G496 and Sd2L-G496 were almost the same as those of Sd1-M535 and Sd2L-M535. Comparison of Figures 4. 2 and 4. 4 shows that the  $T_{50}$  values of recombinant  $\beta$ -amylases Sd1-M535 and Sd2L-M535 were very similar to those of Sd1 and Sd2L grain  $\beta$ -amylases (54.7 °C vs 55.0°C and 52.6°C vs 52.6°C), although the first two amino acids at the N-terminus were missing in Sd1-M535 and Sd2L-M535 compared with Sd1 and Sd2L grain  $\beta$ -amylases. The thermostabilities of recombinant  $\beta$ -amylases with or without the 6xHis tag and the enterokinase recognition site (17 amino acid residues) at the N-terminus of the protein were similar (Appendix B, Table B1). The higher  $T_{50}$  value of Sd1 compared with Sd2L  $\beta$ -amylase was maintained after the deletions.

#### **4. 3. 4 Kinetic parameters of recombinant $\beta$ -amylases**

As shown in Table 4. 1, Sd1-G489 and Sd2L-G489 had lower  $K_m$  values than Sd1-M535 and Sd2L-M535. The  $K_m$  values of Sd1-G489 and Sd2L-G489 were 3.2  $\mu$ M and 8.3  $\mu$ M, respectively, compared to 16.2  $\mu$ M (Sd1-M535) and 16.0  $\mu$ M (Sd2L-M535). Sd1-G496 and Sd2L-G496 had very similar  $K_m$  values to those of Sd1-G489 and Sd2L-G489. No differences in  $k_{cat}$  values were observed among recombinant  $\beta$ -amylases.

Table 4. 1. Kinetic parameters for the hydrolysis of starch by recombinant  $\beta$ -amylases.

$\beta$ -Amylase	$K_m$ ( $\mu$ M)	$k_{cat}$ (U/mg)
Sd1-M535	$16.2 \pm 0.61$	$300 \pm 8$
Sd2L-M535	$16.0 \pm 0.84$	$300 \pm 8$
Sd1-G496	$3.4 \pm 0.18$	$310 \pm 10$
Sd2L-G496	$8.4 \pm 0.71$	$320 \pm 7$
Sd1-G489	$3.2 \pm 0.28$	$310 \pm 9$
Sd2L-G489	$8.3 \pm 0.58$	$320 \pm 6$

#### Structure of the C-terminal region of barley $\beta$ -amylase

Only Sd2L  $\beta$ -amylase was modelled since Sd1  $\beta$ -amylase shares 99.1% sequence identity with Sd2L  $\beta$ -amylase, and has the same cleavage sites at both the N- and C-termini (Eglinton, unpublished data). The modelling of Sd2L  $\beta$ -amylase was based on the solved crystal structure for BBA-7s (PDB identifier 1B1Y) (Mikami *et al.* 1999). Sd2L  $\beta$ -amylase differed from BBA-7s in only 13 amino acids, which included two amino acid substitutions (V233A and L347S), four amino acid residues missing (positions 2-5) and seven mutated amino acids in BBA-7s (M185L, S295A, I297V, S350P, S351P, Q352D, and A376S). Such high sequence homology provides a high degree of confidence in the model structure. The quality of the model was confirmed by its root-mean-square backbone deviation from that of BBA-7s with the value 0.11Å for C  $\alpha$ -atoms (Chothia and Lesk 1986).

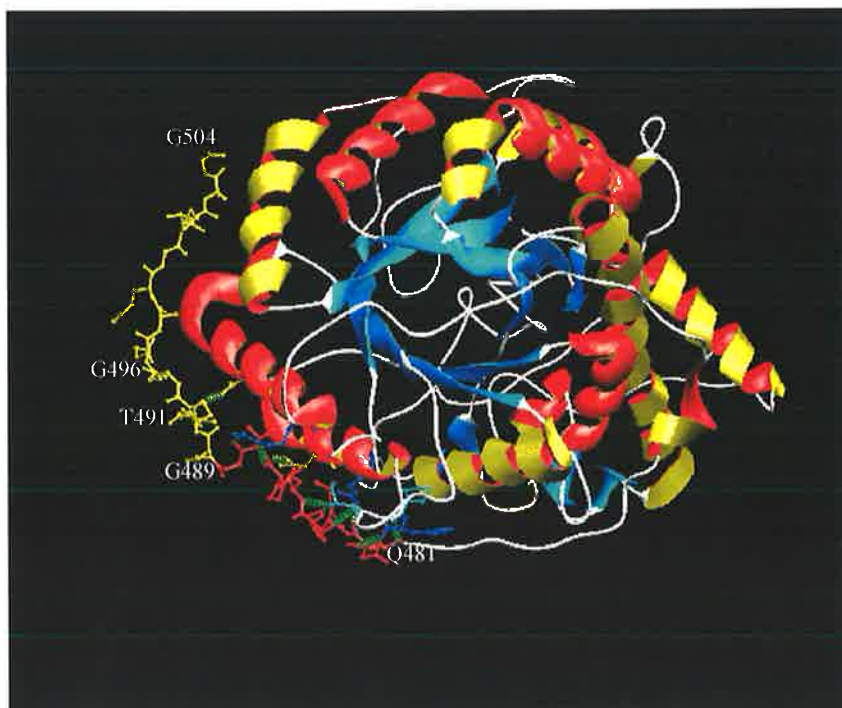


Figure 4. 5. Ribbon diagram of Sd2L  $\beta$ -amylase showing hydrogen bond interactions of the C-terminal residues between Q481-G504 with other parts of the protein. Hydrogen bonds are shown as green dotted lines. The residues from Q481 to V488 (upstream of the four C-terminal glycine-rich repeats) are coloured in red, and the residues from G489 to G504 of the four C-terminal glycine-rich repeats are coloured in yellow. The Figure was generated using the program SPDBV 3.5 (Guex and Peitsch 1997).

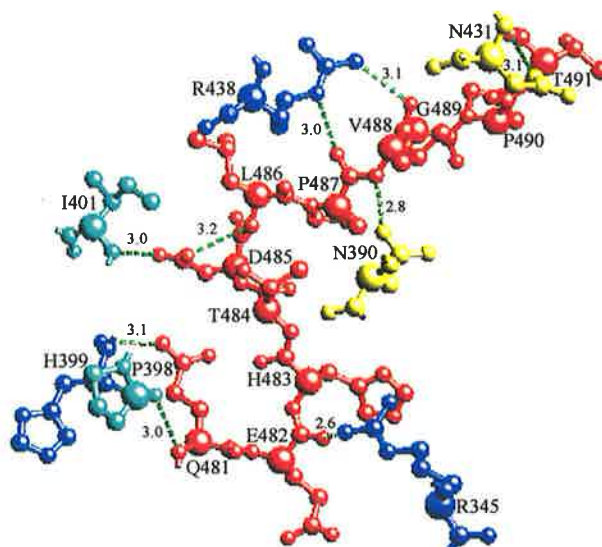


Figure 4. 6. A close-up view of the hydrogen bonds from residues between Q481-T491. Hydrogen bonds are shown as green dotted lines, and bond lengths are shown in angstroms (Å). The C-terminal residues (Q481-T491) are coloured in red. Other residues are coloured in yellow (polar residues), blue (basic residues), and light blue (non-polar residues). The Figure was generated using the program SPDBV 3.5 (Guex and Peitsch 1997).

The residues beyond G504 are absent in the model as they were not included in the structure of BBA-7s. Thus, only the first one and a half repeats (residues between G489-G504) of the four C-terminal glycine-rich repeats is visible in the model of Sd2L  $\beta$ -amylase. Figure 4. 5 presents a ribbon model of Sd2L  $\beta$ -amylase showing the hydrogen bond interactions of residues Q481-G504 with other parts of the protein. There was only one inter-chain hydrogen bond detected within the first one and half repeats (G489-G504). Upstream of the four repeats (from V488), however, more hydrogen bonds have been formed. Eight hydrogen bonds were predicted between residues Q481-V488. Of the eight, seven are inter-chain hydrogen bonds, V488 O-R438 N (3.1Å), V488 N-N390 OD1 (2.8Å), P487 O-R438 NE (3.0Å), D485 OD1-I401 N (3.0Å), E482 O-R345 NH2 (2.6Å), Q481 NE2-H399 O (3.1Å), Q481 N-P398 O (3.0Å), and one is an intra-chain hydrogen bond, D485 OD1-L486 N (3.2Å) (Figure 4. 6).

#### **4. 4 Discussion**

A significant increase in thermostability was observed from both purified Sd1 and Sd2L native  $\beta$ -amylases after proteolytic cleavage following germination (Figure 4. 2). This cleavage also increased the native enzyme's affinity for starch (chapter 3). Both N- and C-termini of barley  $\beta$ -amylases were proteolytically cleaved after germination (Eglinton, unpublished data). The removal of the first two amino acid residues (M1 and E2) at the N-terminus appeared not to be a determinant of the changes in  $\beta$ -amylase properties because no differences in the  $T_{50}$  values were observed between the native grain  $\beta$ -amylases and the recombinant  $\beta$ -amylases Sd1-M535 and Sd2L-M535 in which the first two amino acids at the N-terminus were



removed. Moreover, the thermostability and kinetic properties of the recombinant  $\beta$ -amylases with the 6xHis tag were similar to those without them, and similar to those of the native enzyme (Appendix B, Table B1).

The C-terminal deletions, however, resulted in a significant increase in the enzyme's affinity for starch. Deletions at G489 and G496 both decreased the  $K_m$  values for starch by 2-5-fold (Table 4. 1). A deletion at Q481 (two amino acid differences from H483) was also reported to decrease the  $K_m$  values for starch by 2.6-fold (7). Therefore, different deletions at the C-terminal region all act at a kinetic level by increasing the enzyme's affinity for starch. This result suggests that the removal of the C-terminal tail may create a more favorable environment for substrate binding, presumably by reducing steric hindrance in starch binding.

The C-terminal deletion also affected the thermostability of barley  $\beta$ -amylase, although different deletions had different effects. The deletion at G489 significantly increased the thermostability of the  $\beta$ -amylase, but the deletion at G496 did not change its thermostability. Yoshigi *et al.* (1995a) reported that a deletion at Q481 (upstream of the four repeats) resulted in a significant decrease in the thermostability of the enzyme. It appears, therefore, that G489 is an important proteolytic cleavage site for optimizing the thermostability of  $\beta$ -amylase. Significantly, G489 is precisely located at the beginning of the four glycine-rich repeats (Figure 1. 2). Thus, the cleavage completely removes the four C-terminal glycine-rich repeats. Soybean  $\beta$ -amylase, which has relatively higher thermostability than barley  $\beta$ -amylase (Yoshigi *et al.* 1995b), also lacks the four glycine-rich repeats. Therefore, it would be

interesting to know whether the four C-terminal glycine-rich repeats destabilize the protein.

To look for possible explanations as to why the four C-terminal glycine-rich repeats destabilise the  $\beta$ -amylase structure, Sd2L  $\beta$ -amylase was modelled using the crystal structure for BBA-7s (PDB identifier 1B1Y) (Mikami *et al.* 1999). The four glycine-rich repeats included residues G489-P532. The three-dimensional structure revealed that there is only one hydrogen bond interaction with the other part of the protein between G489-G504 in comparison with many more hydrogen bonds upstream of the four repeat region (from V488) (Figure 4. 5). This observation indicates that the first one and half repeats (G489-G504) do not form a rigid structure. For the remaining repeats, Mikami *et al.* (1999) have reported an incomplete electron density map that indicates a highly disordered main-chain structure beyond G504. Thus, the entire four C-terminal glycine-rich repeat region is an unstable and unstructured peptide chain.

The structural instability of the four C-terminal glycine-rich repeats most probably results from the high degree of chain flexibility imparted by the abundance of glycine. Glycine lacks an  $\alpha$ -carbon, thus has more backbone conformational flexibility and greater configurational entropy than other amino acid residues. Highly flexible chains cannot form defined structures (Schulz and Schirmer 1984). It has been demonstrated that an increase in the rigidity of a flexible region of a protein by replacing glycines with other residues (Hardy *et al.* 1993; Matthews *et al.* 1987) can enhance the protein's thermostability. Therefore, it is necessary to completely

remove the four glycine-rich repeats of barley  $\beta$ -amylase to reduce the chain movement of this region and stabilise the protein. Retention of even a short peptide (P490-G496) containing four glycines is sufficient to destabilise the protein.

More hydrogen bonds are present upstream of the four glycine-rich repeats which reinforce the hydrogen bond network of the region. Therefore, any deletion upstream of the four repeats, such as at Q481, would destroy the hydrogen bond network. Hydrogen bonding plays an important role in protein stability, and an increase in hydrogen bonds has been shown to be a principal determinant of the increased thermal stability of 16 families of proteins including  $(\alpha/\beta)_8$  barrel proteins (Vogt *et al.* 1997). It seems likely that the decreased thermostability of barley  $\beta$ -amylase by the deletion at Q481 (Yoshigi *et al.* 1995a) is due to the disruption of the hydrogen bonds between Q481 and V488. Therefore, an appropriate cleavage site, rather than the length of the C-terminal tail, appears to determine the thermostability of  $\beta$ -amylase.

Barley  $\beta$ -amylase is heat-labile compared with other starch-degrading enzymes. Its activity diminishes rapidly at temperatures above 55°C (Yoshigi *et al.* 1995a). During brewing, however, mashing is performed either isothermally at approximately 65 °C or using a ramped temperature profile from approximately 45 °C-70 °C. These temperatures are required for starch gelatinisation, which in turn, is necessary for rapid and complete starch degradation. The thermal instability of barley  $\beta$ -amylase reduces the efficiency of the saccharifying process in commercial

beer production. Improvement of  $\beta$ -amylase thermostability has become an important target for protein engineering (Yoshigi *et al.* 1995a; Okada *et al.* 1995). The results in this chapter demonstrate that the complete removal of all four glycine-rich repeats at the C-terminal tail significantly increases the thermostability of barley  $\beta$ -amylase. Therefore, control of barley germination conditions is worthy of further investigation to ensure the complete removal of the four glycine-rich repeats at the C-terminal tail. In addition, our results show that the Sd1  $\beta$ -amylase is more thermostable than Sd2L  $\beta$ -amylase regardless of the C-terminal deletions. The characterisation of the structural significance of amino acid substitutions between the  $\beta$ -amylase alleles may also lead to further increases in barley  $\beta$ -amylase thermostability. This work will be discussed in chapter 6.

## Chapter 5

### A single amino acid substitution that determines the IEF band pattern of barley $\beta$ -amylase

---

#### Abstract

Barley  $\beta$ -amylase exhibits two distinct band patterns after isoelectric focusing (IEF), termed Sd1 and Sd2. A comparison of the deduced amino acid sequences revealed five amino acid differences between the two types of  $\beta$ -amylase. To investigate whether the two band patterns are due to these amino acid substitutions, four Sd2L mutants (Sd2L-R115C, Sd2L-D165E, Sd2L-L347S and Sd2L-V430A) were constructed by site-directed mutagenesis. The analysis of IEF band patterns of mutant and wild-type  $\beta$ -amylases revealed that only the replacement of R115 with cysteine converted the Sd2 band pattern to the Sd1 one. The contribution of the R115C substitution to the IEF band pattern of barley  $\beta$ -amylase was further confirmed by generating a Sd1 mutant (Sd1-C115R), where cysteine at this position was in turn replaced by arginine. As a result of this mutation, the Sd1 band pattern was converted into the Sd2 pattern. Calculation of the electrostatic potential and reducing agent treatment revealed that the R115C substitution altered both the net charge on the protein surface and intermolecular disulfide bond interactions, thereby altering the IEF band pattern of barley  $\beta$ -amylase.

## 5.1 Introduction

Barley  $\beta$ -amylase is highly heterogeneous and exists in a number of isoforms with different isoelectric points (pI) in the range of 5-7 (Visuri and Nummi 1972; Evans *et al.* 1997a). In spite of the multiple isoforms, only two distinct band patterns have been identified in cultivated barley, termed Sd1 and Sd2 (Allison 1973; Allison and Swanston 1974; Eglinton and Evans 1996; Evans *et al.* 1997a). Both Sd2L and Sd2H  $\beta$ -amylases exhibit identical Sd2 band patterns (Eglinton and Evans 1996; Evans *et al.* 1997a). The band patterns of Sd1 and Sd2  $\beta$ -amylases remain distinct after germination during which approximately 4 kDa peptide is cleaved from the C-terminus (Lundgard and Svensson 1986), although both enzymes become more basic (Evans *et al.* 1997a).

Sd1 and Sd2  $\beta$ -amylases exhibit different expression levels (Erkkilä *et al.* 1998), thermostability (Eglinton *et al.* 1998; Kihara *et al.* 1998; 1999) and kinetic properties (chapter 3). The band patterns have also been closely associated with malting quality, and it has been suggested that they could be used as a biochemical marker to predict malting quality in barley breeding programs (Swanston 1980; Swanston 1983; Evans *et al.* 1997a). However, the explanation for the two distinct IEF band patterns and their molecular basis has puzzled  $\beta$ -amylase investigators for more than 30 years (Allison 1973; Allison and Swanston 1974; Swanston 1980; Swanston 1983; Evans *et al.* 1997a). An understanding of the biochemical and molecular mechanisms underlying the different band patterns of barley  $\beta$ -amylase will be useful in effectively utilising IEF band pattern as a selection tool in barley breeding programs.



It is known that the two band patterns are the result of two co-dominant alleles at the *Bmy1* locus on chromosome 4H (Allison 1973; Allison and Swanston 1974; Li 1997). To understand the mechanisms controlling the IEF band patterns of barley  $\beta$ -amylase, Sd1 and Sd2L  $\beta$ -amylase cDNAs were cloned, and the contributions of amino acid substitutions between Sd1 and Sd2 barley  $\beta$ -amylase to the two distinct band patterns were evaluated by site-directed mutagenesis. This chapter describes how the two distinct  $\beta$ -amylase band patterns in cultivated barley are due to one single amino acid substitution at position 115.

## **5. 2 Materials and methods**

### **5. 2. 1 Materials**

cDNAs encoding full length Sd1 and Sd2L  $\beta$ -amylases were cloned and sequenced as described as in chapter 4. The GenBank-EMBL-DDBJ accession number of Sd2L  $\beta$ -amylase cDNA is AF300799, and that of Sd1 is AF300800. Purified recombinant Sd1 and Sd2L barley  $\beta$ -amylases with a 46 amino acid deletion at the C-terminal tail (terminating at G489) were also generated as described in chapter 4.

### **5. 2. 2 Site-directed mutagenesis**

The expression plasmids containing the proteolytically cleaved (terminating G489) Sd1 and Sd2L  $\beta$ -amylase cDNAs were constructed as described in chapter 4, and used for site-directed mutagenesis since enzyme analyses are mainly carried out on malted barley.

Site-directed mutagenesis of  $\beta$ -amylase cDNA was performed using a QuikChange site-directed mutagenesis kit as described in chapter 2, section 2. 2. 5. A total of five mutagenic primers (Table 5. 1) were used to obtain five single-mutants (one from Sd1, and four from Sd2  $\beta$ -amylase). Each mutant was obtained using a 5' sense primer and a 3' complementary primer containing the desired mutation. For example, the Sd2 mutant at position 115 was obtained using a 5' sense primer (5'-GGGTGCGGGACGTTCGGCACGTGTGATCCCGACATTTTCTACACCG-3') and a 3' complementary primer corresponding to nucleotides 378-422 of barley  $\beta$ -amylase with a codon (CGT) for arginine to codon (TGT) for cysteine substitution at nucleotide 398. Similarly, the Sd1 mutant at the same position was obtained using a 5' sense primer (5'-GGGTGCGGGACGTTCGGCACGCGTGATCCCGACATTTTCTACACCG-3') and a 3' complementary primer with a codon (TGT) for cysteine to codon (CGT) for arginine substitution at nucleotide 398, and so on. Each mutant was sequenced to confirm that only the desired mutation occurred during the manipulations. The mutants were denoted using the one-letter code with the wild-type residue given first, followed by the position number, and then the new residue. For example, the Sd1 mutant, in which C115 in Sd1  $\beta$ -amylase is replaced with arginine, is referred to as Sd1-C115R.

All of the mutant plasmids were expressed. Recombinant proteins were purified and the 6xHis-tag was removed as described in chapter 4.



Table 5. 1. Oligonucleotides prepared for site-directed mutagenesis

Mutant	Sequence	Position (bp)	Mutation
R115C	5' -GGGTGCGGGACGTCGGCACGtGTGATCCCGACATTTCTACACCG-3'	378-422	CGT→TGT
C115R	5' -GGGTGCGGGACGTCGGCACGcGTGATCCCGACATTTCTACACCG-3'	378-422	TGT→CGT
D165E	5' -GCTTCAGGGAGAACATGAAAGAgTTCTTGGATGCTGG-3'	528-564	GAC→GAG
L347S	5' -CGGAGATGAGGGATTcGGAGCAAAGCTCGC-3'	1080-1109	TTG→TCG
V430A	5' -GGTGGAGGGACAAAACATATGcCAATTTCAAGACCTTGTGTCG-3'	1324-1364	GTC→GCC

The target nucleotides are indicated in lower case. The position of oligonucleotides is numbered according to the  $\beta$ -amylase sequence in reference (Yoshigi *et al.* 1994a).

### 5. 2. 3 Electrophoresis

SDS-PAGE was performed as described in chapter 2, section 2. 2. 2. 1, and IEF was performed as described in chapter 2, section 2. 2. 2. 3.

### 5. 2. 4 Electrostatic calculations

Electrostatic potential maps of the protein surface were obtained by running the GRASP program (Nicholls *et al.* 1991) on a Silicon Graphics Iris Indigo Elan 4000 workstation. The electrostatic potential was calculated using the following parameters: dielectric constant of the protein, 2.0; solvent dielectric constant, 80.0; solvent ionic strength, 150 mM. Only charged residues were taken into account.

### 5. 3 Results

#### 5. 3. 1 IEF band patterns of native Sd1 and Sd2 $\beta$ -amylases

Native Sd1 and Sd2  $\beta$ -amylases gave two distinct IEF band patterns, although both patterns primarily contained four major activity bands (Figure 5. 1). The first difference in banding pattern was that the bands of Sd2  $\beta$ -amylase were more basic than those of Sd1  $\beta$ -amylase. The bands of Sd2  $\beta$ -amylase were at pI 5.65, 6.0, 6.3 and 6.7, while those of Sd1  $\beta$ -amylase were at pI 5.45, 5.70, 6.1 and 6.30. Secondly, Sd1  $\beta$ -amylase had one more band than Sd2  $\beta$ -amylase. The second most basic band of Sd1  $\beta$ -amylase (pI 6.1) was a doublet band, but that of Sd2 (pI 6.3) was a single band.

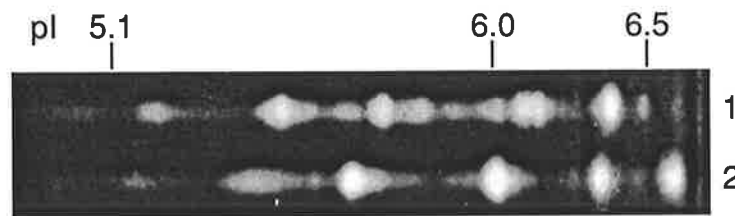


Figure 5. 1. Activity stained IEF of  $\beta$ -amylases purified from malt. Lane 1, Sd1  $\beta$ -amylase; lane 2, Sd2  $\beta$ -amylase.

#### 5. 3. 2 IEF band patterns of recombinant Sd1 and Sd2 $\beta$ -amylases

Recombinant  $\beta$ -amylases exhibited fewer bands than native  $\beta$ -amylases (Fig 5. 2). The three more acidic bands, which existed in native  $\beta$ -amylases, disappeared in both Sd1 and Sd2 recombinant  $\beta$ -amylases. Nevertheless, the IEF band patterns of Sd1

and Sd2  $\beta$ -amylases were still distinct in the recombinant  $\beta$ -amylases. Sd1  $\beta$ -amylase had two bands, while the Sd2  $\beta$ -amylase contained only a single band. In addition, the Sd2  $\beta$ -amylase band was more basic (pI 6.7) than either of the Sd1  $\beta$ -amylase bands (pI 6.1 and 6.3).



Figure 5. 2. Activity stained IEF of purified recombinant malt-type  $\beta$ -amylases. Lane 1, Sd1  $\beta$ -amylase; lane 2, Sd2  $\beta$ -amylase.

### 5. 3. 3 Production of mutant $\beta$ -amylases

The amino acid substitutions of Sd1 and Sd2L  $\beta$ -amylases are listed in Table 5. 2. There are 5 amino acid substitutions at positions 115, 165, 347, 430 and 527. Using the proteolytically cleaved Sd2L  $\beta$ -amylase cDNA as a template, codons CGT for arginine at position 115, GAC for aspartic acid at position 165, TTG for leucine at position 347 and GTC for valine at position 430 were replaced by the corresponding codons TGT for cysteine, GAG for glutamic acid, TCG for serine and GCC for alanine found in Sd1  $\beta$ -amylase, respectively. Thus, four single Sd2L mutants (Sd2L-R115C, Sd2L-D165E, Sd2L-L347S and Sd2L-V430A) were constructed to evaluate the contributions of these amino acid substitutions to the two band patterns.

Moreover, a Sd1 mutant (Sd1-C115R) was also generated by replacing cysteine at position 115 in Sd1  $\beta$ -amylase with arginine. The structure of the 5 mutant constructions are shown in Figure 5. 3.

Table 5. 2 Amino acid substitutions of Sd1 and Sd2L barley  $\beta$ -amylases

Variety	Allele	IEF Pattern	Position				
			115	165	347	430	527
Franklin	<i>Bmy1</i> -Sd1	Sd1	C	E	S	A	M
Schooner	<i>Bmy1</i> -Sd2L	Sd2	R	D	L	V	I

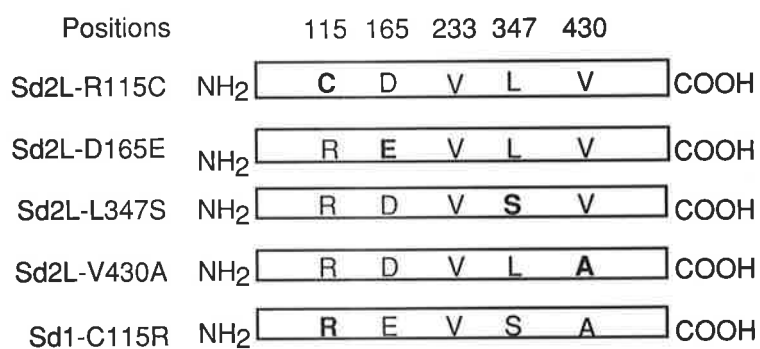


Figure 5. 3. Barley  $\beta$ -amylase mutants. Mutated residues are in bold.

After confirming the amino acid substitutions of each mutant by DNA sequencing, the mutant plasmids were expressed in *E. coli* as active and soluble enzymes. The recombinant proteins were purified to homogeneity, exhibited one single band of 56 kDa (Figure 5. 4), and the 6xHis-tag was removed.

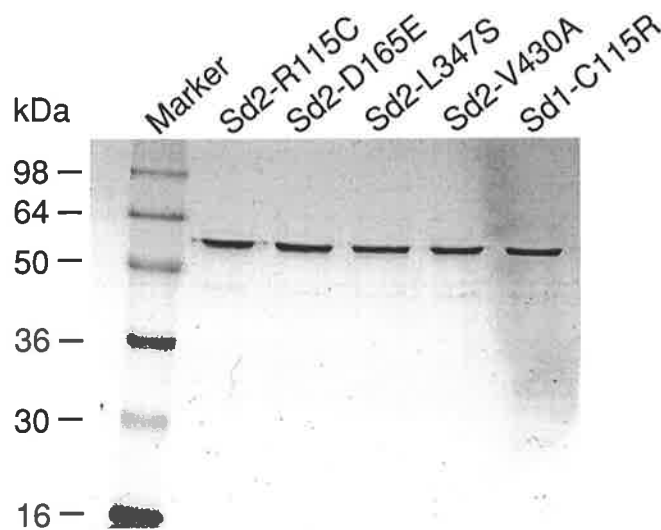


Figure 5. 4. SDS-PAGE (12 %) of the purified mutant  $\beta$ -amylases. Molecular weight marker proteins were simultaneously electrophoresed. The gel was stained with Coomassie brilliant blue R250.

#### 5. 3. 4 IEF band patterns of mutant $\beta$ -amylases

The IEF band patterns of the purified mutant enzymes were examined (Figure 5. 5). Among the four Sd2L mutants, only the Sd2L-R115C mutant band pattern was converted into that of Sd1 (Figure 5. 5, lane 1). All of the other three Sd2L mutants

retained the Sd2 band pattern (Figure 5. 5, lane 2-4). Conversely, in the Sd1 mutant (Sd1-C115R), in which C115 was replaced by arginine, the Sd1 band pattern was converted into the Sd2 pattern (Figure 5. 5, lane 5).

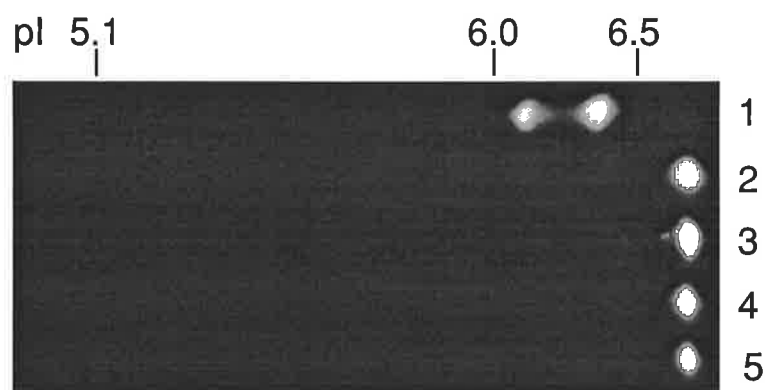


Figure 5. 5. Activity stained IEF of purified mutant  $\beta$ -amylases. lane 1, Sd2L-R115C; lane 2, Sd2L-D165E; lane 3, Sd2L-L347S; lane 4, Sd2L-V430A; lane 5, Sd1-C115R.

### 5. 3. 5 IEF band patterns of recombinant $\beta$ -amylases in the presence of reducing agents

The recombinant Sd1  $\beta$ -amylase exhibited two bands on IEF gels, whereas Sd2  $\beta$ -amylase had only a single band (Figure 5. 2). When R115 in Sd2L  $\beta$ -amylase was replaced with cysteine, the Sd2L-R115C mutant also gave two bands (Figure 5. 5, lane 1). However, the more acidic band of both the Sd1 and Sd2L-R115C mutant  $\beta$ -amylases disappeared when reducing agents were present (Figure 5. 6), whereas the Sd2 and other mutant  $\beta$ -amylases retained the same band pattern as those without reducing agents (data not shown).



Figure 5. 6. Activity stained IEF of recombinant  $\beta$ -amylases in the presence of reducing agent. Lane 1, recombinant Sd1  $\beta$ -amylase with 143 mM  $\beta$ -ME; lane 2, Sd2L-R115C mutant with 143 mM  $\beta$ -ME.

### 5. 3. 6 Electrostatic potential of mutant and wild type $\beta$ -amylases

The electrostatic potentials of the mutant and wild type barley  $\beta$ -amylase proteins were calculated at the level of the solvent-accessible surface (Figure 5. 7). The calculations illustrated that there is a positively charged area (colored blue) on the surface of the Sd2L  $\beta$ -amylase at position 115 (Figure 5. 7b). When the positively charged arginine in Sd2L  $\beta$ -amylase was replaced with cysteine, this positively charged area was extinguished (Figure 5. 7d). Moreover, the surface of the Sd1  $\beta$ -amylase lacked the positively charged area (Figure 5. 7a), which was present in the Sd2L  $\beta$ -amylase. Replacement of C115 with arginine resulted in the generation of the positively charged area around this position (Figure 5. 7c).

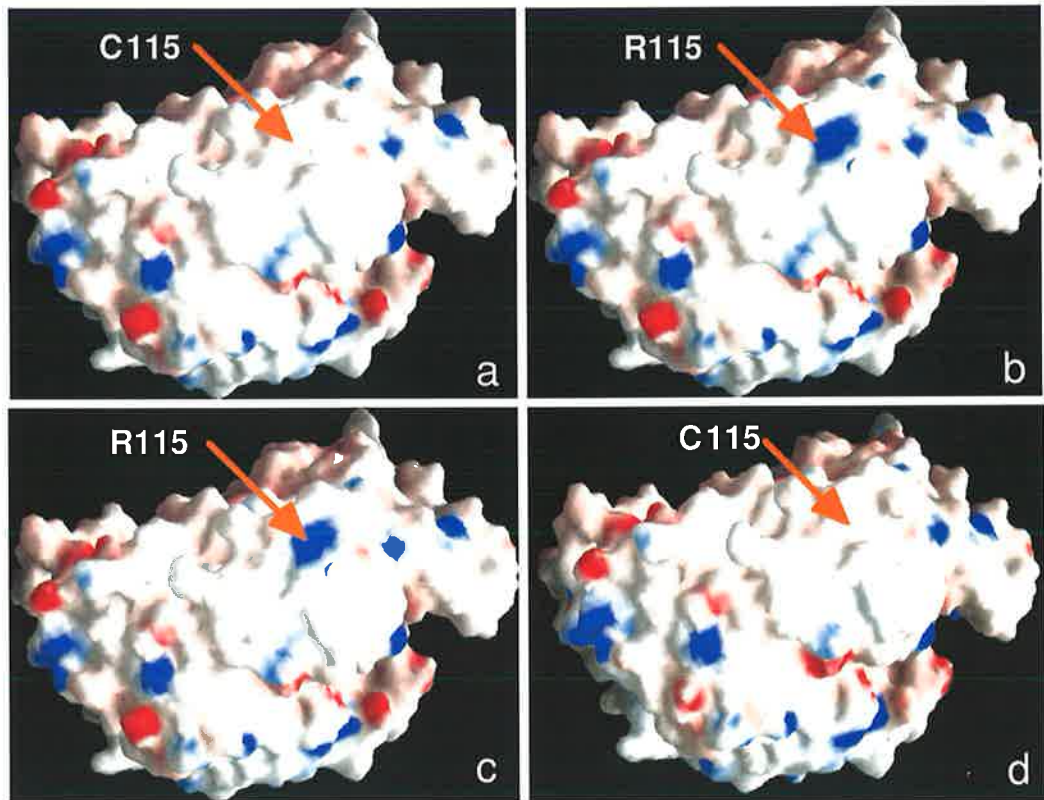


Figure 5. 7. Molecular surfaces of wild-type and mutant barley  $\beta$ -amylases illustrating the electrostatic potential of Sd1(a), Sd2L (b), Sd1-C115R (c) and Sd2L-R115C (d). Positively charged regions are coloured in blue and negatively charged regions are coloured in red. Position 115 is labelled. The figure was generated using GRASP program (Nicholls 1991).



#### 5. 4 Discussion

Although barley  $\beta$ -amylase has multiple bands on IEF gels, only two distinct band patterns have been identified in cultivated barley, termed Sd1 and Sd2 (Allison 1973; Allison and Swanston 1974; Evans *et al.* 1997a). Because Sd2L and Sd2H  $\beta$ -amylases exhibit the same IEF band patterns, only Sd2L  $\beta$ -amylase was used to represent Sd2  $\beta$ -amylase. Based on the comparison of the deduced protein sequences of Sd1 and Sd2L  $\beta$ -amylases, there are five amino acid substitutions at positions 115, 165, 347, 430 and 527 (Table 5. 2). The substitution at 527 is not responsible for the observed differences in the IEF band patterns of Sd1 and Sd2  $\beta$ -amylases, because this residue, lying within the C-terminal tail, is proteolytically cleaved after germination, and the two distinct band patterns of Sd1 and Sd2  $\beta$ -amylases are maintained after the cleavage (Evans *et al.* 1997a).

To define the mechanisms controlling the two distinct band patterns, the four amino acid residues R115, D165, L347 and V430 in Sd2L  $\beta$ -amylase were individually replaced by the corresponding ones found in Sd1  $\beta$ -amylase to construct four Sd2L mutants (Sd2L-R115C, Sd2L-D165E, Sd2L-L347S and Sd2L-V430A). A comparison of IEF band patterns of the mutant and the wild-type proteins showed that only the R115C mutant converted the Sd2 band pattern into the Sd1 band pattern. All of the other mutants retained the same IEF band pattern as the wild-type. The contribution of this single substitution to the  $\beta$ -amylase band pattern was further demonstrated by the Sd1 mutant (Sd1-C115R) in which the Sd1 band pattern was converted into the Sd2 one. This conversion demonstrated that the two distinct IEF

band patterns of barley  $\beta$ -amylase resulted from a single amino acid substitution at position 115, at which arginine is present in all Sd2  $\beta$ -amylases sequenced, but replaced by cysteine in Sd1  $\beta$ -amylase (Erkkilä *et al.* 1998; Kreis *et al.* 1987; Yoshigi *et al.* 1994a).

The basis for the effect of the R115C substitution on the IEF band pattern was assessed by calculating the electrostatic potential on the surface of mutant and wild-type  $\beta$ -amylases. The electrostatic potential maps show that there was a positively charged area in Sd2L  $\beta$ -amylase at position 115 where there is an arginine residue, but not in Sd1  $\beta$ -amylase where a cysteine residue at this position. When R115 in Sd2L  $\beta$ -amylase was substituted by cysteine, the positively charged area disappeared, whilst substitution of arginine at C115 in Sd1  $\beta$ -amylase caused the generation of a positively charged area. These observations indicate that the distribution of surface charges differ between the Sd1 and Sd2  $\beta$ -amylases, which is consistent with the lower pI value for Sd1 than that of Sd2  $\beta$ -amylase. Therefore, the more basic IEF band pattern of Sd2  $\beta$ -amylase resulted from the positively charged arginine residue, and the R115C mutation altered the electrostatic potential on the molecular surface resulting in a change in the pI values of  $\beta$ -amylase.

In addition to the lower pI values, Sd1  $\beta$ -amylase gave one more band than Sd2  $\beta$ -amylase on an IEF gel (Figures 5. 1 and 5. 2). This extra band, however, disappeared when reducing agents were present both in wild-type Sd1  $\beta$ -amylase and the Sd2L-

R115C mutant (Figure 5. 6), indicating that this band is an aggregate of Sd2  $\beta$ -amylase monomers connected by disulfide bridges. Niku-Paavola *et al.* (1973) have also reported that the purified Sd1  $\beta$ -amylase (from the barley variety Pirkka) monomer can easily polymerise when reducing agents are not present. Therefore, the additional band in Sd1  $\beta$ -amylase is apparently due to the cysteine residue at position 115 which can form an intermolecular disulfide bond. These results also suggest that polymerisation from monomeric forms might be one of the reasons for the occurrence of the multiple forms of barley  $\beta$ -amylase. Recombinant  $\beta$ -amylases had fewer bands on an IEF gel than the native  $\beta$ -amylase (Figure 5. 1 and 5. 2). This is most likely because the native  $\beta$ -amylases were a mixture of multiple forms with ragged-ends at the C-terminus as a result of proteolysis after germination (Lundgard and Svensson 1987), whereas the recombinant  $\beta$ -amylases were a single component with one specific C-terminal end at G489 (chapter 4). Therefore, proteolysis may be another reason for the occurrence of the multiple isoforms of barley  $\beta$ -amylase.

The results in this chapter have demonstrated that a single R115C substitution is responsible for the two distinct IEF band patterns of barley  $\beta$ -amylase. This single mutation results in a shift in the electrostatic potential on the protein surface and a modification of intermolecular interactions with disulfide bonds, consequently changing the IEF band pattern. In addition, this substitution results in a change in the enzyme's affinity for starch (chapter 6), indicating that there are associations between the IEF band pattern and the properties of barley  $\beta$ -amylase. IEF band patterns of barley  $\beta$ -amylases have been associated with malting quality, and it has been

suggested that they could be used as biochemical markers to predict malting quality in barley breeding programs (Swanston 1980; Swanston 1983; Evans *et al.* 1997a). To select for malting quality in barley breeding programs have traditionally relied on the measurement of standard malt quality parameters. This is a slow and laborious process, in which the results vary with the environmental conditions. IEF band pattern of  $\beta$ -amylase provides an option for a more precise approach to select for specific  $\beta$ -amylase alleles that are important to malting quality.

## Chapter 6

### The amino acid substitutions of barley $\beta$ -amylase

#### that improve the thermostability and substrate-binding affinity

---

##### Abstract

Three allelic forms of barley  $\beta$ -amylase (Sd1, Sd2H and Sd2L) exhibit different thermostability and kinetic properties. These differences are critical in influencing the malting quality of barley varieties. To understand the molecular basis for the different properties of these three allelic forms, the effects of amino acid substitutions between them were evaluated by site-directed mutagenesis. Results showed that a R115C mutation is responsible for the difference in kinetic properties. Based on the model of Sd2L  $\beta$ -amylase, this substitution resulted in an additional hydrogen bond to V112 which may create a more favourable environment for substrate binding. The different thermostability of  $\beta$ -amylase forms was due to two amino acid substitutions (V233A and L347S), which increased the enzyme's thermostability index  $T_{50}$  by 1.9 °C and 2.1 °C, respectively. The two mutations may increase the thermostability of the enzyme by relieving steric strains and increasing the interaction of the protein surface with solvent water. Although both the V233A and L347S mutations increased the enzyme thermostability, they affected the thermostability in different ways. The replacement of L347 with serine seems to increase the thermostability by slowing the thermal unfolding of the protein during heating, while the mutation of V233 to alanine appears to cause an acceleration of the refolding after heating. Because the different  $\beta$ -amylase properties determined by the three mutations (R115C, V233A and L347S) are associated with barley malting

quality, a mutant with high thermostability and substrate-binding affinity was generated by combining the three preferred amino acid residues C115, A233 and S347. A possible approach to producing better malting quality barley varieties by genetic engineering is discussed.

## 6. 1 Introduction

Three  $\beta$ -amylase alleles, termed *Bmy1*-Sd1, *Bmy1*-Sd2L and *Bmy1*-Sd2H, have been identified at the *Bmy1* locus on chromosome 4H among cultivated barleys. The corresponding enzymes are referred to as Sd2L, Sd1 and Sd2H, and possess low, intermediate, and high thermostabilities, respectively (Eglinton *et al.* 1998). Sd1  $\beta$ -amylase also exhibits a higher affinity for starch than Sd2L  $\beta$ -amylase (chapter 3). These different properties of  $\beta$ -amylases have a significant effect on fermentability (Eglinton *et al.* 1998; Kihara *et al.* 1998; 1999). These results indicate that genetic variation in barley  $\beta$ -amylases directly influences barley malting quality, and an understanding of the molecular basis for the genetic variation may identify strategies to improve the enzyme's properties and, in turn, to enhance the production of fermentable sugars for brewing. Kaneko *et al.* (2000) suggested that the thermostability of  $\beta$ -amylase is determined by amino acid substitutions in the  $\beta$ -amylase gene. To identify which amino acid substitutions are responsible for the different properties of allelic  $\beta$ -amylase forms, Sd1  $\beta$ -amylase cDNA has been cloned, and the contributions of amino acid substitutions between different allelic  $\beta$ -amylase forms have been evaluated by site-directed mutagenesis. This chapter reports on the role of amino acid substitutions at positions 115, 233 and 347 on the observed variations in thermostability and kinetic properties among the three allelic barley  $\beta$ -amylases.

## **6. 2 Materials and methods**

### **6. 2. 1 Sequence alignment of barley $\beta$ -amylases**

Two Sd2L  $\beta$ -amylase sequences from the barley varieties Adorra (Erkkilä *et al.* 1999) and Hiproly (Kreis *et al.* 1987), a Sd2H  $\beta$ -amylase sequence from the barley variety Haruna Nijo (Yoshigi *et al.* 1994a), and a  $\beta$ -amylase sequence from a wild barley *Hordeum vulgare subsp. spontaneum* NPGS PI29689 (abbreviated to *H. spontaneum*) (Erkkilä *et al.* 1999) were obtained from GeneBank databases (the accession numbers are AF061203, X52321, D21349 and AF061204, respectively). Sd1 and Sd2L  $\beta$ -amylases sequenced in chapter 4 were aligned with the four published barley  $\beta$ -amylases using the multiple sequence alignment program Pileup (The Australian National Genomic Information Service-ANGIS).

### **6. 2. 2 Site-directed mutagenesis**

A total of six single mutants (five from Sd2L, and one from Sd1  $\beta$ -amylase) were generated. Four of the five Sd2L single mutants (R115C, D165E, L347S and V430A) were described in chapter 5. Similarly, both Sd2L and Sd1 mutants at position 233 were obtained using a 5' sense primer (5'-GGGAATTCCTAACGATGCCGGACAGTACAATGACACTCCCG-3' or 5'-GGGAATTCCTAACGATGTCGGACAGTACAATGACACTCCCG-3') and a 3' complementary primer corresponding to nucleotides 735-776 of barley  $\beta$ -amylase with codon (GTC) for valine substituted to codon (GCC) for alanine at nucleotide 754. Sd2L-L347S was further mutated to produce a double mutation at positions 233



and 347. Each mutant was sequenced to confirm that only the desired mutation occurred during the manipulations and denoted as described in chapter 5.

### **6. 2. 3 Production of mutant $\beta$ -amylases**

All of the mutant plasmids were expressed, the recombinant proteins were purified as described in chapter 2, section 2. 2. 4, the irreversible thermal inactivation and kinetics of the mutant  $\beta$ -amylases were measured as described in chapter 2, sections 2. 2. 2. 4-2. 2. 2. 9, and protein modelling and structural analyses were performed as described in chapter 2, section 2. 2. 2. 10.

## **6. 3 Results**

### **6. 3. 1 Sequence comparison of three allelic barley $\beta$ -amylases**

Amino acid substitutions among the three allelic barley  $\beta$ -amylase forms are listed in Table 6. 1. The sequence of Sd2L  $\beta$ -amylase from the variety Schooner revealed that it was completely identical with the Sd2L  $\beta$ -amylase from variety Hiproly (Kreis *et al.* 1987) which had a single amino acid substitution at position 527 relative to the Sd2L  $\beta$ -amylase from variety Adorra (Erkkilä *et al.* 1999). The major sequence differences among the three *Bmy1* alleles were limited to the *Bmy1*-Sd1 allele which showed five amino acid differences from *Bmy1*-Sd2L  $\beta$ -amylase (positions 115, 165, 347, 430 and 527) and four amino acid differences from *Bmy1*-Sd2H  $\beta$ -amylase (positions 115, 165, 233 and 430). The Sd2L and Sd2H sequences exhibited three amino acid substitutions at positions 233, 347 and 527. The *Bmy1* allele of a wild

barley *H. spontaneum* (Erkkilä *et al.* 1999) had a sequence that was identical to the *Bmy1*-Sd2H allele from Haruna nijo (Yoshigi *et al.* 1994a).

Table 1. Amino acid substitutions of the barley  $\beta$ -amylase allelic forms

Variety	Alleles	Positions					
		115	165	233	347	430	527
Franklin	<i>Bmy1</i> -Sd1	C	E	V	S	A	M
Schooner	<i>Bmy1</i> -Sd2L	R	D	V	L	V	I
Hiproly <sup>1</sup>	<i>Bmy1</i> -Sd2L	R	D	V	L	V	I
Adorra <sup>2</sup>	<i>Bmy1</i> -Sd2L	R	D	V	L	V	M
Haruna nijo <sup>3</sup>	<i>Bmy1</i> -Sd2H	R	D	A	S	V	M
<i>H. spontaneum</i> <sup>2</sup>	<i>Bmy1</i> -Sd2H	R	D	A	S	V	M

<sup>1</sup> Kreis *et al.* 1987; <sup>2</sup> Erkkilä *et al.* 1998; <sup>3</sup> Yoshigi *et al.* 1994a

### 6. 3. 2 Production of mutant $\beta$ -amylases

In addition to the four Sd2L single mutants (R115C, D165E, L347S and V430A) described in Figure 5. 3 of chapter 5, another Sd2L single mutant (V233A) was generated by replacing the codon GTC for valine at position 233 of Sd2L  $\beta$ -amylase with the codon GCC for alanine that was found in Sd2H  $\beta$ -amylase, since the Sd2L and Sd1  $\beta$ -amylases had the same sequence at this position (Table 6. 1). A Sd2L double mutant (Sd2L-V233A/L347S) was also generated by further replacing V233 of mutant Sd2L-L347S with alanine. Thus, the resultant mutant had the exact same sequence as Sd2H  $\beta$ -amylase (Table 6. 1). In addition, a Sd1 mutant (Sd1-V233A) was also produced. The structures of all of the mutants are shown in Figure 6. 1.

	Positions	115	165	233	347	430	
Sd2L-R115C	NH <sub>2</sub>	<b>C</b>	D	V	L	V	COOH
Sd2L-D165E	NH <sub>2</sub>	R	<b>E</b>	V	L	V	COOH
Sd2L-V233A	NH <sub>2</sub>	R	D	<b>A</b>	L	V	COOH
Sd2L-L347S	NH <sub>2</sub>	R	D	V	<b>S</b>	V	COOH
Sd2L-V430A	NH <sub>2</sub>	R	D	V	L	<b>A</b>	COOH
Sd2L-V233A/L347S (Sd2H)	NH <sub>2</sub>	R	D	<b>A</b>	<b>S</b>	V	COOH
Sd1-V233A	NH <sub>2</sub>	<b>C</b>	<b>E</b>	<b>A</b>	<b>S</b>	<b>A</b>	COOH

Figure 6. 1. Barley  $\beta$ -amylase mutants. Mutated residues are in bold font.

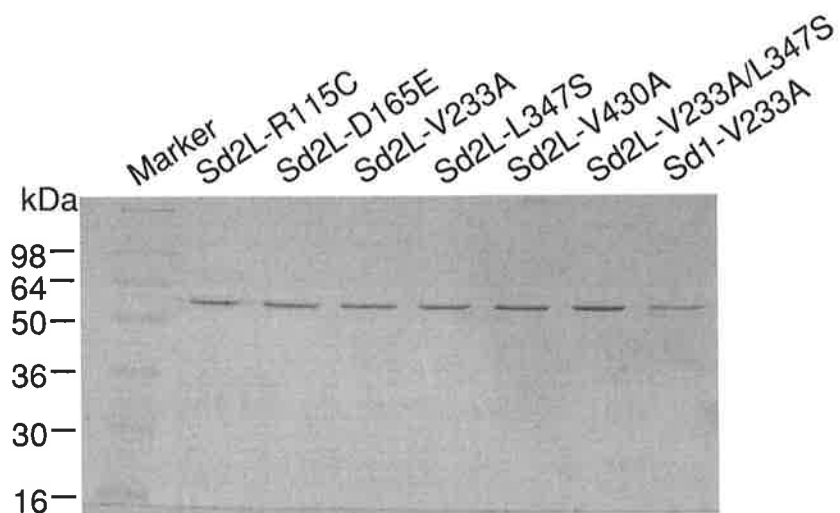


Figure 6. 2. SDS-PAGE of the purified mutant  $\beta$ -amylases stained with Coomassie blue R250.

After confirming the amino acid substitutions of each mutant by DNA sequencing, the plasmids were expressed in *E. coli* as active and soluble enzymes, and purified to homogeneity (Figure 6. 2).

### 6. 3. 3 Thermostability of mutant and wild type $\beta$ -amylases

The thermostability of mutant and wild type enzymes was measured using irreversible thermal inactivation curves (Figure 6. 3) to determine the  $T_{50}$  values (Table 6. 2). The  $T_{50}$  values for Sd2H (Sd2L-V233A/L347S), Sd1 and Sd2L  $\beta$ -amylases were 59.2, 57.3 and 55.2 °C, respectively. Among the five Sd2L single mutants, two mutations (V233A and L347S) resulted in an increase in the  $T_{50}$  values by 1.9 °C and 2.1 °C, respectively, compared with the wild type. All the remaining mutants had little effect on the  $T_{50}$  values.

The important roles the V223A and L347S mutations played in determining the  $\beta$ -amylase thermostability was further demonstrated in the double mutant Sd2L-V233A/L347S, where L347 and V233 of the Sd2L  $\beta$ -amylase were replaced with alanine and serine, respectively. As shown in Figure 3a and Table 3, this mutation enhanced the  $T_{50}$  by 4 °C, the sum of the calculations from the two single mutants Sd2L-V233A and Sd2L-L347S. This result indicates that the two residues had a simple additive effect on increasing the thermostability of  $\beta$ -amylase. This additive effect was further confirmed by the Sd1 mutant (Sd1-V233A). Wild type Sd1  $\beta$ -amylase, with a serine residue at position 347, had a  $T_{50}$  value 2.1 °C higher than the wild type Sd2L  $\beta$ -amylase that had a leucine residue at this position (Table 6. 1). The

single Sd1 mutant (Sd1-V233A) caused another 2.0 °C increase in the  $T_{50}$  value (Figure 6. 3 and Table 6. 2).

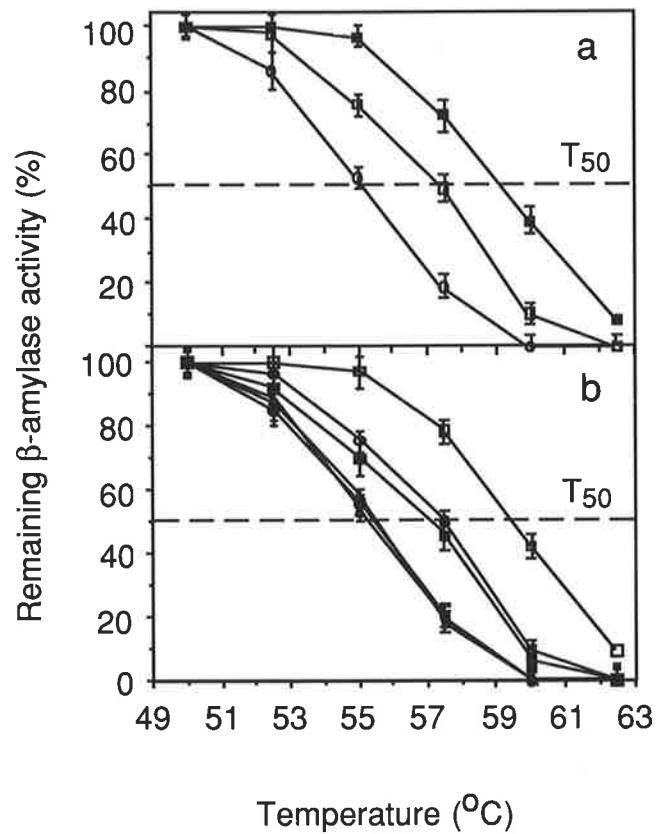


Figure 6. 3. Irreversible thermal inactivation. (a) wild type  $\beta$ -amylases. □ Sd1, ○ Sd2L, ■ Sd2H. (b) mutant  $\beta$ -amylases. □ Sd1-V233A, ○ Sd2L-L347S, ■ Sd2L-V233A, ▲ Sd2L-R115C, ● Sd2L-D165E, ◆ Sd2L-V430A. The activities are expressed as percentages of initial activities. Values are the means of three independent determinations, with the standard deviations shown as bars.

Table 6. 4.  $T_{50}$  values of wild-type and mutant barley  $\beta$ -amylases

Purified $\beta$ -amylase	$T_{50}$ ( $^{\circ}\text{C}$ )	$\Delta T_{50}$ ( $^{\circ}\text{C}$ )
Sd2L (wild-type)	$55.2 \pm 0.4$	-
Sd2L-R115C	$55.3 \pm 0.4$	+ 0.1
Sd2L-D165E	$55.2 \pm 0.2$	0
Sd2L-V233A	$57.1 \pm 0.3$	+ 1.9
Sd2L-L347S	$57.3 \pm 0.4$	+ 2.1
Sd2L-V430A	$55.3 \pm 0.3$	+ 0.1
Sd2L-V233A/L347S (Sd2H)	$59.2 \pm 0.5$	+ 4.0
Sd1 (wild-type)	$57.3 \pm 0.3$	-
Sd1-V233A	$59.4 \pm 0.4$	+ 2.1

$\Delta T_{50}$  is the change in  $T_{50}$  value of the mutant proteins relative to the wild-type protein.

Although both the V233A and L347S mutations increased the  $T_{50}$  values, only the substitution of L347 with serine enabled the maintenance of significantly higher activity than the wild type at higher assay temperatures (Figure 6. 4). The Sd2L-L347S mutant lost activity more slowly than the wild type at temperatures over 55  $^{\circ}\text{C}$ . Only approximately 10 % and 40 % of the activity was lost from Sd2L-L347S when the temperature rose from 55  $^{\circ}\text{C}$  to 57.5  $^{\circ}\text{C}$  and 60  $^{\circ}\text{C}$ , respectively, compared with approximately 30 % and 60 % that were lost from the wild type. The Sd2L-V233A mutant, however, did not have a significant effect on the maintenance of activity when the temperature was increased.

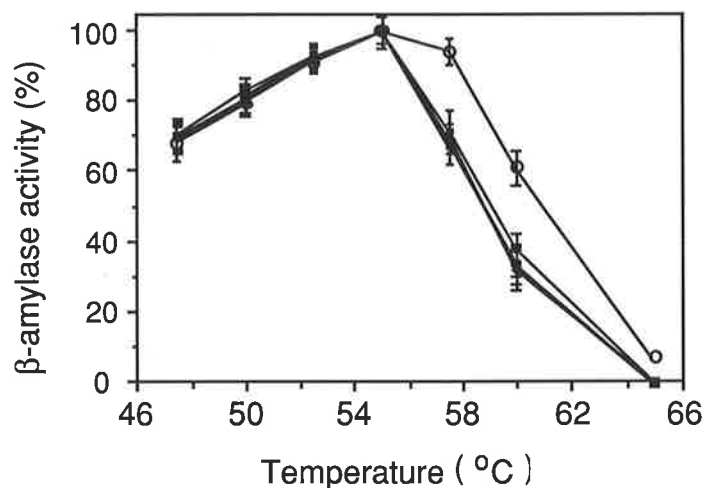


Figure 6. 4. Effect of assay temperature on the activities of mutant and wild type barley  $\beta$ -amylases.  $\circ$  Sd2L-L347S,  $\blacktriangle$  Sd2L-R115C,  $\bullet$  Sd2L-D165E,  $\blacksquare$  Sd2L-V233A,  $\blacklozenge$  Sd2L-V430A. The activities are expressed as percentages of the initial activity. Values are the mean of three independent determinations, with the standard deviation shown as bars.

#### 6. 3. 4 Kinetics of mutant and wild type $\beta$ -amylases

The kinetic constants,  $K_m$  and  $k_{cat}$ , of each mutant and wild type  $\beta$ -amylase were determined from initial rate measurements for the hydrolysis of soluble starch. Table 6. 3 summarises the kinetic parameters of starch hydrolysis catalysed by the mutant and wild type  $\beta$ -amylases. Sd1  $\beta$ -amylase exhibited a 2.5-fold lower  $K_m$  value than Sd2L and Sd2H  $\beta$ -amylases. Mutation results showed that replacement of R115 with cysteine resulted in a decrease in the  $K_m$  value of the enzyme from 8.3 to 3.6  $\mu$ M. Thus, this mutant has almost the same  $K_m$  value for starch as Sd1  $\beta$ -amylase where there is a cysteine residue at this position. For all of the other mutants, however, the

$K_m$  values were almost unchanged. No significant differences in the  $k_{cat}$  value between the mutant and wild type enzymes were observed.

Table 6. 3. Kinetic parameters for the hydrolysis of starch by wild-type and mutant barley  $\beta$ -amylases

Purified $\beta$ -amylase	$k_{cat}$ (U/mg)	$K_m$ ( $\mu$ M)
Sd2L (wild-type)	$300 \pm 12$	$8.3 \pm 0.58$
Sd2L-R115C	$310 \pm 8$	$3.6 \pm 0.28$
Sd2L-D165E	$320 \pm 9$	$8.5 \pm 0.61$
Sd2L-V233A	$316 \pm 11$	$8.2 \pm 0.71$
Sd2L-L347S	$310 \pm 9$	$8.3 \pm 0.68$
Sd2L-V430A	$320 \pm 10$	$8.4 \pm 0.75$
Sd2L-V233A/L347S (Sd2H)	$309 \pm 7$	$8.3 \pm 0.62$
Sd1 (wild-type)	$306 \pm 9$	$3.3 \pm 0.28$
Sd1-V233A	$315 \pm 7$	$3.2 \pm 0.56$

Values are the means of three independent determinations, with the standard deviations shown as  $\pm$ .

### 6. 3. 5 Structural analysis of $\beta$ -amylases

The structural bases of the observed thermostability and kinetic properties of barley  $\beta$ -amylase were investigated using a model based on the solved crystal structure for the sevenfold mutant of barley  $\beta$ -amylase (Mikami *et al.* 1999). The structural quality was ensured by the use of a template that shares 97.3 % sequence identity to



the mutant and the wild type Sd2L barley  $\beta$ -amylases. Nevertheless, the models for each mutant were analysed to ensure that the structures were sufficiently reliable to predict the effects of site-directed mutagenesis. The Ramachandran plot of the main-chain conformational angles of the wild type enzyme revealed that most of the residues in the wild type fall in or near the energetically preferred regions, with the exception of only four non-glycine residues (P191, P471, P485, W446) (Ramakrishnan and Ramachandran 1965; Laskowski *et al.* 1993). No additional residues with poor backbone conformations were identified in the mutant proteins. Superposition of all atoms of the three mutant structures with those of the wild type protein structure resulted in root-mean-square differences for the backbone of 0.112, 0.106 and 0.108 Å for Sd2L-R115C, Sd2L-V233A and Sd2L-L347S, respectively. This indicates that a single amino acid substitution is not likely to significantly affect the backbone structure of the protein. Some small differences in root-mean-square appear to be the logical consequence of the smaller side-chains in the mutants.

Figure 6. 5a shows the locations of residues R115, V233 and L347 in the wild type enzyme (Sd2L  $\beta$ -amylase). R115 is located at the C-terminal turn of the  $\alpha$ -helix of Loop 3 (coloured in red), which is a loop 1- $\alpha$ -helix-loop 2 motif. The long side-chain of arginine extends into the solvent. Inspection of the model showed that the main-chain nitrogen atom of R115 makes a hydrogen bond (distance 3.2 Å) with the main-chain oxygen atom of the adjacent V112 in the  $\alpha$ -helix (Figure 6. 6). In the mutant Sd2L-R115C, the replacement of R115 with cysteine resulted in the formation of an additional hydrogen bond (distance, 2.4 Å) because the SH group of mutated cysteine has the capacity to act as a hydrogen bond donor.

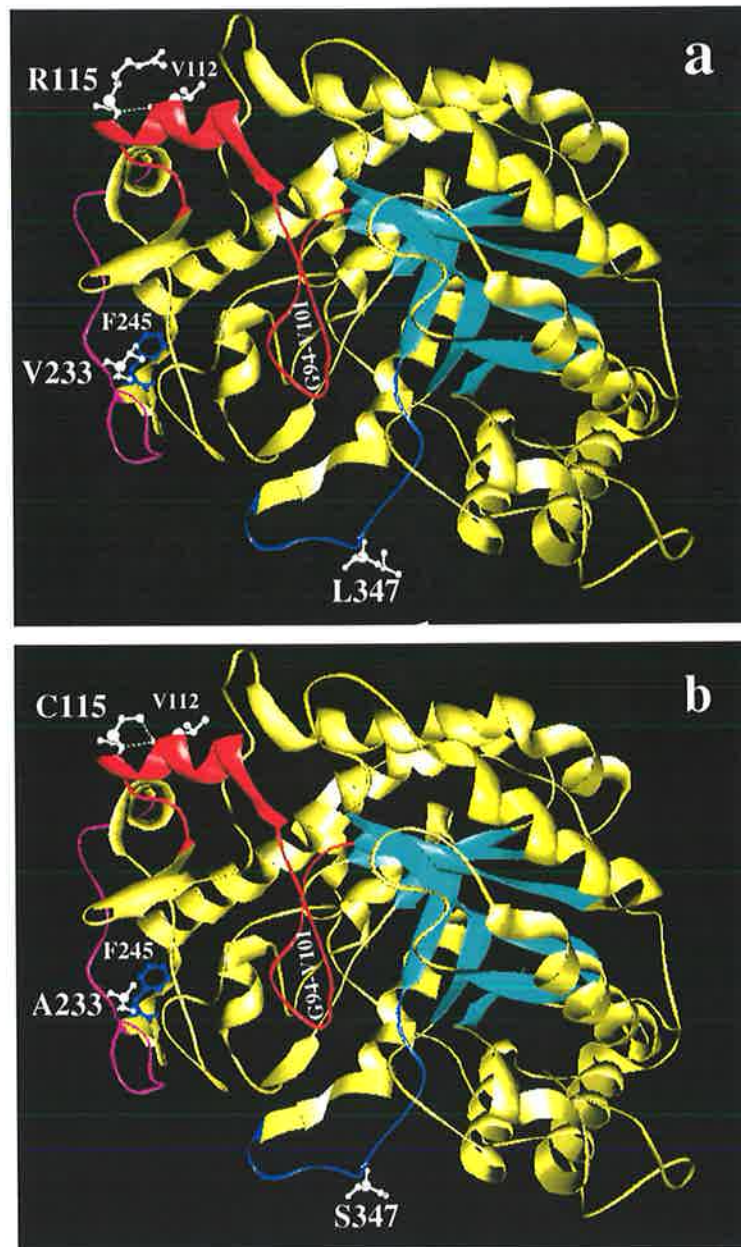


Figure 6. 5. Three-dimensional structures of wild type Sd2L  $\beta$ -amylase (a) and Sd1-V233A mutant (b). Loop 3 is coloured in red, Loop 4 is coloured in pink, and Loop 6 is coloured in blue. The pocket is coloured in aqua. The segment (residues G94-V101) was labelled. Hydrogen bonds are shown as green dotted lines. The Figure was generated using the program SPDBV 3.5 5 (Guex Peitsch 1997).

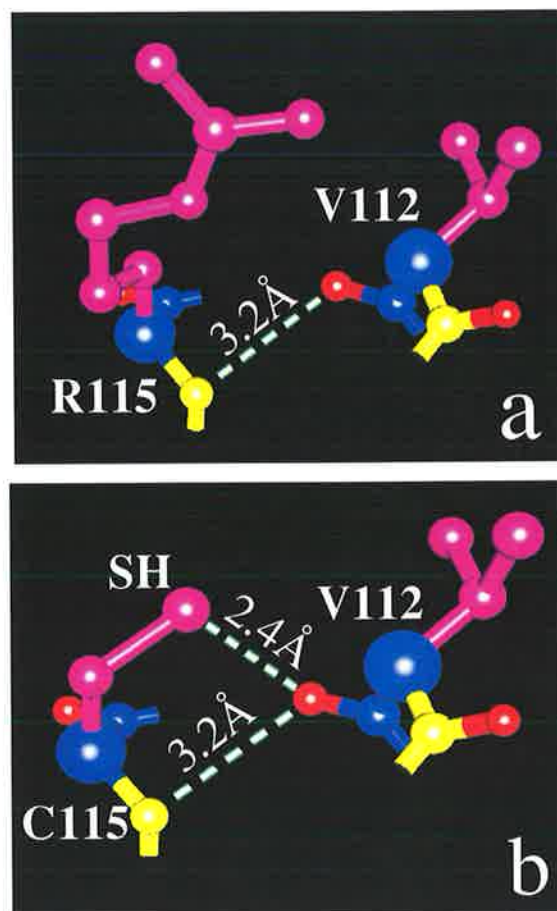


Figure 6. 6. Hydrogen bond interaction(s) between residues 112 and 115 of wild type Sd2L β-amylase (a) and mutant Sd2L-R115C (b). Side-chain is coloured pink, oxygen is coloured in red, nitrogen is coloured yellow, and carbon is coloured blue. Hydrogen bonds are shown as green dotted lines. The Figure was generated using the program SPDBV 3.5 (Guex Peitsch 1997).

Both V233 and L347 residues are located in a loop region (Figure 6. 5). V233 lies on Loop 4 (coloured in pink) pointing to the interior. The side-chain of this residue is close to surrounding residue F245. The residue L347, however, lies on Loop 6 (coloured in blue), pointing into the solvent. The side-chain of this residue is completely solvent-exposed. A structural analysis shows that neither residue is involved in hydrogen bond interactions with neighbouring residues in the wild type Sd2L  $\beta$ -amylase, nor in the Sd2L-V233A and Sd2L-L347S mutant proteins.

#### 6. 4 Discussion

Sequence comparison of the Sd1, Sd2L and Sd2H  $\beta$ -amylases showed there were six amino acid exchanges at positions 115, 165, 233, 347, 430 and 527 (Table 6. 1). The substitution at position 527 was not responsible for the observed differences in the thermostability and kinetic properties, because this residue, lying within the C-terminal region, is proteolytically cleaved after germination, and the differences in the thermostability and kinetic properties of the  $\beta$ -amylase forms are maintained after germination (Eglinton *et al.* 1998; chapter 4). The contribution of the remaining five amino acid substitutions to the thermostability and kinetic properties of barley  $\beta$ -amylase was evaluated by individually replacing the residues in Sd2L  $\beta$ -amylase with the corresponding ones in Sd1 or Sd2H  $\beta$ -amylase.

Recombinant Sd1  $\beta$ -amylase had a lower  $K_m$  value than the Sd2H and Sd2L  $\beta$ -amylases (Table 6. 3), indicating that this allelic  $\beta$ -amylase form has higher affinity for substrate than the Sd2H and Sd2L  $\beta$ -amylases. This is consistent with the result

from native purified  $\beta$ -amylases (chapter 3). Among the mutants, only the replacement of R115 with cysteine caused a reduction in the  $K_m$  value; by approximately 2.5-fold. Thus, the mutant exhibited a very similar  $K_m$  value to that of Sd1  $\beta$ -amylase, suggesting that this substitution is responsible for the kinetic differences among the three allelic barley  $\beta$ -amylase forms. A structural analysis shows that the R115C mutation occurs in the  $\alpha$ -helix of Loop 3 (Figure 6. 5). Loop 3 is an essential part of the active center (Mikami *et al.* 1993; 1994; Laederach *et al.* 1999). In particular, the opening and closing movement of the loop segment (residues 94-101, corresponding to residues 96-103 in soybean  $\beta$ -amylase) is involved in the binding of the substrate into the active site of the enzyme (Laederach *et al.* 1999). The R115C mutation resulted in the formation of an additional hydrogen bond with the main-chain oxygen atom of V112 (Figure 6. 6). Although there is no experimental evidence that the removal of the positively charged R115 affects the dipoles across the  $\alpha$ -helix electric field, it seems likely that the  $\alpha$ -helix in the mutant might be stabilised by the additional hydrogen bond. This may create a more favourable environment for substrate binding.

Recombinant Sd2H, Sd1 and Sd2L  $\beta$ -amylases exhibited high, intermediate and low  $T_{50}$  values, respectively (Figure 6. 3a and Table 6. 2), reflecting their different thermostabilities as native  $\beta$ -amylases. The replacement of V233 and L347 with alanine and serine increased the  $T_{50}$  values by 1.9 °C and 2.1 °C, respectively. The contributions of the two residues to the thermostability of barley  $\beta$ -amylase were additive. All other mutations had little effect on the  $T_{50}$  values. These results suggest

that the two amino acid substitutions at 233 and 347 are responsible for the different thermostability of the three allelic  $\beta$ -amylase forms, and that alanine and serine at the two positions are the preferred residues for enhancing thermostability. Soybean  $\beta$ -amylase, which has a relatively high thermostability compared to barley  $\beta$ -amylase (Yoshigi *et al.* 1995b), also contains alanine and serine at these two positions (Totsuka and Fukazawa 1993).

Both V233A and L347S substitutions are “large-to-small” exchanges. Residue 233 points into the interior, and its side-chain is very close to F245, which may cause some unfavourable strain (Figure 6. 5a). As shown in Figure 5b, the mutant side-chain of alanine is much smaller than that of valine. This reduction of the side-chain volume in the mutant may relieve some steric strain. Thus, the reason for the increased thermostability caused by the V233A mutation may be the reduction of the side-chain volume. In the case of the L347S substitution, the size of the side-chain may not be important for structural stability because this residue is completely solvent-exposed, and does not have any interactions with neighbouring residues. In addition to the difference in volume, the L347S substitution is an exchange from a hydrophobic residue to a hydrophilic one. The polar residue serine has a hydroxyl group that can hydrogen bond to solvent water. A protein with more hydrogen bonds to its solvent should gain energetic stability. It is therefore likely that the increased thermostability of the Sd2L-L347S mutant is correlated to the hydrophilic property, especially to the interactions of the protein surfaces with the surrounding water.

Although both V233A and L347S mutations led to increased thermostability, they

affected the thermostability in different ways. The replacement of L347 with serine significantly increased the capability to maintain activity when the assay temperature was increased (Figure 6. 4). This suggests that this serine residue is crucial for slowing the thermal unfolding of the protein and maintaining a heat-stable conformation of  $\beta$ -amylase against thermal denaturation. Thus, this mutation would be expected to recover some of the  $\beta$ -amylase activity that is lost from heat denaturation during kilning and protect the enzyme activity at higher temperatures during mashing. In contrast, the Sd2L-V233A mutant did not improve the capability of the enzyme to maintain activity at higher temperatures (Figure 6. 4), suggesting that this replacement does not slow thermal unfolding of the protein during heating. Thus, the increased thermostability of the V233A mutation is most probably due to an acceleration of refolding after heating. Consequently, this mutation would only protect the enzyme from heat denaturation in the kilning process.

The results in this chapter have demonstrated that the different thermostabilities and kinetic properties of the three allelic barley  $\beta$ -amylase forms are due to different combinations of three preferred residues; C115, A233 and S347. Sd2L  $\beta$ -amylase, with all three unfavourable residues (R115, V233 and L347) had low thermostability and affinity for substrate. Sd1, containing the preferred residue C115, showed high affinity for substrate, but its thermostability was lower than that of Sd2H  $\beta$ -amylase. Sd2H  $\beta$ -amylase, carrying two preferred residues, A233 and S347, exhibited high thermostability, but its affinity for substrate was lower than that of Sd1  $\beta$ -amylase. The  $\beta$ -amylase properties determined by the three residues appear to be associated

with the malting quality of different barley varieties. Sd2L varieties have typically low fermentability, while the fermentabilities of Sd1 and Sd2H varieties are generally similar (Eglinton *et al.* 1998). Thus, a  $\beta$ -amylase mutant (Sd1-V233A) containing all of the three preferred residues was generated. This mutant had almost the same  $T_{50}$  value as Sd2H  $\beta$ -amylase and a very similar  $K_m$  value to Sd1  $\beta$ -amylase, indicating that the mutant combined both the high thermostability and high substrate-binding affinity. At present, no barley cultivar carries all three preferred residues. Techniques for barley transformation are now available (Nuutila *et al.* 1999), and the introduction of a  $\beta$ -amylase gene containing all three preferred residues may result in the production of improved malting quality barley varieties.



## General discussion

---

$\beta$ -Amylase catalyses the release of maltose from the non-reducing ends of starch. The enzyme is a key determinant of diastatic power, and thus particularly important for the production of fermentable sugars in the brewing industry where a large quantity of starch needs to be converted into fermentable sugars. In most commercial malts, however,  $\beta$ -amylase activity is insufficient, and reported to be the rate-limiting enzyme in starch degradation during mashing (MacGregor 1996; Sjöholm *et al.* 1995). Therefore, it would be useful to increase  $\beta$ -amylase activity in germinating barley grain in order to enhance extract fermentability. The experiments conducted in this thesis were directed towards understanding the enzymatic characteristics of barley  $\beta$ -amylase, and using this knowledge to improve the enzyme's properties by molecular manipulation.

There are three allelic  $\beta$ -amylase forms (Sd1, Sd2L and Sd2H) in cultivated barley (Eglinton *et al.* 1998), but only two distinct IEF band patterns (Sd1 and Sd2) have been identified as Sd2L and Sd2H exhibit an identical band pattern despite differing thermostability (Evans *et al.* 1997a). To understand the enzymatic characteristics, Sd1 and Sd2L  $\beta$ -amylases were purified from both barley grain and malt of the barley varieties Franklin and Schooner, so that kinetic and thermostability analysis could be conducted with the purified enzymes. The investigation demonstrated that:

- (1). the three allelic forms of barley  $\beta$ -amylase exhibit different thermostability and kinetic properties.
- (2). the enzyme has increased thermostability and substrate-binding affinity for starch after germination, during which approximately 4 kDa

peptide is removed from the C-terminal tail of the 60 kDa protein. These results indicate that both genetic variation and post-translational modification control the properties of the enzyme, and suggest that understanding the molecular mechanisms for these effects might lead to the development of strategies to improve the enzyme's characteristics.

Particular emphasis was placed on understanding the molecular basis for the effect of post-translational modification on the enzymatic characteristics. The C-terminal tail of barley  $\beta$ -amylase contains four glycine-rich repeats. The proteolytic cleavage at this region during germination is non-specific, and produces several  $\beta$ -amylase forms with different C-terminal terminations (Lundgard and Svensson 1987). To understand how the different cleavages affect the enzyme properties, cDNAs encoding barley  $\beta$ -amylases with different C-terminal deletions were cloned, and recombinant  $\beta$ -amylases generated. The results demonstrated that different cleavages at the C-terminus of the protein had different effects on thermostability, although all of the cleavages increased the affinity for starch. Only the complete deletion of the four C-terminal glycine-rich repeats significantly increased the enzyme's thermostability. Incomplete deletions with one repeat remaining did not change the thermostability. An inspection of a homology-based model of Sd2L  $\beta$ -amylase revealed that the four glycine-rich repeat region of barley  $\beta$ -amylase is a very flexible and unstable structure, whose presence limits the stability of the protein in response to heat. Because the proteolytic cleavage of barley  $\beta$ -amylase is a step-wise process from the C-terminus of the protein (Lundgard and Svensson 1987), the degree of

peptide cleavage in the C-terminal tail is dependent on the cleavage conditions, such as protease concentration, cleavage time, etc. Therefore, further investigations into the effect of germination conditions on the proteolytic cleavage of barley  $\beta$ -amylase are required. This will potentially identify germination conditions which ensure the complete removal of the destabilising four C-terminal glycine-rich repeats from barley  $\beta$ -amylase during malting and increase the enzyme's thermostability during mashing.

The different properties of the three allelic forms of barley  $\beta$ -amylase have a critical role in determining the malting quality of barley varieties (Eglinton *et al.* 1998; Kihara *et al.*, 1998; 1999). To understand the molecular mechanism for the effects of this genetic variation on enzymatic characteristics, Sd1 and Sd2L  $\beta$ -amylase cDNAs were cloned, and the nucleotide sequences compared with those of the published Sd2L and Sd2H  $\beta$ -amylases. The comparison revealed six amino acid substitutions at positions 115, 165, 233, 347, 430 and 527. Residue 527 is not responsible for the different properties of the three allelic  $\beta$ -amylases, because this residue, lying in the C-terminal tail, is removed after germination. The contributions of remaining five substitutions to the enzyme properties were evaluated by site-directed mutagenesis.

Results showed that the R115C mutation is responsible for the differences in the kinetic properties of the enzyme. This substitution resulted in the formation of an additional hydrogen bond, which may create a more favourable environment for substrate binding. The R115C substitution was also the determinant for the two

distinct IEF band patterns of barley  $\beta$ -amylase since it altered both the net charges on the protein surface and intermolecular interactions via disulfide bonds. The explanation for the two band patterns has puzzled  $\beta$ -amylase investigators for more than 30 years (Allison 1973; Allison and Swanston 1974; Swanston 1980; Swanston 1983; Evans *et. al.* 1997a). The discovery of the biochemical and molecular mechanisms underlying the different band patterns of barley  $\beta$ -amylase will be useful in utilising the band pattern as a selection tool in barley breeding programs. Selection for malting quality in barley breeding programs has traditionally relied on the measurement of standard malt quality parameters. This is a slow and laborious process, in which the results vary with the environmental conditions. Electrophoresis is a qualitative test, as results are not affected by the environment in which the plants are grown. Electrophoresis also has an other advantage over the traditional malt quality measurement. The test is quick, simple, and can be applied to half grains, with the other half grown on to produce a healthy plant, so it could be introduced at a very early stage of a breeding program to predict the malting quality of potential barley varieties. Therefore, IEF band pattern of  $\beta$ -amylase provides an option for a more precise approach to select for specific  $\beta$ -amylase alleles important to malting quality.

The different thermostabilities of the  $\beta$ -amylase forms were due to two amino acid substitutions (V233A and L347S), which increased the enzyme's thermostability

index  $T_{50}$  by 1.9°C and 2.1°C, respectively. The reasons for this increased thermostability seems to be the relieving of steric strain and the interaction of the protein surface with solvent water. However, these explanations need to be confirmed by crystallising and subjecting the mutant proteins to x-ray analysis. Although both V233A and L347S mutations increased the thermostability of the enzyme, they affected the thermostability in different ways. The replacement of L347 with serine seems to increase thermostability by slowing the thermal unfolding of the protein during heating. Thus, this mutation would be expected to recover some  $\beta$ -amylase activity from heat denaturation during kilning and protect the enzyme activity at higher temperatures during mashing. The mutation of V233 to alanine, however, appears to be due to an acceleration of any refolding that occurs after heating. Thus, the increased thermostability of the V233A mutation is most probably due to an acceleration of refolding after heating. Consequently, this mutation would only protect the enzyme from heat denaturation that occurs during the kilning process.

The results from the site-directed mutagenesis experiments demonstrated that the different thermostability and kinetic properties of the three allelic barley  $\beta$ -amylase forms were due to different combinations of the three preferred residues C115, A233 and S347. This suggested that combining the three preferred residues might produce an  $\beta$ -amylase with high thermostability and substrate-binding affinity,  $\beta$ -amylase mutant (Sd1-V233A) containing all three preferred residues was therefore generated. This mutant demonstrated very similar substrate-binding affinity to Sd1  $\beta$ -amylase

and almost the same thermostability as Sd2H  $\beta$ -amylase, indicating that the mutant has improved characteristics that combine high thermostability and substrate-binding affinity. Thus, this investigation recommends a superior  $\beta$ -amylase type for selection by Australian Barley Improvement Programs.

The apparent sub-optimal levels of  $\beta$ -amylase activity during mashing are due to the quality, rather than the quantity of the enzyme. Barley  $\beta$ -amylase, representing approximately 1-2% of total barley protein (MacGregor *et al.* 1971; Hejgaard & Boisen 1980; Evans *et al.* 1997a), is relatively thermolabile compared with other starch-degrading enzymes. A significant proportion of barley  $\beta$ -amylase activity is lost during the mashing process. My investigations demonstrated that barley  $\beta$ -amylase can be manipulated to be more thermostable and to have a higher affinity for starch by a combination of amino acid substitutions and removal of the unstable C-terminal tail. Other researchers have also manipulated  $\beta$ -amylase to make it more thermostable (Okada *et al.* 1995; Yoshigi *et al.* 1995b). The increased thermostability could be of significant benefit to the brewing industry. The mutant enzyme with enhanced thermostability is expected to have an improved ability to survive thermal challenges in the malthouse or brewery. The higher affinity of the mutant  $\beta$ -amylase may also result in a higher yield of fermentable sugars during the mashing process. Although the concentration of starch in barley grain is much higher than the enzyme's  $K_m$  value for starch, it is possible that the enzyme may be better able to hydrolyse starch under conditions where the concentration of starch becomes limiting, such as towards the end of saccharification in the mashing process of

brewing, thereby improving wort fermentability. As shown in Figure 3. 5, Sd1  $\beta$ -amylase (higher substrate-binding affinity for starch) showed a higher reaction rate than Sd2L  $\beta$ -amylase at the non-saturating 50  $\mu$ M starch concentration. Simulated mashing experiments may be useful for assessing the practical impact of mutant proteins on the production of fermentable sugars for brewing and wort fermentability. However, the influence of the wild type  $\beta$ -amylase will need to be taken into account. In addition, wort fermentability (or the production of fermentable sugars) is due to the effects of starch degrading enzymes. The efficiency of any starch degrading enzyme in mashing is these, in part, influenced by the degree of its interaction with other starch degrading enzymes, so that the influence of any particular enzyme on fermentability will be constrained by the levels and characteristics of the other starch degrading enzymes.

Results from this thesis have given an indication that protein engineering can be a valuable method for improving the properties of barley  $\beta$ -amylase. In particular, reliable methods for the production of transgenic barley are now available (Nuutila *et al.* 1999; Lörz *et al.* 2000; Okada *et al.* 2000), so it should be possible to incorporate a desirable Sd2L  $\beta$ -amylase mutant gene into the genome of transgenic barley. Thus, protein engineering may have an application in barley breeding programs to provide barley varieties with significantly improved malting quality. Protein engineering has also been used by many researchers to enhance the stability of other proteins mainly by introducing ion pairs (Vogt *et al.* 1997), reducing the entropy of unfolding of the protein (Matthews *et al.* 1987), reducing the size of hydrophobic pockets in the

protein (Argos *et al.* 1979), removing the exposed loop on a protein surface (Thompson and Eisenberg 1999), or generating internal hydrogen bonds to link together potentially unstable regions (Hardy *et al.* 1993). However, this technology requires detailed knowledge of the enzyme's three-dimensional structure. Although the structure of barley  $\beta$ -amylase is available (Mikami *et al.* 1999), the properties governing the protein's stability are not completely understood. Further investigations are needed to comprehensively understand the factors which affect protein folding and stability. By understanding the structure and function, it should be possible to further manipulate barley  $\beta$ -amylase by protein engineering.



## Appendix A

### Additional results of $\beta$ -amylase Purification

Table A1. Enzyme yields during the purification of  $\beta$ -amylase from Sd1 malt

Purification step	yield		activity (U/mg)	recovery (%)	purification (-fold) <sup>a</sup>
	protein (mg)	activity (U)			
Crude extraction	3763	514684	137	100	
20-60% (NH <sub>4</sub> ) <sub>2</sub> SO <sub>4</sub>	1568	309607	198	60	1.4
Chromatography I	935	265930	285	52	2.1
Chromatography II					
Peak 1	18	15843	900	3	6.6
Peak 2	19	17781	913	3	6.7
Peak 3	154	148044	961	29	7

<sup>a</sup> Calculated on the basis of specific activity (U/mg protein)

Table A2. Enzyme yields during the purification of  $\beta$ -amylase from Sd2L malt

Purification step	yield		activity (U/mg)	recovery (%)	purification (-fold) <sup>a</sup>
	protein (mg)	activity (U)			
Crude extraction	3170	386874	122	100	
20-60% (NH <sub>4</sub> ) <sub>2</sub> SO <sub>4</sub>	1554	301918	194	78	1.6
Chromatography I	594	203022	342	53	2.8
Chromatography II					
Peak 4	96	78697	819	20	6.7
Peak 5	70	65183	934913	17	7.7
Peak 6	39	21316	548	5	4.5

<sup>a</sup> Calculated on the basis of specific activity (U/mg protein)

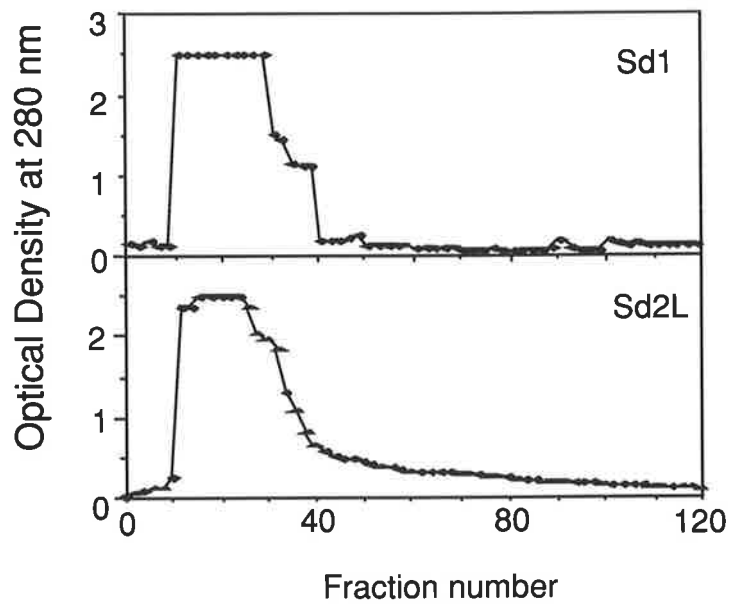


Figure A1. Chromatography of Sd1 and Sd2L malt  $\beta$ -amylases on the first anion exchange column (pH 7.0).

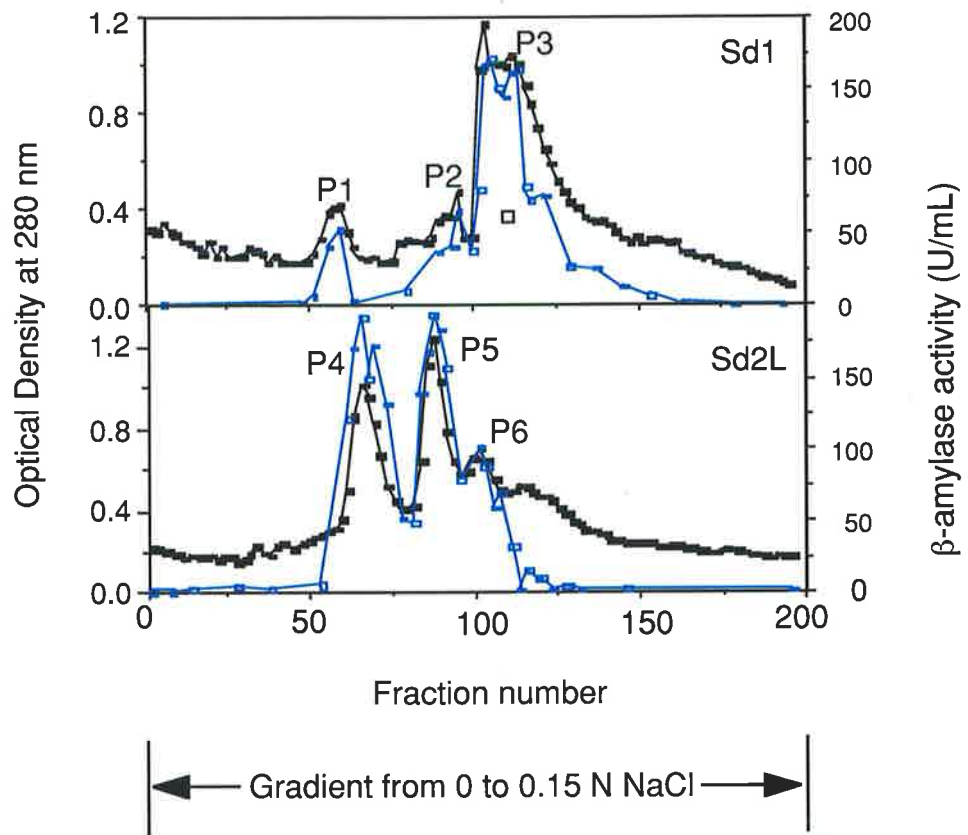


Figure A2. Chromatography of Sd1 and Sd2L malt  $\beta$ -amylases on the second anion exchange column (pH 8.5). black line, OD 280; blue line,  $\beta$ -amylase activity.

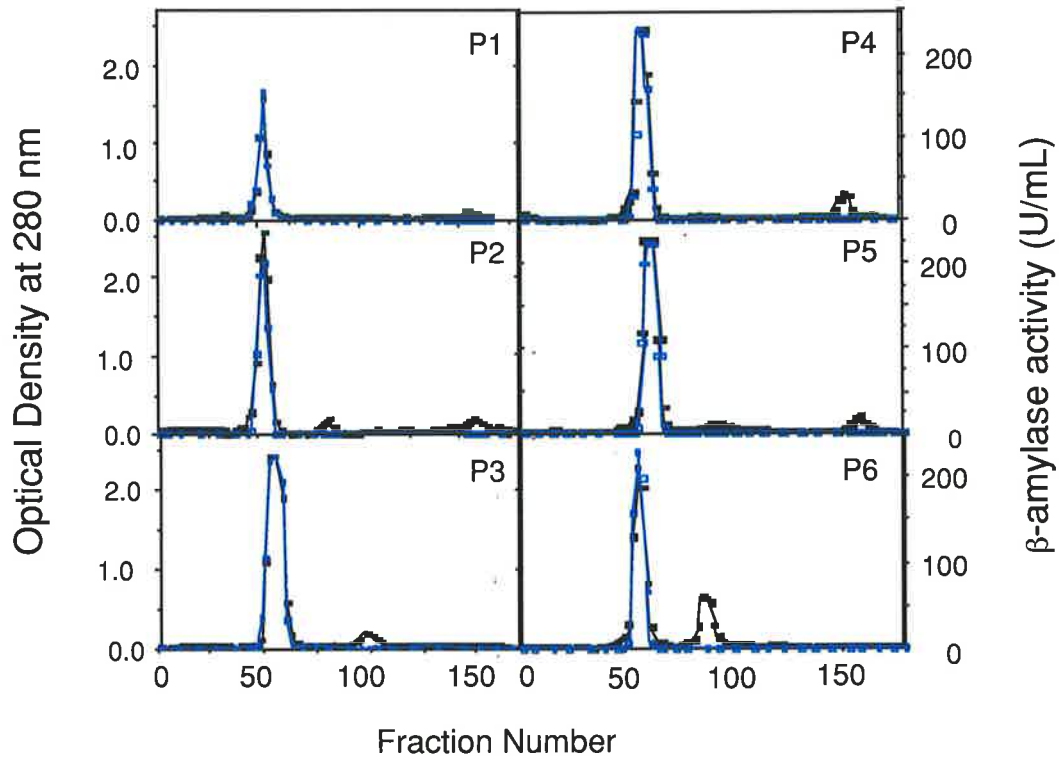


Figure A3. Re-chromatography of aliquots of the  $\beta$ -amylase peaks from the second anion exchange column on gel filtration column (Bio-gel P60). black line, OD 280; blue line,  $\beta$ -amylase activity.

## Appendix B

### Additional results of $\beta$ -amylase clone and recombinant protein analysis

---

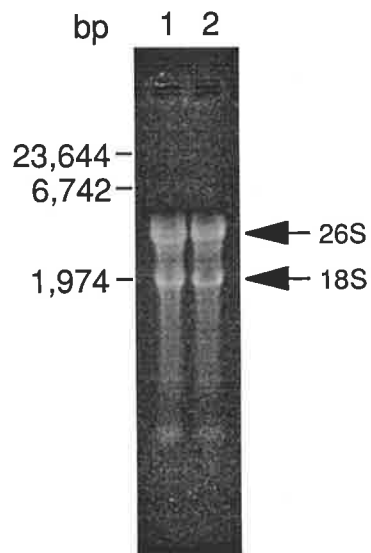


Figure B1. Agarose gel electrophoresis of total RNA extracted from Franklin (lane 1) and Schooner (lane 2) barley grain.

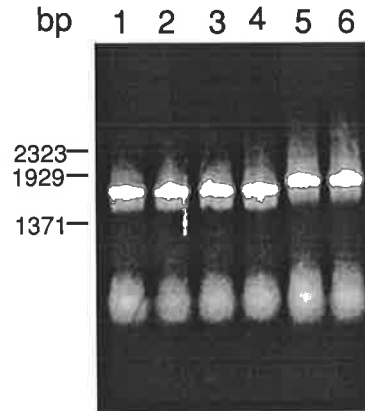

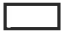


Figure B2. Agarose gel electrophoresis of PCR amplified products of Sd1-489 (lane 1), Sd2L-489 (lane 2), Sd1-496 (lane 3), Sd2L-496 (lane 4), Sd1-535 (lane 5), Sd2L-535 (lane 6).



Figure B3. Restriction map of  $\beta$ -amylase cDNA. The numbers represent the nucleotide pair of the sequence.  coding region (extends from 56 bp to 1660 bp of the cDNA sequence).  non-coding region.

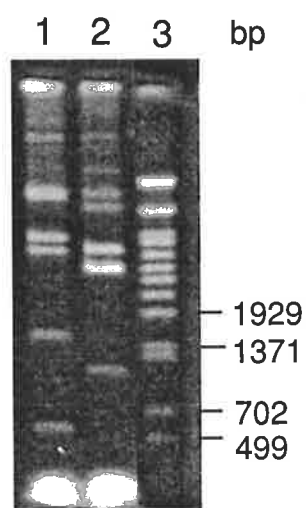


Figure B4. Restriction analysis of the recombinant  $\beta$ -amylase by digestion with BamH 1. lane 1, the cell line carrying the  $\beta$ -amylase plasmid with the correct orientation of the insert; lane 2, the cell line carrying the  $\beta$ -amylase plasmid with the reverse orientation of the insert; lane 3, marker.



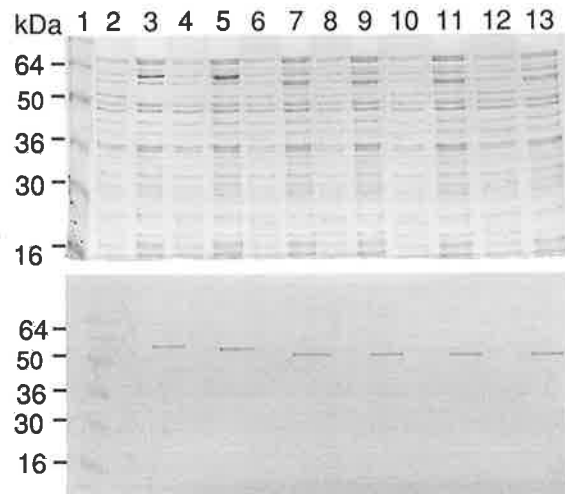


Figure B5. Expression analysis of the recombinant  $\beta$ -amylase. The upper panel is SDS-PAGE, the lower panel is on immuno-blot. lane 1, molecular markers; lanes 2, 4, 6, 8, 10 and 12 were non ITPG induced Sd1-535, Sd2L-535, Sd1-496, Sd2L-496, Sd1-489 and Sd2L-489, lanes 3, 5, 7, 9, 11, and 13 were ITPG induced Sd1-535, Sd2L-535, Sd1-496, Sd2L-496, Sd1-489 and Sd2L-489.

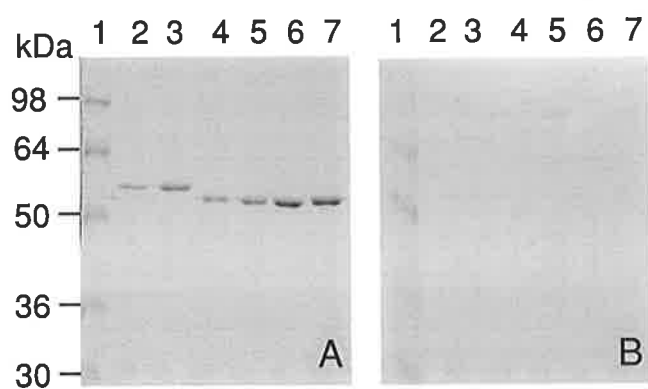


Figure B6. Evidence of the complete cleavage of the 6xHis-tag from fusion proteins.

A. SDS-PAGE of enterokinase-digested proteins, B. Immuno-blot using anti-His antibody. Lane 1, marker; lane 2, Sd1-535; lane 3, Sd2L-535; lane 4, Sd1-496; lane 5, Sd2L-496; lane 6, Sd1-489; lane 7, Sd2L-489.

Table B1.  $T_{50}$  values ( $^{\circ}\text{C}$ ) of recombinant  $\beta$ -amylases with and without the 6xHis tag.

$\beta$ -Amylase	$T_{50}$ values ( $^{\circ}\text{C}$ )	
	With the 6xHis tag	Without the 6xHis tag
Sd1-M535	$55.7 \pm 0.3$	$55.0 \pm 0.3$
Sd2L-M535	$52.4 \pm 0.3$	$52.6 \pm 0.2$
Sd1-G496	$55.2 \pm 0.2$	$55.0 \pm 0.4$
Sd2L-G496	$52.4 \pm 0.4$	$52.7 \pm 0.3$
Sd1-G489	$57.5 \pm 0.3$	$57.6 \pm 0.4$
Sd2L-G489	$55.5 \pm 0.4$	$55.2 \pm 0.2$

## Appendix C

### Buffers, stock solutions and media

---

All general laboratory reagents were at least analytical grade in standard. Solutions were prepared under sterile conditions with ultra-pure water and autoclaved where appropriate.

#### 1 Buffers and stock solutions

**Acrylamide stock solution:** 30 % (w/v) acrylamide, 0.8 % bis-acrylamide.

**$\beta$ -Amylase extraction buffer:** 10 mM EDTA, 0.1 M Monothioglycerol (MTG), pH 5.0.

**$\beta$ -Amylase dilution buffer:** 0.1 M maleic acid buffer containing 2.8 mg/mL BSA, 0.02 % (w/v) Sodium Azide, 1 mM Na<sub>2</sub>EDTA, pH 6.2.

**10xCIAP buffer:** 0.5 M Tris-HCl, 10 mM MgCl<sub>2</sub>, 1 mM ZnCl<sub>2</sub> and 10 mM spermidine, pH 9.0.

**Coomassie gel de-stain solution (per litre):** 100 mL of methanol, 100 mL of glacial acetic acid, 800 mL of H<sub>2</sub>O.

**Coomassie gel stain solution (per litre):** 1 g of Coomassie blue R-250, 450 mL of methanol, 450 mL of H<sub>2</sub>O, 100 mL of glacial acetic acid.

**Dephosphorylation stop buffer:** 273  $\mu$ L of 1xTE buffer, 12  $\mu$ L of 5M NaCl and 15  $\mu$ L of 10 % SDS.

**10xDNA sample loading buffer:** 100 mM Tris-HCl, 200 mM Na<sub>2</sub>EDTA, 0.25 % bromophenol blue, 0.25 % xylene cyanol FF, and 30 % Ficoll type 4000.

**HRP colour development solution:** add 30 mg of 4-chloro-naphthol, 10 mL of pre-chilled methanol, 40 mL of TBS and 30  $\mu$ L of  $H_2O_2$ .

**I/KI solution:** dissolve 6.5 g of  $I_2$  and 19.5 g of KI in 1 L of water.

**10xMOPS Buffer:** 500 mM MOPS, 10 mM  $Na_2EDTA$ , pH 7.0.

**10xMutagenesis reaction buffer:** 100 mM KCl, 100 mM  $(NH_4)_2SO_4$ , 200 mM Tris-HCl, 20 mM  $MgSO_4$ , 1 % Triton X-100, 1 mg/mL nuclease-free BSA, pH 8.8.

**N3 buffer:** 3 M Sodium acetate, pH 4.8.

**Nelson Reagent:**

Solution A, dissolve 25 g of ammonium molybdate [ $(NH_4)_6Mo_7O_{24} \cdot 4H_2O$ ] in 450 mL of water, add 21 mL of concentrated  $H_2SO_4$ .

Solution B, dissolve 3 g of Sodium Arsenate ( $Na_2HAsO_4 \cdot 7H_2O$ ) in 25 mL of water.

Add solution B to solution A slowly with mixing and incubate the solution for 24-48 hours at 37  $^{\circ}C$  to stabilise the colour.

**P1 buffer:** 50 mM glucose, 25 mM Tris-HCl, 10 mM  $Na_2EDTA$ , pH 8.0,

**P2 buffer:** 0.2 M NaOH, 10 % SDS.

**10xPBS:** 137 mM NaCl, 2.7 mM KCl, 1.5 mM  $KH_2PO_4$ , 4.3 mM  $Na_2HPO_4$ , pH 7.5.

**10xPCR buffer:** 500 mM KCl, 200 mM Tris-HCl, 25 mM  $MgCl_2$ , 1 mg/mL BSA, pH 8.4.

**Phenol/chloroform/iso-amyl alcohol (25:24:1):** redistilled phenol was saturated with

0.5 M Tris-HCl, pH 8.0, then mixed with chloroform and iso-amyl alcohol.

**Protein gel electrophoresis buffer:** 25 mM Tris-HCl, 192 mM glycine, 0.1 % SDS, pH 8.3.

**Protein transfer buffer:** 25 mM Tris-HCl, 192 mM glycine, 20 % (v/v) methanol, 0.05 % SDS, pH 8.1-8.3.

**REB buffer:** 100 mM Tris-HCl, 4 % Sarkosyl, 10 mM Na<sub>2</sub>EDTA, pH 8.0.

**10xrEK cleavage buffer:** 200 mM Tris-HCl, 200 mM NaCl, 2 mM CaCl<sub>2</sub>, 50 % glycerol, pH 7.4.

**RNA extraction buffer:** 0.2 M Tris-HCl, 0.1 M KCl, 0.025 M EGTA, 0.035 M MgCl<sub>2</sub>, 1 % Triton X-100, 0.5 % sodium deoxycholate, 1 mM spermidine, 5 mM β-ME, 0.5 M sucrose, pH 9.0.

**10xRNA loading buffer:** 250 μl of 50 % glycerol, 1 mM Na<sub>2</sub>EDTA, 10 mg of bromophenol blue, 249 μL of DEP'd H<sub>2</sub>O, final volume of 500 μL.

**5xSDS-PAGE sample buffer:** 60 mM Tris-HCl, 25 % glycerol, 2 % SDS, 14.4 mM β-ME, 0.1 % bromophenol blue, pH 6.8.

**Somogyi I:**

Solution A, add 15 KNa tartrate and 30 Na<sub>2</sub>CO<sub>3</sub> to H<sub>2</sub>O, allow complete dissolution, bring to 300 mL with H<sub>2</sub>O, then add 20 g of NaHCO<sub>3</sub>.

Solution B, dissolve 180 g of Na<sub>2</sub>SO<sub>4</sub> with H<sub>2</sub>O in a final volume of 500 mL.

Boil solution A and solution B to completely degas. Then cool to room temperature, add solution A to solution B and make the volume to 1 L.

**Somogyi II:** dissolve 5 g of  $\text{CuSO}_4 \cdot 5\text{H}_2\text{O}$  and 45 g of  $\text{Na}_2\text{SO}_4$  in water in a final volume of 250 mL.

**Sonication buffer:** 50 mM Na-phosphate, 300 mM NaCl, pH 7.8.

**10xTAE buffer:** 400 mM Tris-HCl, 10 mM  $\text{Na}_2\text{EDTA}$ , pH 8.0.

**10xT4 DNA ligase buffer:** 300 mM Tris-HCl, 100 mM  $\text{MgCl}_2$ , 100 mM DTT, 10 mM ATP, pH 7.8.

**TFB buffer:** 10 mM MES, 45 mM  $\text{MnCl}_2$ , 100 mM RbCl, 10 mM  $\text{CaCl}_2$ , 3 mM hexamine cobalt chloride, pH 6.3, sterile filter.

**TFB 1 buffer:** 100 mM RbCl, 50 mM  $\text{MnCl}_2$ , 30 mM potassium acetate, 10 mM  $\text{CaCl}_2$ , 15 % glycerol, pH 5.8, sterile-filter.

**TFB 2 buffer:** 10 mM MOPS, 10 mM RbCl, 75 mM  $\text{CaCl}_2$ , 15 % glycerol, pH 6.8, sterile filtered.

**10xTBS:** 0.15 M NaCl, 10 mM Tris-HCl, pH 7.5.

**1xTE buffer:** 10 mM Tris-HCl, 1 mM  $\text{Na}_2\text{EDTA}$ , pH 8.0.

**Wash buffer:** 50 mM Na-phosphate, 300 mM NaCl, 10 % glycerol, pH 6.0.

## 2. Media

**LB medium (per litre):** 10 g of Bacto-Tryptone, 5 g of yeast extract, 10 g of NaCl, pH 7.0.

**LB agar:** 15 g of agar per litre LB medium.

**SOB medium (100 mL):** add 2 g of Bacto-Tryptone, 0.5 g of Bacto-yeast extract, 1 mL of 1M NaCl and 0.25 mL of 1M KCl to 97 mL of water. Stir to dissolve. Autoclave and cool down to room temperature. Add 1 mL of 2M Mg<sup>2+</sup> stock (1M MgCl<sub>2</sub>·6H<sub>2</sub>O/1M MgSO<sub>4</sub>·7H<sub>2</sub>O) and 1 mL of 2M filter-sterilised glucose. Bring to 100 mL with water. Filter the complete medium through a 0.2 µm filter unit. The final pH should be 7.0.

**NZY Broth (per liter):** 10 g of NZ amine (casein hydrolysate), 5 g of yeast extract, 5 g of NaCl, adjust to pH 7.5 using NaOH and autoclave. Add 12.5 mL of 1 M MgCl<sub>2</sub>, 12.5 mL of 1 M MgSO<sub>4</sub> and 20 mL of 20 % (w/v) glucose before use.

**Psi-broth:** LB medium, 4mM MgSO<sub>4</sub>, 10 mM KCl.



## References

---

- Allison, M. J. (1973) Genetic studies on the  $\beta$ -amylase isozymes of barley malt. *Genetica* 44, 1-15.
- Allison, M. J. and Swanston, J. S. (1974) Relationships between  $\beta$ -amylase polymorphisms in developing, mature and germinating grains of barley. *J. Inst. Brew.* 80, 285-291.
- Arends, A. M., Fox, G. P., Henry, R. J., Marschke, R. J. and Symons, M. H. (1995) Genetic and environmental variation in the diastatic power of Australian barley. *J. Cereal Sci.* 21, 63-70.
- Baba, T. and Kainuma, K. (1987) Partial hydrolysis of sweet-potato starch with  $\beta$ -amylase. *Agric. Biol. Chem.* 51, 1365-1371.
- Bradford, M. M. (1976) A rapid and sensitive method for the quantitation of microgram quantities of protein utilising the principle of protein dye binding. *Anal. Biochem.* 72, 248-254.
- Briggs, D. E. (1973) Hormones and carbohydrate metabolism in germinating cereal grains. In 'Biosynthesis and its control in plants', Milborrow, B. V. ed. pp 219-277, Academic Press, New York.
- Chothia, C. and Lesk, A. M. (1986) The relation between the divergence of sequence and structure in proteins. *EMBO J.* 5, 823-826.
- Cheong, C. G., Eom, S. H., Chang, C., Shin, D. H., Song, H. K., Min, K., Moon, J. H., Kim, K. K., Hwang, K. Y. and Suh, W. (1995) Crystallisation, molecular replacement solution, and refinement of tetrameric  $\beta$ -amylase from sweet potato. *Proteins* 21, 105-117.

- Cleland, W. W. (1979) Substrate inhibition. *Methods Enzymol* 63, 500-513.
- Cox, K. H. and Goldberg, R. B. (1988) Analysis of plant gene expression. In 'Plant Molecular Biology, A Practical Approach', Shaw, C. H. ed, pp 1-8. IRL Press, Washington DC.
- Daussant, J. and Laurière, C. (1990). Detection and partial characterisation of two antigenically distinct  $\beta$ -amylase in developing kernels of wheat. *Planta* 181, 505-511.
- Daussant, J., Sadowski, J., Rorat, T., Mayer, C. and Laurière, C. (1991) Independent regulatory aspects and post-translational modifications of two  $\beta$ -amylases of rye. *Plant Physiol.* 96, 84-90.
- Delcour, J. A. and Verschaeve, S. G. (1987) Malt diastatic power. Part II. A modified EBC diastatic power assay for the selective estimation of  $\beta$ -amylase activity. Time and temperature dependence of the release of reducing sugars. *J. Inst. Brew.* 93, 296-301.
- Eglinton, J. K. and Evans, D. E. (1996) Identification of the *beta*-amylase isoelectric focusing band pattern in barley (*Hordeum vulgare* L.). *Barley Genet. Newslett.* 27, 8-12.
- Eglinton, J. K., Langridge, P. and Evans, D. E. (1998) Thermostability variation in alleles of barley *beta*-amylase. *J. Cereal Sci.* 28, 301-309.
- Erkkilä, M. J., Leah, R., Ahokas, H. and Cameron-Mills, S. V. (1998) Allele-dependent barley grain  $\beta$ -amylase activity. *Plant Physiol.* 117, 679-685.
- Evans, D. E., Macleod, L. C., Eglinton, J. K., Gibson, C. E., Zhang, X., Wallace, W., Skerritt, J. H. and Lance, R. C. M. (1997a) Measurement of *beta*-

- amylase in malting barley (*Hordeum vulgare L.*). Part 1: Development of a quantitative ELISA for *beta*-amylase. *J. Cereal Sci.* 25, 229-239.
- Evans, D. E., Wallace, W., Lance, R. C. M and Macleod, L. C. (1997b) Measurement of *beta*-amylase in malting barley (*Hordeum vulgare L.*). Part 2: The effect of germination and kilning. *J. Cereal Sci.* 26, 241-250.
- Gibson, T. S., Solah, V., Glennie-Holmes, M. R. and Taylor, H. R. (1995) Diastatic power in malted barley: contributions of malt parameters to its development and the potential of barley grain  $\beta$ -amylase to predict malt diastatic power. *J. Inst. Brew.* 101, 277-280.
- Giese, H. and Hejgaard, J. (1984) Synthesis of salt soluble proteins in barley. Pulse-labelling study of grain filling in liquid-cultured detached spikes. *Planta* 161, 172-177.
- Grime, K. H. and Briggs, D. E. (1995) Release and activation of barley  $\beta$ -amylase. *J. Inst. Brew.* 101, 337-343.
- Guerin, J. R., Lance, R. C. M. and Wallace, W. (1992) Release and activation of barley *beta*-amylase by malt endopeptidases. *J. Cereal Sci.* 15, 5-14.
- Guex, N. and Peitsch, M. C. (1997) SWISS-MODEL and the Swiss-Pdb viewer: An environment for comparative protein modelling. *Electrophoresis* 18, 2714-2723.
- Hammond-Kosack, M. C. U., Holdsworth, M. J. and Bevan, M. W. (1993) *In vivo* footprinting of a low molecular weight glutenin gene (LMWG-1D1) in wheat endosperm. *EMBO J.* 12, 545-554.
- Hara-Nishimura, I., Nishimura, M. and Daussant, J. (1986) Conversion of free  $\beta$ -amylase to bound  $\beta$ -amylase on starch granules in the barley endosperm

- during desiccation phase of seed development. *Protoplasma* 134, 149-153.
- Hardie, D. G. (1975) Control of carbohydrase formation by gibberellic acid in barley endosperm. *Phytochem.* 14, 1719-1722.
- Hardy, F., Vriend, G., Veltman, O. R., Vinne, van der B., Venema, G. and Eijsink, V. G. H. (1993) Stabilisation of *Bacillus stearothermophilus* neutral protease by introduction of prolines. *FEBS Lett.* 317, 89-92.
- Hejgaard, J. (1976) Free and protein-bound  $\beta$ -amylase of barley grain. Characterisation by two-dimensional immuno-electrophoresis. *Physiol. Plant.* 38, 293-299.
- Hejgaard, J. (1978) 'Free' and 'bound'  $\beta$ -amylases during malting of barley. Characterisation by two-dimensional immunoelectrophoresis. *J. Inst. Brew.* 84, 43-46.
- Hejgaard, J., and Boisen, S. (1980) High lysine proteins in Hiproly barley breeding: identification, nutritional significance and new screening methods. *Hereditas* 93, 311-320.
- Hizukuri, S. and Osaki, S. (1978) A rapid Smith-degradation for the determination of non-reducing terminal residues of (1 $\rightarrow$ 4)- $\alpha$ -D-glucans. *Carbohydr. Res.* 63, 261-264.
- Kaneko, T., Kihara, M. and Ito, K. (2000) Genetic analysis of  $\beta$ -amylase thermostability to develop a DNA marker for malt fermentability improvement in barley, *Hordeum vulgare* L.. *Plant Breeding* 119, 197-201.

- Kihara, M., Kaneko, T. and Ito, K. (1998) Genetic variation of  $\beta$ -amylase thermostability among varieties of barley, *Hordeum vulgare* L., and relation to malting quality. *Plant Breeding* 117, 425-428.
- Kihara, M., Kaneko, T., Ito, K., Aida, Y. and Takeda, K. (1999). Geographical variation of  $\beta$ -amylase thermostability among varieties of barley (*Hordeum vulgare*) and  $\beta$ -amylase deficiency. *Plant Breeding* 118, 453-455.
- Kreis, M., Williamson, M., Buxton, B., Pywell, J., Hejgaard, J. and Svendsen, I. (1987) Primary structure and differential expression of  $\beta$ -amylase in normal and mutant barleys. *Eur. J. Biochem.* 169, 517-525.
- Kreis, M., Williamson, M. S., Shewry, P. R., Sharp, P. and Gale, M. (1988) Identification of a second locus encoding  $\beta$ -amylase on chromosome 2 of barley. *Genet. Res. Camb.* 51, 13-16.
- Kitamoto, N., Yamagata, H., Kato, T., Tsukagoshi, N. And Udaka, S. (1988) Cloning and sequencing of the gene encoding thermophilic  $\beta$ -amylase of *Clostridium thermosulfurogenes*. *J. Bacteriol.* 170, 5848-5854.
- Kunze, W. (1996) Wort product. In 'Technology Brewing and Malting', Wainwright T. Translated, pp 171-316, VLB, Berlin.
- LaBerge, D. E. and Marchylo, B. A. (1983) Heterogeneity of the  $\beta$ -amylase enzymes of barley. *J. Am. Soc. Brew. Chem.* 41, 120-124.
- LaBerge, D. E. and Marchylo, B. A. (1986) Changes in  $\beta$ -amylase enzymes during kernel development of barley and the effect of papain as an extractant. *J. Am. Soc. Brew. Chem.* 44, 16-19.

- Laederach, A., Dowd, M. K., Coutinho, P. M. and Reilly, P. J. (1999) Automated docking of maltose, 2-deoxymaltose, and maltotetraose into the soybean  $\beta$ -amylase active site. *Proteins: Struct. Funct. Genet.* 37, 166-175.
- Laemmli, U. K. (1971) Cleavage of structural proteins during the assembly of the head of bacteriophage T4. *Nature* 227, 680-685.
- Laskowski, R. A., MacArthur, M. W., Moss, D. S. and Thornton, J. M. (1993) PROCHECK: a program to check the stereochemical quality of protein structures. *J. Appl. Crystallogr.* 26, 283-291.
- Laurière, C., Laurière, M. and Daussant, J. (1986) Immunohistochemical localisation of  $\beta$ -amylase in resting barley seeds. *Physiol. Plant.* 67, 383-388.
- Li, C. (1997) Genetic control of hydrolytic enzymes in germinated barley (*Hordeum vulgare L.*). Chapter 3. Sequence variation, isoenzyme type and activity QTL of beta-amylase in barley (*Hordeum vulgare L.*). pp 57-65. Thesis for the degree of Doctor of philosophy at the University of Adelaide.
- Lizotte, P. A., Henson, C. A. and Duke, S. H. (1990) Purification and characterisation of pea epicotyl  $\beta$ -amylase. *Plant Physiol.* 92, 615-621.
- Lörz, H., Serazetdinova, L., Leckband, G. Lutticke, S. (2000) Transgenic barley – a journey with obstacles and milestones. 8<sup>th</sup> International Barley Genetics Symposium, 22-27 October, Adelaide, ed. S.J. Logue, pp 189-193.
- Lundgard, R. and Svensson, B. (1986) Limited proteolysis in the carboxy-terminal region of barley  $\beta$ -amylase. *Carlsberg Res. Commun.* 51, 487-491.

- Lundgard, R. and Svensson, B. (1987) The four major forms of barley  $\beta$ -amylase. Purification, characterisation and structural relationship. *Carlsberg Res. Commun.* 52, 313-326.
- MacGregor, A. W., LaBerge, D. E. and Meredith, W. O. S. (1971) Changes in barley kernels during growth and maturation. *Cereal Chem.* 48, 255-269.
- MacGregor, A. W. (1996) Malting and brewing science: challenges and opportunities. *J. Inst. Brew.* 102, 97-102.
- MacGregor, A. W., Bazin, S. L., Macri, L. J. and Babb, J. C. (1999) Modelling the contribution of *alpha*-amylase, *beta*-amylase and limit dextrinase to starch degradation during mashing. *J. Cereal Sci.* 29, 161-169.
- Mannervik, B. (1982) Regression analysis, experimental error, and statistical criteria in the design and analysis of experiments for discrimination between rival kinetic models. *Methods Enzymol.* 87, 370-390.
- Matthews, B. W., Nicholson, H. And Becktel, W. J. (1987) Enhanced protein thermostability from site-directed mutations that decrease the entropy of unfolding. *Proc. Natl. Acad. Sci. USA* 84, 6663-6667.
- McCleary, B. V. and Sheehan, H. (1987) Measurement of cereal  $\alpha$ -amylase: A new assay procedure. *J. Cereal Sci.* 6, 237-251.
- McCleary, B. V. and Codd, R. (1989) Measurement of  $\beta$ -amylase in cereal flours and commercial enzyme preparations. *J. Cereal Sci.* 9, 17-33.
- Mikami, B., Hehre, E. J., Sato, M., Katsube, Y., Hirose, M., Morita, Y. and Sacchettini, J. C. (1993) The 2.0 - Å resolution structure of soybean  $\beta$ -amylase complexed with  $\alpha$ -cyclodextrin. *Biochemistry* 32, 6836-6845.

- Mikami, B., Degano, M., Hehre, E. J. and Sacchettini, J. C. (1994) Crystal structure of soybean  $\beta$ -amylase reacted with  $\beta$ -maltose and maltal: active site components and their apparent roles in catalysis. *Biochemistry* 33, 7779-7787.
- Mikami, B., Yoon, Hye-Jin and Yoshigi, N. (1999) The crystal structure of the sevenfold mutant of barley  $\beta$ -amylase with increased thermostability at 2.5 Å resolution. *J. Mol. Biol.* 285, 1235-1243.
- Mikami, B. (2000) Structure of  $\beta$ -amylase: X-ray crystallographic analysis. In 'Glycoenzymes', Ohnishi, M. Ed., pp 55-81, Japan Scientific Societies Press, Tokyo.
- Misra, U. K. and French, D. (1960) Inhibition and action pattern of  $\beta$ -amylase in presence of maltose. *Biochem. J.* 77, 1.
- Nakatani, H. (1997) Monte carlo simulation of multiple attack mechanism of  $\beta$ -amylase-catalysed reaction. *Biopolymers* 42, 831-836.
- Nanmori, T., Nagai, M., Shimizu, Y., Shinke, R. and Mikami, B. (1993) Cloning of the  $\beta$ -amylase gene from *Bacillus cereus* and characteristics of the primary structure of the enzyme. *Appl. Environ. Microbiol.* 59, 623-627.
- Nelson, N. (1944) Photometric adaptation of the Somogyi method for the determination of glucose. *J. Biol. Chem.* 153, 375-380.
- Nicholls, A., Sharp, K. and Honig, B. (1991) Protein folding and association: insights from the interfacial and thermodynamic properties of hydrocarbons. *Proteins* 11, 281-296.



- Nielsen, G. and Johansen, H. B. (1986) Proposal for the identification of barley varieties based on the genotypes for 2 hordein and 39 isoenzyme loci of 47 reference varieties. *Euphytica* 35, 717-728
- Niku-Paavola, M. L., Skakoun, A., Nummi, M. and Daussant, J. (1973) The polymorphism of barley  $\beta$ -amylase. *Biochem. Biophys. Acta* 322, 181-184.
- Nitta, Y., Isoda, Y., Toda, H. and Sakiyama, F. (1989) Identification of glutamic acid 186 affinity-labelled by 2,3-epoxypropyl  $\alpha$ -D-glucopyranoside in soybean  $\beta$ -amylase. *J. Biochem.* 105, 573-576.
- Nomura, K., Mikami, B. and Morita, Y. (1986) Interaction of soybean  $\beta$ -amylase with glucose. *J. Biochem.* 100, 1175-1183.
- Nummi, M., Vilhunen, R. and Enari, T. M. (1965)  $\beta$ -amylase: I.  $\beta$ -amylases of different molecular size in barley and malt. *Eur. Brew. Conf. Proc. 10th Congr.* pp. 52-61, Stockholm.
- Nuutila, A. M., Ritala, A., Skadsen, R. W., Mannonen, L and Kauppinen, V. (1999) Expression of fungal thermotolerant endo-1,4-beta-glucanase in transgenic barley seeds during germination. *Plant Mol. Biol.* 41, 777-783.
- Okada, Y., Yoshigi, N., Sahara, H. and Koshino, S. (1995) Increase in thermostability of recombinant barley  $\beta$ -amylase by random mutagenesis. *Biosci. Biotech. Biochem.* 59, 1152-1153.
- Okada, Y., Kihara, M., Kuroda, H., Yoshigi, N. and Ito, K. (2000) Cloning and sequencing of the promoter region of the seed specific  $\beta$ -amylase gene from barley. *J. Plant Physiol.* 156, 762-767.

- Peitsch, M. C. (1995) Protein modelling by E-mail. *Bio/Technology* 13, 658-660.
- Peitsch, M. C. (1996) ProMod and swiss-Model: Internet-based tools for automated comparative protein modelling. *Biochem. Soc. Trans.* 24, 274-279.
- Perella, F. W. (1988) EZ-FIT: A practical curve-fitting microcomputer program for the analysis of enzyme kinetic data on IBM-PC compatible computers. *Anal. Biochem.* 174, 437-447.
- Ramakrishnan, C. and Ramachandran, G. N. (1965) PROCHECK: Stereochemical criteria for polypeptide and protein chain conformation. *Biophys. J.* 5, 909-993.
- Robinson, C. R. and Sauer, R. T (1998) Optimising the stability of single-chain proteins by linker length and composition mutagenesis. *Proc. Natl Acad. Sci. USA* 95, 5929-5934.
- Rorat, T., Sadowski, J., Irzykowski, W., Ziegler, P. and Daussant, J. (1995) Differential expression of two  $\beta$ -amylase genes of rye during seed development. *Physiol. Plant.* 94, 19-24.
- Sadowski, J., Rorat, T., Cooke, R. and Delseny, M. (1993) Nucleotide sequence of a cDNA clone encoding ubiquitous  $\beta$ -amylase in rye (*Secale cereale* L.). *Plant Physiol.* 102, 315-316 .
- Schulz, G. E. and Schirmer, R. H. (1984) Thermodynamics and kinetics of polypeptide chain folding. In 'Principles of protein structure' Cantor, C. R. ed., pp 149-165. Springer-Verlag New York Inc, New York.

- Shewry, P. R., Parmar, S., Buxton, B., Gale, M. D., Liu, C. J., Hejgaard, J. and Kreis, M. (1988) Multiple molecular forms of  $\beta$ -amylase in seeds and vegetative tissues of barley. *Planta* 176, 127-134 .
- Shinke, R. (1988)  $\beta$ -Amylases. In 'Handbook of amylases and related enzymes. Their sources, isolation methods, properties and applications', The Amylase Research Society of Japan ed., pp 81-99, Pergamon Press, Oxford.
- Sjöholm, K., Macri, L. J. and MacGregor, A. W. (1995) Is there a role for limit dextrinase in mashing? In '*Proc. 25<sup>th</sup> Cong. Eur. Brew. Conv.*' pp 277-284, Oxford University Press, Oxford.
- Sopanen, T. and Laurière, C. (1989) Release and activity of bound  $\beta$ -amylase in a germinating barley grain. *Plant Physiol.* 89, 244-249.
- Stenholm, K. and Home, S. (1999) A new approach to limit dextrinase and its role in mashing. *J. Inst. Brew.* 105, 205-210.
- Swanston, J. S. (1980) The use of electrophoresis in testing for high diastatic power in barley. *J. Inst. Brew.* 86, 81-83.
- Swanston, J. S. (1983) An alternative approach to breeding for high diastatic power in barley. *Euphytica* 32, 910-924.
- Takeda, Y., Guan, H. P. and Preiss, J. (1993) Branching of amylose by the branching isoenzymes of maize endosperm. *Carbohydr. Res.* 240, 253-263.
- Thompson, M. J. and Eisenberg, D. (1999) Transproteomic evidence of a loop-deletion mechanism for enhancing protein thermostability. *J. Mol. Biol.* 290, 595-604.

- Totsuka, A. and Fukazawa, C. (1993) Expression and mutation of soybean  $\beta$ -amylase in *Escherichia coli*. *Eur. J. Biochem.* 214, 787-794.
- Totsuka, A., Nong, V. H., Kadokawa, H., Kim, C.-S., Itoh, Y. and Fukazawa, C. (1994) Residues essential for catalytic activity of soybean beta-amylase. *Eur. J. Biochem.* 221, 649-654.
- Totsuka, A. and Fukazawa, C. (1996) Functional analysis of Glu380 and Leu383 of soybean  $\beta$ -amylase: A proposed action mechanism. *Eur. J. Biochem.* 240, 655-659.
- Uozumi, N., Matsuda, T., Tsukagoshi, N. and Udaka, S. (1991) Structure and functional roles of cysteine residues of *Bacillus polymyxa*  $\beta$ -amylase. *Biochemistry* 30, 4594-4599.
- Vikstøl-Nielsen, A., Christensen, T. M. I. E., Bojko, M. and Marcussen, J. (1997) Purification and characterisation of  $\beta$ -amylase from leaves of potato (*Solanum tuberosum*). *Physiol. Plant.* 99, 190-196.
- Visuri, K. and Nummi, M. (1972) Purification and characterisation of crystalline  $\beta$ -amylase from barley. *Eur. J. Biochem.* 28, 555-565.
- Vogt, G., Woell, S. and Rrgos, P. (1997) Protein thermal stability, hydrogen bonds, and ion pairs. *J. Mol. Biol.* 269, 631-643.
- Yoshigi, N., Okada, Y., Sahara, H. and Koshino, S. (1994a) PCR cloning and sequencing of the  $\beta$ -amylase cDNA from barley. *J. Biochem.* 115, 47-51.
- Yoshigi, N., Okada, Y., Sahara, H. and Koshino, S. (1994b) Expression in *Escherichia coli* of cDNA encoding barley  $\beta$ -amylase and properties of recombinant  $\beta$ -amylase. *Biosci. Biotech. Biochem.* 58, 1080-1086.

Yoshigi, N., Sahara, H. and Koshino, S. (1995a) Role of the C-terminal region of  $\beta$ -amylase from barley. *J. Biochem.* 117, 63-67.

Yoshigi, N., Okada, Y., Maeba, H., Sahara, H. and Tamaki, T. (1995b) Construction of a plasmid used for the expression of a sevenfold-mutant barley  $\beta$ -amylase with increased thermostability in *Escherichia coli* and properties of the sevenfold-mutant  $\beta$ -amylase. *J. Biochem.* 118, 562-567.